THESIS

REMOTE SENSING AND APPARENT ELECTRICAL CONDUCTIVITY TO CHARACTERIZE SOIL WATER CONTENT

Submitted by

Alfonso de Lara

Department of Soil and Crop Sciences

In partial fulfillment of the requirements

For the Degree of Master of Science

Colorado State University

Fort Collins, Colorado

Fall 2016

Master's Committee:

Advisor: Raj Khosla

Louis Longchamps
Phil Westra

ABSTRACT

REMOTE SENSING AND APPARENT ELECTRICAL CONDUCTIVITY TO CHARACTERIZE SOIL WATER CONTENT

Improvement in water use efficiency of crops is a key component in addressing the increasing global water demand. The time and depth of the soil water monitoring are essential when defining the amount of water to be applied to irrigated crops. Precision irrigation (PI) is a relatively new concept in agriculture, and it provides a vast potential for enhancing water use efficiency while maintaining or increasing grain yield. As part of site-specific farming, PI needs to be explored, tested, and evaluated which continues to be a research issue. Neutron probes (NPs) have consistently been used for studies as a robust and accurate method to estimate soil water content (SWC). Remote sensing derived vegetation indices have been successfully used to estimate variability of Leaf Area Index and biomass, which are related with root water uptake. Crop yield has not been evaluated on a basis of SWC as explained by NPs in time and at different depths. One among many challenges in implementing PI is the reliable characterization of the soil water content (SWC) across spatially variable fields. For this purpose, commercial retailers are employing apparent soil electrical conductivity (EC_a) to create irrigation prescription maps. However, the accuracy of this method has not been properly studied at the field scale. The objectives of this study were (1) to determine the optimal time and depth of SWC and its relationship to maize grain yield (2) to determine if satellite-derived vegetation indices coupled with SWC could further improve the relationship between maize grain yield and SWC (3) to assess the potential of EC_a

measurement to characterize spatial distribution of SWC at field scale, and (4) to determine whether soil properties coupled with EC_a could further improve the characterization of the SWC. For objectives 1 and 2, the study was conducted on maize (*Zea Mays* L.) irrigated in two fields in northern Colorado. Soil water data was collected at five soil depths (30, 60, 90, 120 and 150 cm), 21 and 12 times at Site I and II, respectively. Three vegetation indices were calculated on seven dates (Emergence to R3). Maize grain yield was harvested at the physiological maturity at each NPs location. Automated model selection of SWC readings to assess maize yield consistently selected three dates spread around reproductive growth stages for most depths (p value < 0.05). For objectives 3 and 4, the study was conducted on two fields located in northeastern Colorado. In-field SWC was measured using neutron probes at 41 and 31 locations for Site I and II respectively. Soil EC_a measurements were acquired using Geonics EM38-MK2 unit. In addition, cation exchange capacity, clay, organic matter and salt content were coupled with soil EC_a to estimate SWC. Data analysis was performed using the statistical software R. Statistical correlations and multiple linear regressions were obtained from the properties that were statistically significant (p value < 0.05). Results of the study showed that the SWC readings at the 90 cm depth had the highest correlations with maize yield, followed closely by the 120 cm. When coupled with remote sensing data, models improved by adding vegetation indices representing the crop health status right before the reproductive growth stage (V9). Thus, SWC monitoring at reproductive stages combined with vegetation indices could be a tool for improving maize irrigation management. Likewise, the SWC was found to be statistically different across EC_a derived zones, indicating that EC_a was able to accurately characterize average differences in SWC across management zones. Organic matter and salt content significantly improved the SWC

assessment when combined with the EC_a. The development of prescription maps for variable rate irrigation should be tailor made depending on the specific field characteristics influencing SWC.

ACKNOWLEDGEMENTS

I want to thank the CSU Precision Agriculture laboratory head members, Dr. Raj Khosla and Dr. Louis Longchamps for their support, guidance and expertise. Also to Ann Hess and Phil Turk from Natural Sciences, for their statistics knowledge and patience needed to help me on the realization of my work.

Further, I would like to thank my fellow colleges, Rafael Siqueira, Adriano Anselmi, Marcelo Chan Fu Wei, and Emmanuel Deleon who help me in different ways on my thesis.

To my family and friends, for their unconditional support, love and motivation over the last years, making possible the realization of my work. Without them, I would not be who I am today.

DEDICATION

For my parents, Juan Carlos de Lara and Maria de los Angeles Aldalur.

And my siblings, Juan Manuel and Maria Jesus.

TABLE OF CONTENTS

LIST OF TABLES

LIST OF FIGURES

LIST OF APPENDICIES

CHAPTER 1

SOIL WATER CONTENT AND HIGH-RESOLUTION IMAGERY: MAIZE YIELD

INTRODUCTION

Since the beginning of human civilization, humans have realized the importance of water in cultivating crops. A better understanding of this resource has led humankind to expand its range by means of more productive and efficient crop water management (Tanner and Sinclair, 1983). As the world's population continues to grow, there is an increase in water scarcity which has created an extra interest in evaluating the relationship between water use and crop yield. Given the limited possibilities to expand land surface, it is necessary to intensify every viable aspect of cereal production systems, especially the ones that are water sensitive. Interactions between crop, climate, water and soil are not simple. Many processes are involved and continuous research has been done to understand this complexity (Johl, 2013). Soil hydraulic properties vary within fields, even on seemingly uniform land areas (Nielsen et al., 1973). The spatiotemporal variability of soil water content is regulated by factors such as topographic features (Moore et al., 1988), soil properties (Henninger et al., 1976), land use (Famiglietti et al., 1999), climatic variability (Hawley et al., 1983), and vegetation distribution (Mohanty et al., 2000). An accurate comprehension of soil water content behavior is important for soil hydrological research in areas such as irrigation scheduling and site-specific agriculture (Hupet and Vanclooster, 2002).

More than half of the irrigation in the U.S. is used for growing cereals, and 29% is used just for maize (*Zea mays* L.) (Howell, 2001). Maize is one of the most important crops in terms of worldwide grain production. The global dedicated area and yield have been increasing over time, with a total production of 1016 million tonnes in 2013 (FAO., 2015). The largest producer is the

United States, with about 41 percent of the world's total production (Steduto et al., 2012). Maize seeds have several uses, from human and animal consumption to alcohol for biofuel and the manufacturing of plastic, among others. Maize production requires large amounts of water, therefore, it is important to better understand the relationship between its yield and soil water to sustain high levels of productivity.

Water resources are pushed to the limits through increasing water demands. Part of the solution for a sustainable productivity is the improvement of the water use efficiency. Water use efficiency is a term that has multiple meanings in relation to crop production. One definition refers to the amount of water that is utilized by the crop rather than lost as evaporation from the soil surface or drained out of the root's range (Condon et al., 2004). Plant water-use efficiency (WUE) is defined as the amount of carbon gained per unit of land area per unit of water used (Steduto, 1996). Crops vary their response to water deficits in terms of WUE. For some crops, the WUE will increase with the increase in water deficit (Johl, 2013). In case of maize, the WUE will decrease if a water shortage is equally spread over the total growth period. The impact of a water deficit also varies throughout the growing season depending on how sensitive the crop is at that specific growth stage. Broadly speaking, for maize, the critical periods are emergence, and reproductive growth stages (Johl, 2013). This suggests that not only the amount of water availability is crucial, but the timing of water availability is important as well. Therefore, it is important to irrigate when the yield response is maximum. However, the effect of water supply on yield is site specific and not so clear, due to the complex interactions between soil, climate, and the crop (Hanks, 1983).

Maintaining soil water levels within a certain range prevents hydric stress and leaching of agrochemicals. Field capacity (FC) is the maximum amount of water that remains after drainage due to gravity and Wilting point (WP) is the minimum amount of water at which plants can no

longer extract water from the soil. Available water-holding capacity (AWC) is the difference between these two points, which is the maximum water that the soil can retain for plant uptake. The quantity of water accessible to the plants is the available soil water, and it could be anywhere from zero at WP, to the maximum at FC (Martin et al., 2014). Measuring and monitoring soil water conditions provides valuable information to determine the amount of water to be applied to crops under irrigation systems (Muñoz-Carpena et al., 2004). Neutron moisture meters, also known as neutron probes (NP), have been used for studies of soil water content for a long time (Evett et al., 2009). The volume sensed with a single access tube is generally enough to provide precision and statistical power. Neutron probe reading has shown to be a robust and accurate (± 0.005 m^3 m^{-3}) method to estimate soil water content (Muñoz-Carpena et al., 2004). Other advantages are that different soil depths can be measured by a single probe, it measures a large volume of soil (sphere of influence with 10-40 cm radius depending on water content, compared to about 3 cm radius of the Time Domain Reflectometry method), NP readings are not affected by soil salinity and has a stable soil-specific calibration (Muñoz-Carpena et al., 2004). Nonetheless, since it is a volumetric method, it does not indicate how strongly the soil retains water. Thus, the same total volumetric water content might be more or less available to plants depending on soil characteristics such as texture, organic matter, and the presence of salts (Martin et al., 2014).

Even though the vegetation growth shows to be heterogeneous across field, most soil water studies for the purpose of water application consider it as being uniform. Farmers often notice spatial variability of crop within fields. Thus, it is logical that the water extraction is not uniform, leading to the need for an investigation on the effect of spatial distribution of vegetation and its influence on the spatial pattern of soil water content. In early studies, Lull and Reinhart (1955) found that vegetation is one of the primary factors affecting soil moisture changes. Hupet and

Vanclooster (2002) discussed a non-negligible role of the evapotranspiration of plants in the soil moisture patterns for the shallow layers. There were significant correlations between the vegetation growth and root water uptake, and they concluded that for fields without significant slope, vegetation would act as the main controlling factor of the soil water spatial structure. Likewise, Teuling and Troch (2005) found that vegetation can either create or destroy spatial variability on the superficial soil layers (20 to 30 centimeters), depending on soil texture and on the precipitation deficit. Similarly, Gao et al. (2014) explained that vegetation could affect water levels by altering the soil properties, particularly near the soil surface. Altering runoff, shading the land surface, non-uniform rates of soil evaporation, and changing soil hydraulic conductivity by way of root activity, are examples of how plants can shape soil water variability (Pan and Wang, 2009). However, the conclusions were different in experiments that studied deeper soil water readings. Vachaud et al. (1985) described a strong temporal stability on grass, olive, and wheat fields, with no effects on soil water variability by root extraction nor by irrigation.

Little research has focused on the importance or explanatory significance of soil water content readings at different depths. Longchamps et al. (2015) suggested that to develop stable irrigation management zones, the spatial pattern of soil water content measured at 45 cm deep was more stable than at 15 cm deep, where readings were more erratic. This may be due to the higher root water consumption and other meteorological conditions closer to the surface (Biswas and Si, 2011). Further, Longchamps et al. (2015) proposed the use of variable rate irrigation only when the roots are deep enough and soil water content shows more stable spatial patterns, and not at the beginning of the season when more randomness in soil water content occurs. With a stronger spatial dependency of the soil water content (SWC) at greater depth, fewer sensor locations would be necessary to measure soil moisture and characterize the soil water content profile.

Hupet and Vanclooster (2002) found a positive relation between root water uptake (0-75 cm depth) and leaf area index (LAI, the ratio of one-sided green leaf area to ground area) in maize, supporting the idea of spatially variable water consumption due to spatially variable crop growth. Given these conditions, it may be necessary to add a crop attribute to account for spatial variability in water consumption. Remote sensing has been used to characterize crop effect on SWC in several studies (Holzman et al., 2014; Wang and Qu, 2009). Vegetation indices derived from remote sensing have been successfully used to estimate spatial variability of crop LAI and biomass (Wiegand et al., 1991) and yield (Ashcroft et al., 1990). Remote estimation of LAI at different scales can be achieved by measuring spectral reflectance (Rouse et al., 1974). The development of these vegetation indices are based on the sensitivity of chlorophyll content in leaves to reflect red and near infrared radiation, showing a negative and positive correlation, respectively (Knipling, 1970). Making use of this relationship, vegetation indices capture the variability by combining them in the form of different ratios (Myneni and Hall, 1995). One of the oldest and most popular indices is the Normalized Difference Vegetation Index (NDVI), which has been widely used to measure the abundance and chlorophyll activity in the leaves (Rouse et al., 1974). The extent of NDVI use varies from small research plots to global investigations, and its popularity is due to the ease of collecting data on generic spectral bands required for its calculation ((Near Infrared – Red)/(Near Infrared + Red)), and availability in most remote sensing systems (Walthall et al., 2004).

The NDVI has potential to be used as a variable to characterize spatial variability of crop water consumption, showing a nonlinear relationship with LAI. However, NDVI is crop specific, thus the need for re-parameterization for different cover types (Viña et al., 2011). In addition, when LAI in maize canopies is higher than 2.0, NDVI is normally insensitive to changes (Gitelson et al.,

2003). Saturation of NDVI happens because the red spectral range used for its calculation is highly absorbed by chlorophyll (Lichtenthaler, 1987), and the depth of light penetration into the leaf is low (Kumar and Silva, 1973). Researchers have studied other spectral regions to overcome this issue. For example, radiation in the red-edge region penetrates deeper into the leaves because chlorophyll has a lower absorption coefficient, and does not saturate at moderate to high chlorophyll contents (Gitelson et al., 1996; Gitelson et al., 2002) . Viña et al. (2011) found that among various vegetation indices evaluated, the Red-edge Chlorophyll Index (RECI) was the only one that did not require different model coefficients for the remote estimation of green LAI in different crop types (re-parameterization). It could also be used for an accurate estimation of LAI for crop canopies ranging from 0 to more than 6 m^2 of vegetation per m^2 of soil. The RECI calculation is simply the ratio of near-infrared to the red-edge band minus one. Delegido et al. (2013) found that the Red-edge Normalized Difference Vegetation Index (RENDVI), which uses the red-edge band rather than the red band, does not saturate at high LAI values and is strongly related to the physiological status of the plant for a wide range of crops and conditions. This represents an advantage for precision farming purposes. The calculation of this index is similar to NDVI, but the red band is replaced by one located in the red-edge region (Gitelson and Merzlyak, 1994). More recently, Nguy-Robertson et al. (2012) proposed the use of a combination of indices on maize and soybean (which have contrasting canopy architectures and leaf structures), arguing that the RENDVI works best for low to moderate LAI values, and RECI works best for moderate to high LAI values.

Since biomass is related to water uptake (Hupet and Vanclooster, 2002), accounting for the seasonal biomass variability can provide useful information on the characterization of the soil water content and yield relationship. In this manner, remote sensing combined with soil water

sensors can perhaps be used to depict the in-season soil moisture profiles for the major land cover types (Huete et al., 1999). Studies on temporal vegetation variability over numerous biome types in North and South America were well represented by the Moderate Resolution Imaging Spectroradiometer (MODIS) sensor (Huete et al., 2002). Particularly, MODIS NDVI and Enhanced Vegetation Index (EVI), were found to accurately assess the temporal vegetation cover changes. Compared to NDVI, EVI is more sensitive to canopy structural variations, such as LAI, canopy type, plant physiognomy and canopy structure (Gao et al., 2000). The EVI was designed to perform better under high biomass conditions where NDVI would saturate, minimize canopy background signal variations, and also to make use of the blue band's sensitivity to the atmosphere to correct for aerosol influences (Pinty et al., 1993).

Review of current literature indicates that the relationship between soil water content and crop yield is not so clear. Moreover, neutron probes and grain yield relationship has not been thoroughly studied from a time and depth perspective. The hypothesis of this study is that soil water content measured at different times and depths is spatially related to grain yield. This could provide useful information for developing and installing soil water sensors at the field scale. In addition, a better interpretation of the data provided by sensor measurements could optimize irrigation water management.

The objectives of this study were (1) to determine the optimal time and depth of soil water measurements and its relationship to maize grain yield, and (2) to determine if satellite-derived vegetation indices coupled with soil water measurements could further improve the relationship between maize grain yield and soil water measurements.

MATERIALS AND METHODS

Study sites

This study was conducted in 2015 at two sites. Both sites were located at Colorado State University's Agricultural Research Development & Education Center (ARDEC), in Larimer County, Colorado. Site I was field number 3130 (40°39'57.4"N, 104°59'53.1"W), and Site II was named Kerbel (40°40'39.8"N, 104°59'50.8"W), which was located straight north of Site I. Site I was under a continuous maize cropping system and irrigated by a center-pivot irrigation system with variable rate prescription capability. Site II was under a maize cropping system with uniform furrow irrigation extending from north to south.

Site I was located on a field mapped as having Kim loam (Fine-loamy, mixed, active, calcareous, mesic Ustic Torriorthents) and Nunn clay loam (Fine, smectitic, mesic Aridic Argiustolls). These soils are characterized as being very deep, well drained, with 1 to 3 percent slopes (Soil Survey Staff, 2000). The Kim series has negligible to very high runoff depending on the slope and moderately slow to slow permeability. Available water storage in profile is very high (about 67.3 cm), and the soil is nonsaline to slightly saline (0.0 to 4.0 mmhos cm^{-1}). The Nunn series has low to high runoff and moderate permeability. Available water storage in profile is high (about 23.1 cm), and the soil is nonsaline (0.1 to 1 mmhos cm^{-1}). Site II was on a field mapped as having Garret loam (Fine-loamy, mixed, superactive, mesic Pachic Argiustolls). This soil is characterized as well to somewhat excessively drained, slow runoff and rapid permeability, with 0 to 1 percent slopes (Soil Survey Staff, 2003). Available water storage in profile is very high (about 32.8 cm), and the soil is nonsaline to slightly saline (0.0 to 2.0 mmhos cm^{-1}).

Temperatures for the 2015 study year followed the historic average. The 1995-2015 average annual precipitation at ARDEC was 272.9 mm. During the year 2015, both sites had high

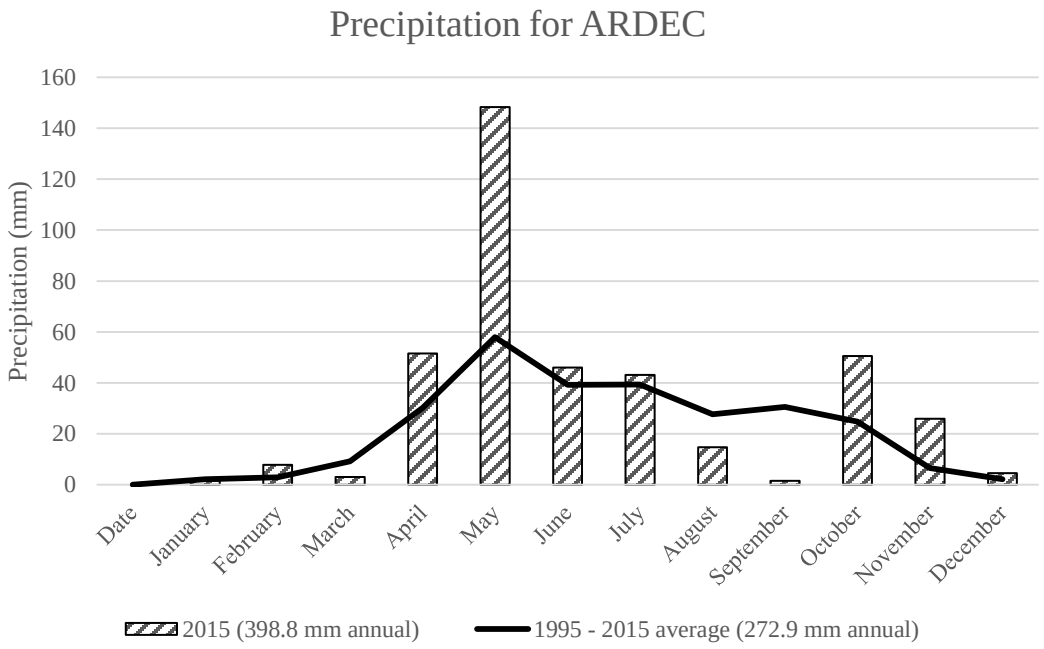

Figure 1.1. Monthly precipitation (mm) registered at ARDEC location for the 2015 (bar plots) and historic monthly average precipitation recorded from 1995 to 2015 (line).

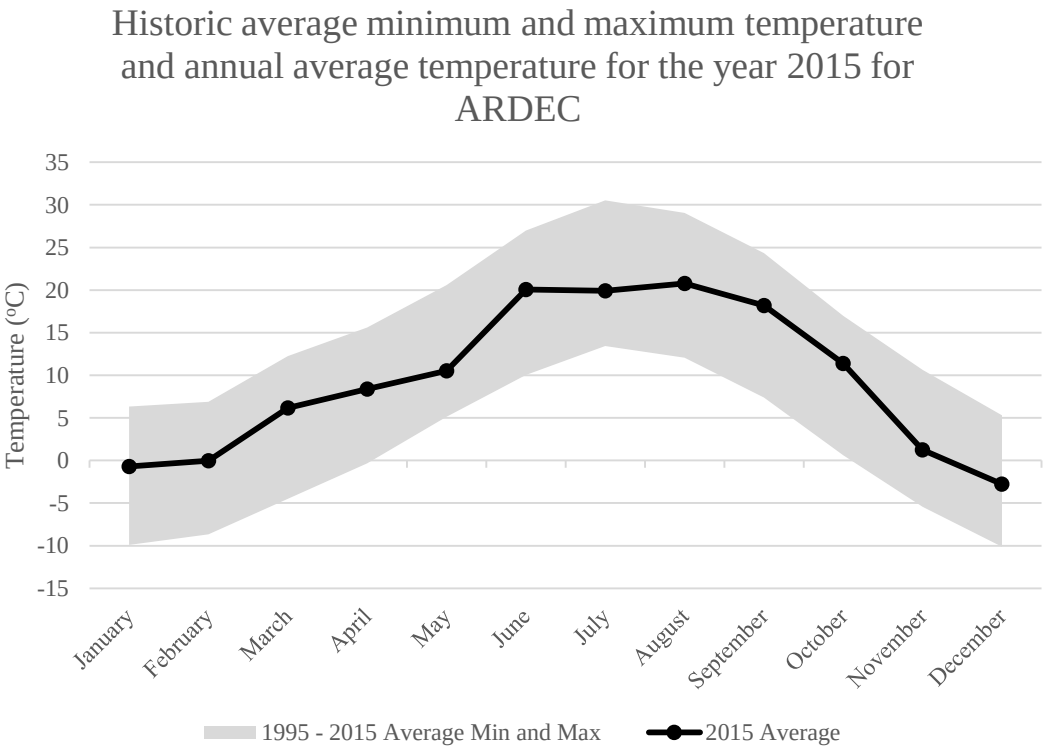

Figure 1.2. Monthly average temperature (ºC) registered at ARDEC location for 2015 (line) and monthly average of minimum and maximum temperature for 1995 to 2015 (gray area).

rainfall. During the early season, April and May, the monthly precipitation average was particularly high, 20 and 90 mm above the series average, respectively. Historic precipitation and temperatures for the last two decades and for year 2015 at ARDEC site can be seen in Figures 1.1 and 1.2, respectively. In summary, weather conditions were wetter than average but temperatures were normal (Colorado Agricultural Meteorological Network, 2015).

Experimental procedure

Cultivation practices

Due to the above average amounts of precipitation at the beginning of the crop growing season, fields were wet and working conditions were poor at average planting date. Maize (*Zea mays* L.) variety Dekalb DKC46-20VT3 was planted on May 28th at Site I. The planter used was a Monosem (NG+3 Series) with a six-row precision vacuum system and inter-row width of 76.2 cm. Plant population rate was 94,000 seeds per hectare. For Site II, maize hybrid Mycogen 2V357 was planted on April 30th, prior to the rainstorm events. The planter used was a six-row John Deere Maxemerge 7300 with an inter-row width of 76.2 cm. Plant population was 83,000 seeds per hectare.

Soil water data collection

This study was part of a large on-going multi-disciplinary project. For the purpose of this study, soil water data was collected at five soil depths (30, 60, 90, 120 and 150 cm) utilizing a neutron probe (Model 503 DR Hydroprobe, CPN International, Martinez, CA). In addition to the original NP readings, average SWC for depths up to 60, 90 and 150 cm were computed, assuming constant bulk density of soil for those depths. For Site I, readings were taken 21 times during the

crop growing season, on a biweekly basis from June 19th to August 28th. For Site II, readings were taken 12 times during the growing season but at time intervals of one to two weeks, from June 8th to September 29th. A total of 18 access tubes were installed on each site (Figure 1.3 and Figure 1.4), and their geo-positions were all logged using a differential-corrected Trimble™ Ag 114 global position system (DGPS) unit. The arrangement of the NP access tubes was in an aligned

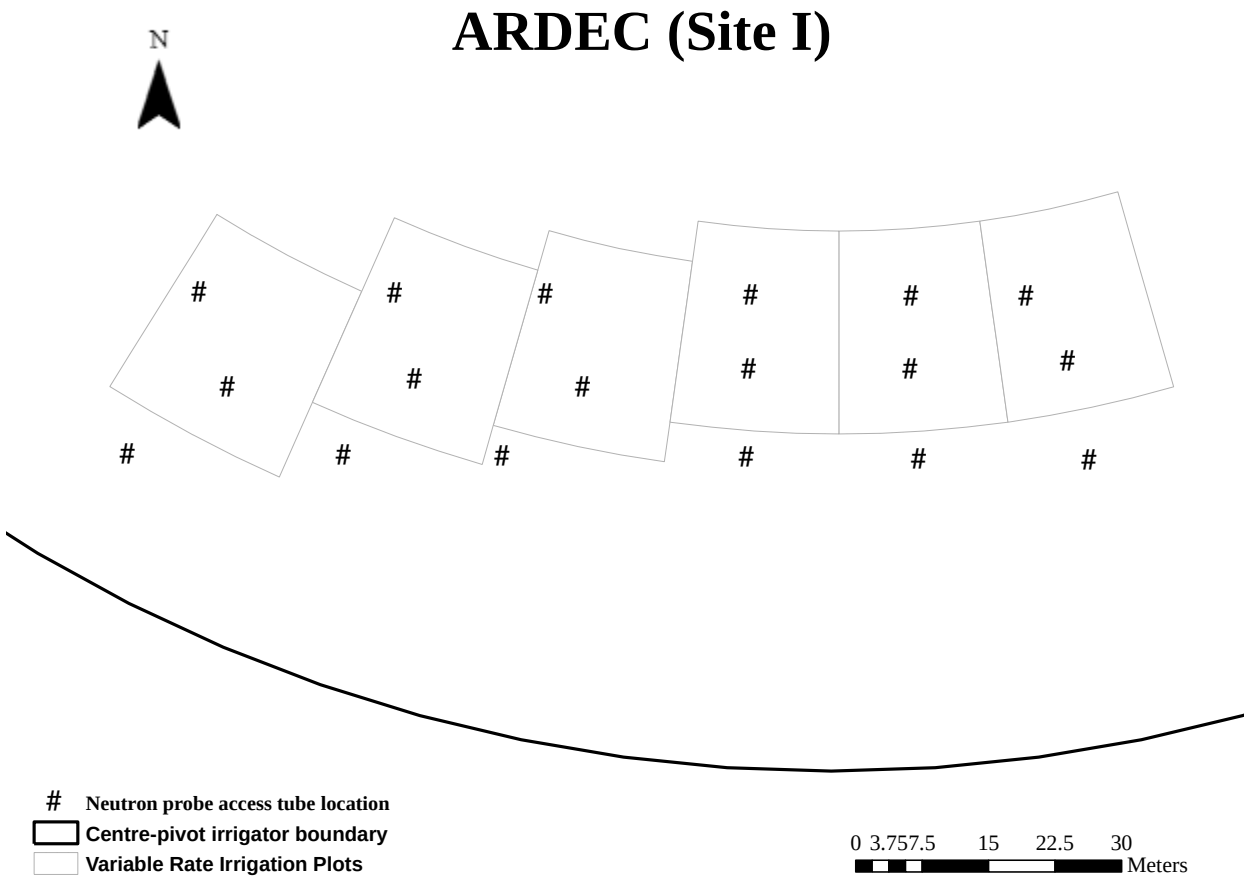

Figure 1.3. Map of Site I showing neutron probe access tubes locations.

samplig design at both experimental locations. Access tubes were positioned within crop rows. For Site I, 12 of the 18 access tubes were located under a variable rate irrigation (VRI) area that was part of another study, and the remainder 6 access tubes were located in a uniform rate irrigation

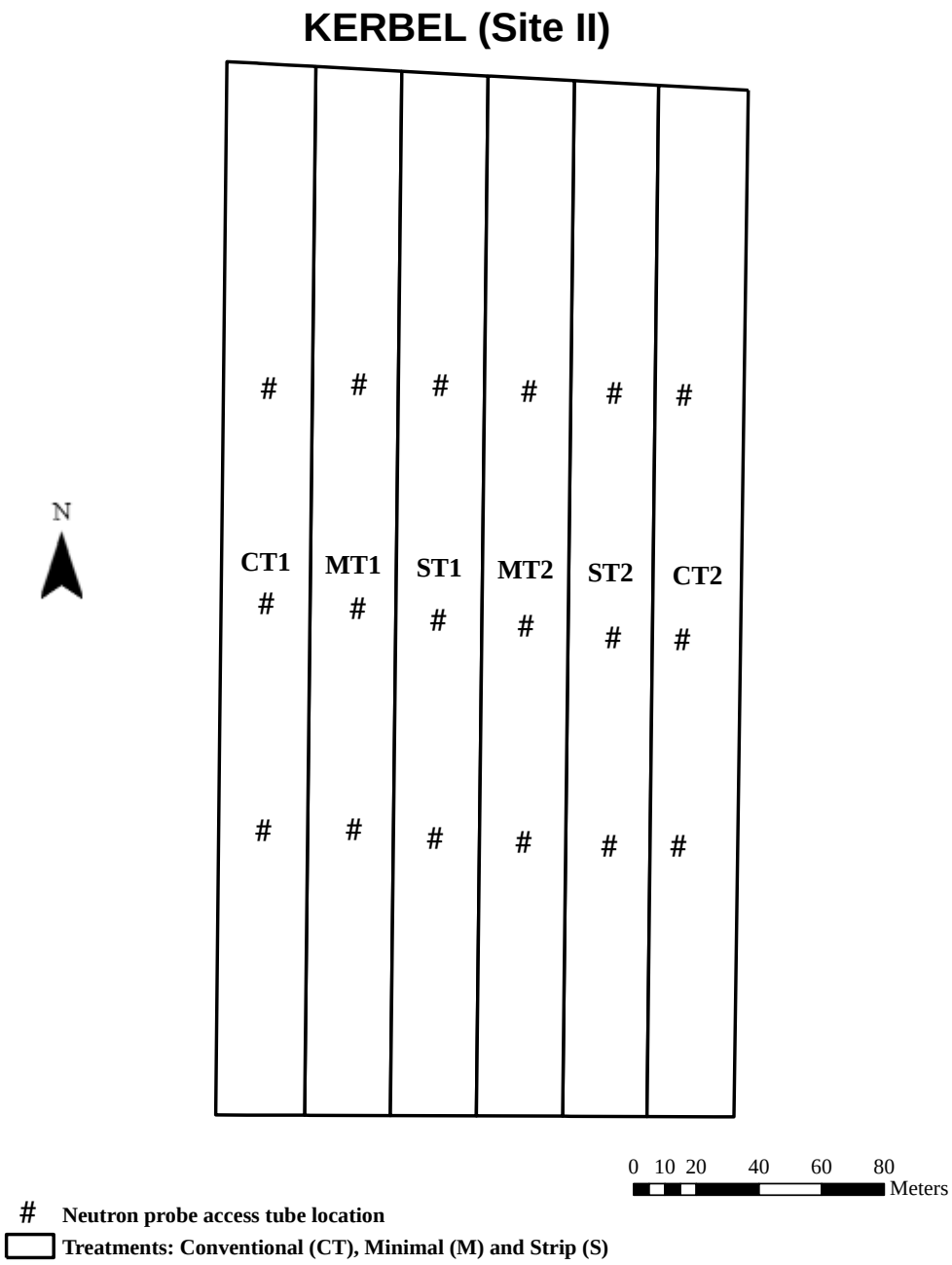

Figure 1.4. Map of Site II showing neutron probe access tubes locations.

area. A Valley variable rate irrigation pivot (Valmont Industries, Valley, NE) was used to provide variable rates of irrigation. The reason for the access tubes distribution was to create variability in water availability with irrigation applications of 40%, 60%, 80%, 100%, 120% and 140% of the

crop evapotranspiration (ET), while the uniform rate was always 100% of the ET. The Site I was irrigated from July 22th to September 24th. For Site II, three different tillage systems were present as part of another study. Access tubes were evenly distributed on the three tillage systems (conventional, minimal and strip) with two replications. The Site II was irrigated from July 7th to September 1th.

Neutron probe based soil moisture measurement technique is widely documented in literature (Evett et al., 2009; Hanson and Kaita, 1997; Longchamps et al., 2015; Muñoz-Carpena et al., 2004; Sheets and Hendrickx, 1995; Stone et al., 1955; Vachaud et al., 1985). The NP emits fast neutrons and part of them are slowed down by the hydrogen atoms present in the soil water. Therefore, the number of slow neutrons is a direct estimate of soil moisture (Stone et al., 1955). Every time the NP is used, a standard measurement was acquired with the sensor located in the probe enclosure to obtain a "count ratio" which consists of the division of the actual field readings by the standard.

Remote sensing data

Satellite images at both sites were obtained by the RapidEye system (BlackBridge, Berlin, Germany), which consist of five identical satellites equipped with a Jena Spaceborne Scanner JSS 56 sensor with a ground sampling distance (nadir) of 6.5 m and a pixel size (orthorectified) of 5 m. Each sensor is able to collect image data in five distinct bands of the electromagnetic spectrum: blue (440-510 nm), green (520-590 nm), red (630-730 nm), red-edge (690-730 nm) and near-infrared (NIR) (760-850 nm). Remotely sensed data was acquired for a total of seven dates distributed across the crop growing season (on June 4th, June 13th, June 27th, July 11th, July 23th, August 9th and August 30th). Image data was provided and processed by FarmLogs (Ann Arbor,

MI, USA). Three different vegetation indices (NDVI, RECI, and RENDVI) were calculated from combinations of data collected over seven dates (Table 1.1). Hence, a total of 21 (7 dates x 3 vegetation indices) high-resolution maps (at 5 m spatial resolution) were obtained.

Ancillary vegetation indices from the Moderate Resolution Imaging Spectroradiometer (MODIS) sensors were provided by The Oak Ridge National Laboratory Distributed Active Archive Center (ORNL DAAC). Onboard of two satellites (Aqua and Terra) with a revisit period of one to two days, these Hyper-Spectral sensors collect data in 36 different bands. Part of the MODIS Land Products, MOD13Q1 consists on the EVI index (ORNL DAAC, 2008). Data is released every 16-day composite periods at 250-meter spatial resolution. The MOD13Q1 image extent covered both sites for the same mosaic. The EVI was utilized given its high sensitivity over dense maize vegetation conditions and less interference of the soil background (Table 1.1). Imagery were obtained every 16 days for the 2015, resulting in a total of 21 images.

Table 1.1 Vegetation Indices evaluated in the study.

Index†	Formulation‡	Source	Resolution	Reference
NDVI	$\frac{NIR - Red}{NIR + Red}$	RapidEye	5 m	(Rouse et al., 1974)
RECI	$\frac{NIR}{Red\_edge} - 1$	RapidEye	5 m	(Gitelson and Merzlyak, 1994; Gitelson and Merzlyak, 1997)
RENDVI	$\frac{NIR - Red\_edge}{NIR + Red\_edge}$	RapidEye	5 m	(Delegido et al., 2013)
EVI	$2.5 * \frac{NIR - Red}{1 + NIR + 6 * Red - 7.5 * Blue}$	MODIS	250 m	(Huete et al., 1999)

† NDVI, Normalized Difference Vegetation Index; RECI, Red Edge Chlorophyll Index; RENDVI, Red Edge Normalized Difference Vegetation Index; EVI, Enhanced Vegetation Index

‡ The NDVI, RECI and RENDVI formulation names NIR, Red, Red edge refers to RapidEye's band 5 (760 – 850 nm), band 3 (630 – 685 nm) and band 4 (690 – 730 nm), respectively. The EVI formulation names NIR, Red, Blue refers to MODIS's band 2 (841 – 876 nm), band 1 (620 – 670 nm) and band 3 (459-479 nm), respectively.

Crop yield data

Both sites were harvested at maize physiological maturity. At Site I, aboveground maize biomass was harvested by hand around the neutron probe locations. At Site II, maize was harvested with a six-row CASE 1660 Combine, which was equipped with a yield sensor and GPS to measure spatial distribution of grain yield at Site II. The GPS unit used was Real Time Kinematic (RTK) technology enabled, with a high precision (maximum error of 2.54 cm). Yield map data was cleaned and processed by Connected Farm (a division of Trimble Navigation Limited). Additional processing to obtain yield values for the specific NP locations was also performed. All Geographic Information System analysis and data processing were performed using ArcMap 10.2.2 and MapInfo 7.0 with the FarmGPS 1.56 toolbox.

Statistical analysis

Data analysis was performed using the R statistical software (R Core Team, 2016). Tillage treatments at Site II were tested for possible effects on maize yield using the "ANOVA" function (analysis of variance) of the R package "car" (John Fox and Sanford Weisberg, 2011). Correlation analysis (Pearson's Correlation with p value = 0.05) was performed to study the relationship between SWC, remote sensing data, and yield values. Further, polynomial models were tested given the quadratic relationship between SWC and yield shown in the literature (Andrade and Sadras, 2000). Coefficient of determination of the quadratic relationship between SWC and maize yield was obtained by fitting polynomial models to the SWC values against yield using the "poly" function, R package "stats" (R Core Team, 2016). Regression, analysis of variance, and analysis of covariance were also performed by fitting linear models to assess maize yield using SWC, and SWC coupled with remote sensing data. Automated model selection was performed with the

"dredge" function, R package "MuMIn" (Kamil Barton, 2016), which generated a list of all possible models sorted by explanatory power. Given the ratio of the sample size to the number of predictors was less than 40, the corrected version of the Akaike Information Criteria (AICc) guided selection of the preferred model (Burnham and Anderson, 2003).Both methods measure how well the models fit the same data, but the "corrected version" adjusts for finite sample sizes. In other words, AICc is essentially AIC with a greater penalty for extra parameters. Burnham and Anderson (2003) gave a detailed description of AIC usage for comparison of multiple models. Comparison of full and simpler models for significant differences were executed using the "ANOVA" function from the base R package (p value = 0.05).

Best dates model

Automated model selection computes every possible predictors combination (soil water measurement for each date in this case) to estimate the response variable. Therefore, due to restrictions in the number of degrees of freedom for modeling, filtering the available dates was necessary. Most relevant dates from the single correlation output were used for further modeling. Likewise, to decrease the number of predictors and increase the statistical power, only linear regression models were included. Automated model selection was performed for each of the five depths and the for the average of the entire soil profile, in search for the more frequents dates.

Best depth model

Knowing the depth that best explains maize yield would be of interest for situations where additional depth monitored by soil water sensors to install translates into additional cost. It is notably the case for measuring soil moisture using time-domain reflectometer probes or

tensiometers. For that purpose, two different methods to test which depth better explained the maize yield were implemented.

Best depth for each date model:

For each of the most relevant date, automated model selection was performed using the depths as independent variables. Most important dates definition criterion was the same as in the "best dates model", filtering by significant correlation with yield.

Best depth including all dates model:

The r^2 values were calculated for each depth including only the most relevant dates. The purpose was to compare full models for each depth. The full models consisted in obtaining the models showing the total explanatory power reached by each depth including the same dates as predictors, therefore, a fair method to make comparisons.

Imagery model

Vegetation indices could be used to estimate spatial variability in biomass produced across a field, hence could be hypothesized that vegetation indices have potential to differentiate plant's soil water uptake capability across a field. Automated model selection was used to test inclusion of vegetation indices as explanatory variables to the previous SWC "best dates model". Only significant NP dates identified in "best dates model" analysis were used for further improvement by inclusion of an "imagery model", i.e., incorporating vegetation indices to the model. If no NP dates were found significant in "best dates model", no further analysis were conducted for this site. For the six imagery available dates, one index at a time was included with the average soil water content for depths down to 150 cm (mean of the entire profile) to assess yield.

RESULTS AND DISCUSSION

Optimal time and depth of soil water content to assess maize grain yield

Maize tasseling was observed around August 8th (DOY 220) and July 24th (DOY 205) at Site I and II respectively. This difference (about 15 days) in tasseling time could be attributed to a difference in planting date of May 28th and April 30th for Site I and II, respectively. For Site I, mean yield value was 14.5 Mg ha^{-1} and ranged from 11.2 Mg ha^{-1} to 15.8 Mg ha^{-1}. Neutron count ratio (NCR) ranged from 1.10 to 1.97 across all dates and depths. The average yield at Site II was 12.3 Mg ha^{-1} and ranged from 11.5 Mg ha^{-1} to 13.4 Mg ha^{-1}. The NCR ranged from 0.20 to 2.10. Results from ANOVA tests showed that tillage systems at Site II did not have a significant effect on the maize yield (p value < 0.05). Therefore, tillage was not taken into account for further analysis. Pearson's Correlation was calculated between NCR and yield values (See Appendix A). Polynomial transformation of the NCR values improved the explanation of the yield variance at Site I, but not at Site II. Multiple significant coefficients of determination (r^2) from the quadratic model between NCR readings and maize yield was observed for Site I (Table 1.2), but very few for Site II (Table 1.3). For Site II, only 7 out of 96 comparisons were significant (Table 1.3), among which four were for the highest soil depth (150 cm).

Scatterplots of the average NCR for soil depths down to 150 cm (average of full profile) against maize yield are shown for both, Sites I and II in Figure 1.5 and Figure 1.6 respectively. Site I showed an increase in yield with higher levels of water content, following a quadratic negative relationship. This indicates that yield increased with increasing NCR until it reached a yield plateau at intermediate NCR values and then, as more irrigation was applied, yield decreased. Conversely, Site II did not show a consistent trend. For the average NCR of depths down to 150 cm against yield, significant relationship between yield and NCR was only observed on DOY 169.

Table 1.2 Coefficient of determination (r^2) between neutron probe (NP) and yield for Site I at different depths and different days of the year (DOY). The r^2 was indicated when a significant (*p* value < 0.05) correlation coefficients was observed, and non-significant relationship were indicated by a hyphen (-).

	Depth							
NP DOY†	30 cm	60 cm	90 cm	120 cm	150 cm	$\bar{x}$ 30 – 60 cm	$\bar{x}$ 30 – 90 cm	$\bar{x}$ 30 – 150 cm
170	-	-	-	-	-	-	-	-
175	-	-	-	-	-	-	-	-
177	-	-	-	-	-	-	-	-
181	-	-	-	-	-	-	-	-
184	-	-	-	-	-	-	-	-
188	-	-	-	-	-	-	-	-
191	-	-	-	-	-	-	-	-
195	-	-	-	-	-	-	-	-
198	-	-	-	-	-	-	-	-
202	-	-	-	-	-	-	-	-
205	0.36	-	-	-	-	-	-	-
209	0.48	-	-	-	-	-	-	-
212	0.62	0.33	-	-	-	-	0.38	-
216	0.66	0.37	-	-	-	-	0.46	0.45
219	-	0.50	-	0.34	0.56	0.47	0.37	0.44
222	0.70	0.48	-	-	0.50	0.70	0.57	0.58
226	0.36	0.48	0.62	0.66	-	0.43	0.54	0.58
230	0.71	0.54	-	0.64	0.41	0.74	0.60	0.64
233	0.70	0.59	0.44	0.61	0.60	0.76	0.72	0.74
237	0.65	0.59	0.46	0.57	0.74	0.74	0.72	0.75
240	0.72	0.58	0.57	0.76	0.70	0.77	0.75	0.76

† Neutron probe Day of year measurement

The figure 1.6 indicates that no robust relationships existed between NCR and yield. Such an observation is quite different than that observed for Site I. It is interesting to note that the Site II of this study had an irrigation system that maintained uniform irrigation application rates for the entire field to match crop's ET and perhaps maintained a soil water content that was not limiting to the crop yield. In addition, the same soil water volumetric content under different tillage systems may also mean a different water availability for plants. The large variance in NCR values attributed to the tillage treatments at Site II may have altered the relationship between the SWC and yield values as is reflected in poor correlations presented in Table 1.3.

Table 1.3 Coefficient of determination (r^2) between neutron probe (NP) and yield for Site II at different depths and different day of the year (DOY). The r^2 was indicated when a significant (*p* value < 0.05) correlation coefficients was observed, and non-significant relationship were indicated by a hyphen (-).

	Depth							
NP DOY†	30 cm	60 cm	90 cm	120 cm	150 cm	x̄ 30 – 60 cm	x̄ 30 – 90 cm	x̄ 30 – 150 cm
159	-	-	0.38	-	-	-	-	-
169	-	-	0.34	-	-	-	-	0.34
175	-	-	-	-	-	-	-	-
182	-	-	-	-	-	-	-	-
191	-	-	-	-	-	-	-	-
204	-	-	-	-	-	-	-	-
211	-	-	-	-	-	-	-	-
224	-	-	-	-	0.43	-	-	-
232	-	-	-	-	0.54	-	-	-
258	-	-	-	-	0.64	-	-	-
265	-	-	-	-	-	-	-	-
272	-	-	-	-	0.59	-	-	-

† Neutron probe Day of year measurement

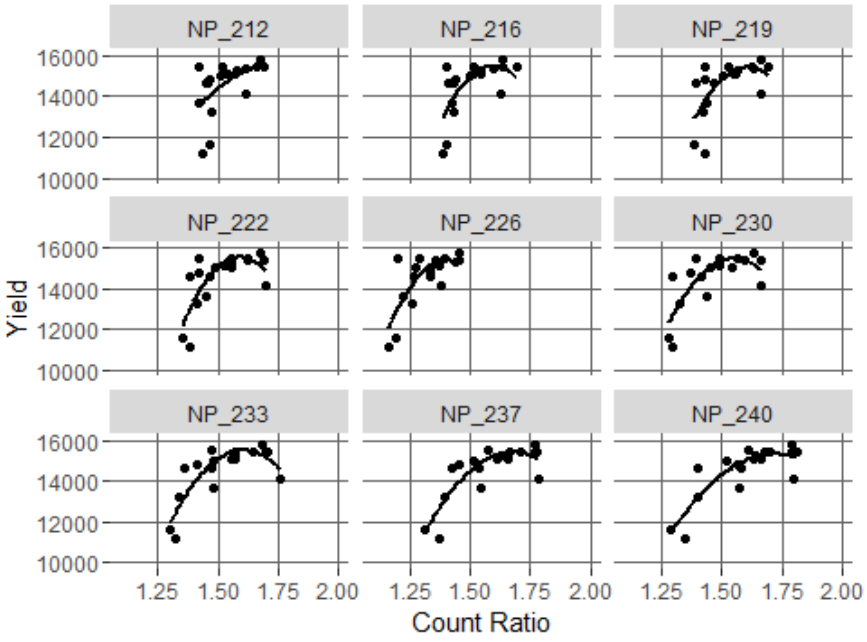

Figure 1.5. Neutron probe count ratio average for soil depths from 30 to 150 cm against yield scatterplots at Site I for the last nine dates. Regression lines represent the two-degree polynomial model line fit for each neutron probe (NP) date indicated in day of the year above each plot.

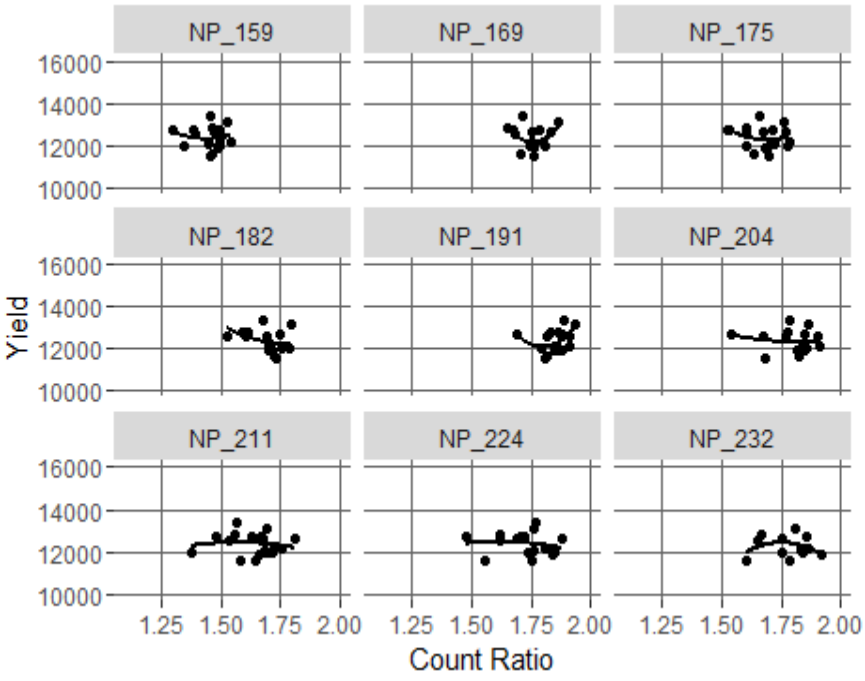

Figure 1.6. Neutron probe count ratio average for soil depths from 30 to 150 cm against yield scatterplots at Site II for the first nine dates. Regression lines represent the two-degree polynomial model line fit for each neutron probe (NP) date indicated in day of the year above each plot.

At Site I, SWC measurements acquired closer to the crop's reproductive growth stages showed a stronger correlation with yield. This seems to coincide with the critical period for irrigation around flowering when plants are more susceptible to water stress. Stronger correlations between SWC and yield validate that during this stage the impact of soil water levels on yield is highest. Even though correlation between SWC and yield was only observed for Site I, there was a notable decrease in the neutron probe reading values for both sites. This occurred one week after the start of tasseling, on DOY 226 for Site I and DOY 211 for Site II respectively, and is indicated with bold arrows in Figures 1.7 and 1.8. This decrease in the SWC could be explained by the higher water demand of crops occurring at early reproductive stages, increase in root depth from 45 cm to more than 120 cm, crop reaches maximum biomass and leaf area index (over 5 m^2/m^2 for maize),

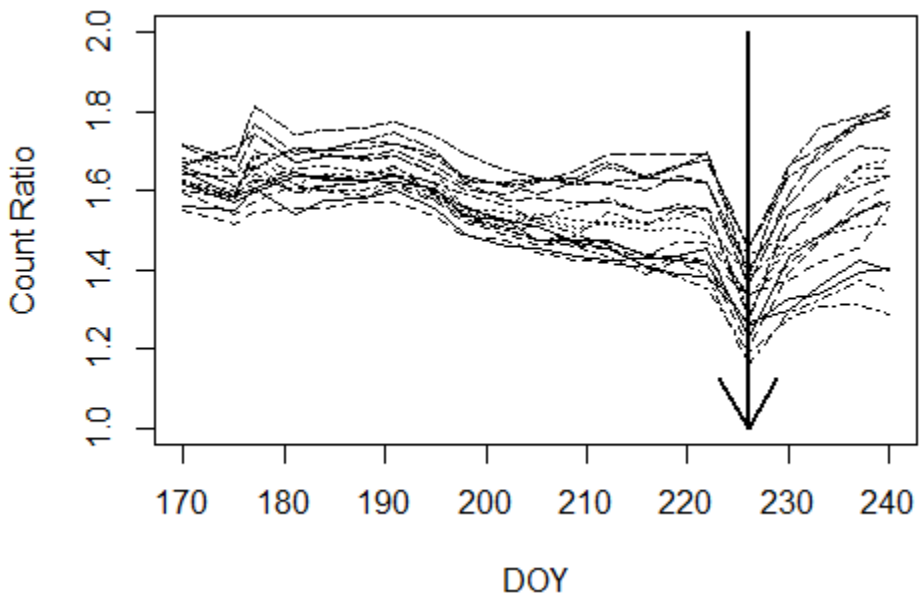

Figure 1.7. Neutron probe (NP) count ratio average for soil depths from 30 to 150 cm along the crop growing season in Day of the year (DOY) for Site I. General decrease in all NP readings after tasseling is marked with a bold arrow that occurred at August 14th (DOY 226).

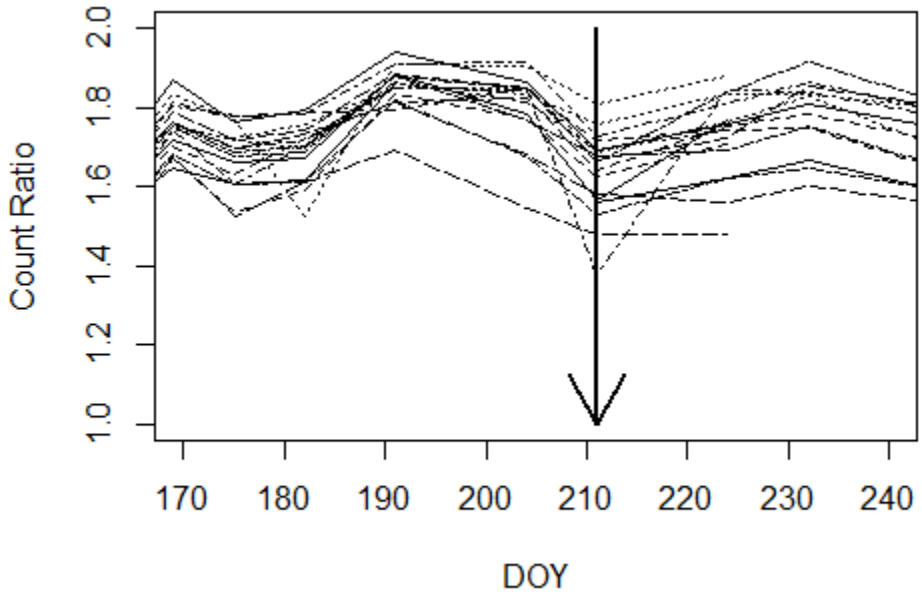

Figure 1.8. Neutron probe (NP) count ratio average for soil depth from 30 to 150 cm along the crop growing season in Day of the year (DOY) for Site II. General decrease in all NP readings after tasseling is marked with a bold arrow that occurred at July 30th (DOY 211).

and crop prepares for pollination (Kranz et al., 2008). This is especially true for maize, for which this critical period is short and more acute than most other crops (Andrade and Sadras, 2000).

Best dates model

From the coefficients of determination (Table 1.2), only the neutron probe readings from the 11 latest dates (i.e. from DOY 205 to DOY 240) were significant for Site I. Table 1.4 shows the dates selected by the best models to explain maize yield at each measurement depth. The SWC measurements from the DOY 222, 226 and 237 had the highest number of significant contribution to the model across soil depths with 3 of 5 possible appearances each. The first variable (DOY 222) coincides with the beginning of tasseling, which was observed at Site I for the first time at DOY 220. The next variable (DOY 226) coincides with a noticeable decrease in soil water reading values, when maize plant water uptake is expected to be at the maximum rate due to high demand (Kranz et al., 2008). Finally, the last variable (DOY 237) provided important information about the water status when tasseling ended. Soil moisture readings that are close in time are correlated, and thereby present collinearity and redundancy. In other words, one reading could be predicted from the previous or the following. However, DOY 222 and 226 are close in time of measurement and are included in three of the five original depth models (on the 60, 90 and 120 cm depth models). This could be explained by a marked decrease for all NP reading values on DOY 226 (Figure 1.7). For this specific date SWC readings, there was no collinearity with previous and following SWC readings and thus provided valuable information to assess yield. When calculating the best model for the integrated SWC for soil depths from 30 to 150 cm (average of the entire soil profile), automated model selection determined at DOY 219, 226 and 237 ($r^2 = 0.77$) were the best predictor

dates, including two of the three previously reported most relevant dates. No best date model was significant for Site II.

Table 1.4 Dates selected by the best model for each depth for Site I. Total number of significant contributions to the model across soil depths for each day of the year is indicated in the bottom row of the table. Most selected dates by the model are highlighted in bold.

Depth	NP DOY†											r^2	*p* value
	205	209	212	216	219	**222**	**226**	230	233	**237**	240		
30 cm	-	-	X	-	X	-	-	-	-	X	-	0.83	<0.001
60 cm	-	-	-	-	-	X	X	-	-	-	X	0.72	<0.001
90 cm	-	-	-	-	-	X	X	-	-	X	-	0.80	<0.001
120 cm	-	X	-	-	X	X	X	X	-	-	-	0.89	<0.001
150 cm	-	X	-	-	-	-	-	-	-	X	-	0.64	<0.001
Total	0	2	1	0	2	3	3	1	0	3	1	-	-

† Neutron probe Day of year measurement

The Table 1.2 presents the R-squared coefficients for Site I. The majority of the NP measurements and yield correlations were stronger (e.g. r^2= 0.72 for the average for soil depths from 30 to 150 cm) as the crop approached maturity. This may suggest that the later the SWC readings are acquired, the better they would characterize the yield variability. Even though the values on DOY 237 for the soil depths down to 150 cm were linearly correlated (r^2 = 0.53) to yield, including DOY 219 and 226 in the best date model was a significant (*p* value < 0.05) improvement (r^2 = 0.77) over the simpler model (i.e. only DOY 237 values). Results indicate that when all SWC measurement dates are available to assess maize yield, the optimal dates would coincide with crop reproductive stage such as tasseling. This was observed for correlations made with SWC measured at individual depths and also for the average SWC estimated for the entire soil profile readings.

Best depth model

Best depth for each date model:

Based on the regression analysis performed for Site I (Table 1.5), the 30 cm soil depth SWC reading appears to be the most explicative one, for 8 of 11 dates (73% of the time) when NCR was a significant predictor of maize yield. Moreover, when the superficial reading (30 cm) was selected as the only predictor of maize yield, NCR was observed to be significant for 7 of 11 reading dates (64% of the time). This follows previous observations on the coefficients of determination between NCR readings and yield (Table 1.2) for which the first 30 cm had the most frequent high values. Nevertheless, the explanatory power of the first 30 cm strongly depends on the date of acquisition, with r^2 values ranging from 0.36 (DOY 205) to 0.72 (DOY 240). Results from this study indicate that strength of the models increases as the measurements were closer to the tasseling period (i.e. DOY 222). No best soil depth model was found to be significant for Site II.

Best depth for all dates model:

The r^2 values were calculated for SWC for each soil depth with all 11 dates included as model predictors (Table 1.8). The SWC readings at 90 cm soil depth had the strongest relationship ($r^2 = 0.93$) with maize yield, followed closely by the SWC readings at the120 cm soil depth ($r^2 = 0.92$). The SWC readings at soil depths of 60 cm and 150 cm failed to describe maize yield when all available dates were added. Still, the SWC readings at 30 cm soil depth reading model returned a good fit ($r^2 = 0.85$).

In the "best soil depth for each date" approach, models were computed for each SWC reading date independently (Table 1.5), and the SWC measured at 30 cm soil-depth was found to be the best explanatory soil depth for most of the dates for which SWC was acquired. However,

when all dates are contained in the model ("best depth for all dates"), the 90 and 120 cm soil depths yielded the highest r^2 (Table 1.6). From the "best dates model" approach (Table 1.4), the most frequently chosen dates (DOY 222, DOY 226 and DOY 237) were identical to the ones selected

Table 1.5 Neutron probe readings (NP) acquired on various days of the year (DOY) at specific soil depths and corresponding coefficients of determination for the best model to assess maize yield for each date at Site I. The most often selected soil depth is highlighted in bold.

NP	Soil depth					r^2	*p* value
	30 cm	60 cm	90 cm	120 cm	150 cm		
205	X	-	-	-	-	0.30	0.02
209	X	-	-	-	-	0.41	0.00
212	X	-	X	-	-	0.60	0.00
216	X	-	-	-	-	0.59	0.00
219	-	-	-	X	-	0.34	0.01
222	X	-	-	-	-	0.63	0.00
226	-	-	-	X	-	0.59	0.00
230	-	-	X	X	-	0.67	0.00
233	X	-	-	-	-	0.59	0.00
237	X	-	-	-	-	0.65	0.00
240	X	-	-	-	-	0.71	0.00
Total	8	0	2	3	0		

† Neutron probe Day of year measurement

Table 1.6. Soil depths and corresponding coefficients of determination for the model that included all dates on which soil water content was acquired to assess maize yield at Site I. The r^2 was indicated when a significant (*p* value < 0.05) correlation coefficients was observed, and non-significant relationship were indicated by a hyphen (-).

Soil depth	r^2
30 cm	0.85
60 cm	-
90 cm	0.93
120 cm	0.92
150 cm	-

in the "best soil depth for each date" approach, models were computed for each SWC reading date independently (Table 1.5), and the SWC measured at 30 cm soil-depth was found to be the best explanatory soil depth for most of the dates for which SWC was acquired. However, when all dates

are contained in the model ("best depth for all dates"), the 90 and 120 cm soil depths yielded the highest r^2 (Table 1.6). From the "best dates model" approach (Table 1.4), the most frequently chosen dates (DOY 222, DOY 226 and DOY 237) were identical to the ones selected by 90 cm soil depth model. Such a finding suggests that under our study conditions at Site I, the 90 cm soil depth reading had the largest potential to assess maize yield, specifically during the tasseling period. It is worth pointing out that maize root depth and water requirements reach their maximums during the early reproductive stage (Kranz et al., 2008). Nevertheless, when single date models were analyzed, the 30 cm soil depth reading clearly showed to be the most important to explain maize yield for the rest of the times when SWC reading were acquired. Even though the r^2 values associated with each date varied considerably, every model showed to be statistically significant (p value < 0.05).

Significant positive correlations between SWC and maize yield were found at Site I, but not at Site II. The deeper SWC readings showed significant relationships with maize yield later during the growing season as compared to readings acquired at shallow soil depths. Similar trend was detected by Hupet and Vanclooster (2002), explaining that plant's water uptake first affects the surface soil layers. Common wisdom among farmers in Colorado (personal communication) is that ample irrigation at the beginning of the crop season builds a storage of water in the soil to be used later in the season when water requirements are highest. Our results seemed to provide scientific basis to support farmer's technique, known as soil water "banking" (Fipps, 1995). We found that generally in the crop growing season, shallow SWC was the most important parameter for the purpose of yield determination. However, at early to mid-reproductive crop growth stages when crop water demand is the highest, deeper SWC was crucial and played the largest role in the grain yield formation. Furthermore, a significant decrease in SWC of the entire profile was

observed for both sites one week after the beginning of tasseling. At Site I, this observation was part of the "best dates model". Findings from this study suggest that at the tasseling growth stage (VT) there is narrow window of perhaps five days, when the SWC of the entire profile is critical. During this period, root water uptake rate might be remarkably high and the irrigation may not able to physically keep up with the crop water consumption (Fipps, 1995). Similarly, Calviño et al. (2003) found a strong association between the water availability during the period bracketing flowering and maize yield over two rainfed fields. Therefore, deeper soil water availability might be the largest yield limiting factor at this stage, and accumulating water in the soil profile (e.g. water "banking") could be a feasible solution.

The positive correlations observed in this study between SWC and grain yield indicated that higher values of SWC resulted in higher yields, which logically agrees with previous studies that showed a strong relationship between SWC, yield and plant's transpiration (Calviño et al., 2003; Hanks, 1983). However, this was not the case for Site II. The absence of correlations between SWC and yield may be attributed to the different tillage treatments presented on the field, which could potentially shift soil water storage patterns (da Silva et al., 2001). Even though the SWC can be explained in large extent by the soil texture (Vachaud et al., 1985), the soil structure is also an important component of the water availability to plants, and could be affected by different tillage treatments (Pagliai et al., 2004). At Site I, spatial variability of the SWC started to explain maize yield from the initiation of irrigation (i.e. DOY 203) to the last NP reading. Prior to the initiation of irrigation, no significant coefficient of determination was observed (Table 1.2). These results suggest that the spatial variability in soil moisture induced by the VRI treatments was the main factor explaining the grain yield, and its impact on yield varied throughout the season. Similarly, Hanks (1983) reported variable returns on maize yield with comparable applied water,

but with different irrigation timing. Both studies indicated the strong dependency of the irrigation water efficiency, relative to the crop's growth stage.

Hupet and Vanclooster (2002) suggested an important role of maize vegetation in explaining soil water variability. Through root water uptake, plants partially controlled the temporal dynamics of the spatial SWC variability. In other words, vegetation affected the SWC patterns. However, in this study, differences in biomass yield is attributed to the soil water variability. Since all of the crop inputs (i.e. seed genetic information, fertilization dose), but irrigation, were uniform, one would logically deduce that vegetation biomass differences were spatially variable due to soil water availability across the study site. Any difference between SWC and biomass development would be due to uncontrolled factors influencing the soil water availability to plants and its growth (weed patches, diseases, etc.). Teuling and Troch (2005) reported that on a rainfed maize field, the spatial variability of water uptake by the vegetation creates additional variance. The additional variance could accentuate the relationship between the soil water variability and yield patterns. In the present study, the later statement may be part of the explanation why the higher coefficients of determination between SWC and yield values were observed later in the season. This suggest that site-specific irrigation management, targeting spatially variable AWC, would have maximum impact later in the season, when water patterns are more related to crop's yield. Likewise, Longchamps et al. (2015) suggested that variable rate irrigation may be more practical when roots are deep enough (below 45 cm) where SWC spatial patterns are more stable.

Practical implications:

In a practical sense, deeper SWC readings at early crop reproductive growth stages were the most critical measurements to characterize maize yield. Surface soil layers are the first to be

watered. Consequently, the SWC of deeper layers frequently becomes a limitation for crop yield because SWC at deeper depth are more susceptible to remain dryer than the surface layers. In addition, plant root growth may increase water depletion at deeper soil layers. Sharp and Davies (1985) tested the effect of water depletion on root growth of greenhouse maize plants grown in soil columns and found that water deficient maize plants tended to grow deeper roots, which resulted in higher water depletion at the deeper layers of soil. Djaman and Irmak (2012) observed similar results on field grown maize plants in Nebraska, where rainfed plants were the ones that extracted the most (19%) water from the 60 – 90 cm soil depth and the least (39%) from 0 – 30 cm soil depth as compared to fully irrigated plants, which extracted the least (10%) from the 60 – 90 cm depth and the most (51%) from the 0 – 30 cm depth. This suggests that dryer surface layers lead to dryer soil profile in the presence of maize plants because of the plant root growth pattern adaptation under water deficit conditions. It is thus logical to envisage a correlation in SWC at surface and deep soil layer when maize plants are growing in a field.

Our results suggest that the superficial soil layers would be the most appropriate to monitor when the purpose of soil water measurements is to ascertain crop water requirements throughout the crop growing season. This would be especially useful for soil water monitoring when only a limited number of sensors can be installed at a single soil depth. If the depth of the measurements can change during the growing season, in particular during the early-mid reproductive growth period, deeper SWC monitoring would be more appropriate for a more efficient irrigation management. When analyzed from the perspective of best dates to describe yield, complementary results were found. The dates selected in the best models were often the ones corresponding to early-mid reproductive stages. Similar dates distribution was observed when modeling for the average SWC of the full profile. Evidences suggest that when maize reaches its maximum root

depth and water requirements, the impact of the SWC on the crop yield is the most important (Howell et al., 1997). Therefore, proper irrigation management is necessary in order to establish sufficient SWC during this crucial crop period. A potential solution could be to plan irrigation management practices that replenishes soil moisture in deeper soil layers, while accounting for infiltration and other soil factors affecting the vertical movement of water through the soil profile.

Imagery model

Remote sensing was used to capture seasonal variations in crop biomass. A single EVI pixel was collected throughout the season at each study site. Due to the large spatial resolution (pixel size of 5.25 ha), soil or crop reflectance from the adjacent fields slightly influenced the EVI index values at both sites. However, given the different maize growth in time and amount compared with the neighboring fields (fields of winter wheat (*Triticum aestivum* L.)), the dynamics of the temporal biomass fluctuation were well captured. Temporal variation of biomass described by the EVI are depicted in Figures 1.9 and 1.10 for Site I and II respectively. The peak growth period occurred around DOY 237 and DOY 226 for Site I and II respectively. Since Site I was planted 28 days later than Site II, it was logical to observe such lag in crop growth stages between the two locations. Figures 1.11 and 1.12 illustrate the spatial variability in crop biomass for the two study sites as characterized by the three vegetation indices acquired near the peak growth stages. Spatial resolution of these images was 25 square meters (0.0025 ha).

For Site I, NDVI ranged from 0.11 to 0.79, RECI ranged from 0.21 to 3.53, and RENDVI ranged from 0.06 to 0.45, across all dates for which SWC was acquired. For Site II, NDVI ranged from 0.13 to 0.76, RECI ranged from 0.26 to 3.36, and RENDVI ranged from 0.08 to 0.43, across all dates for which SWC was acquired. Pearson's correlation coefficient was calculated between

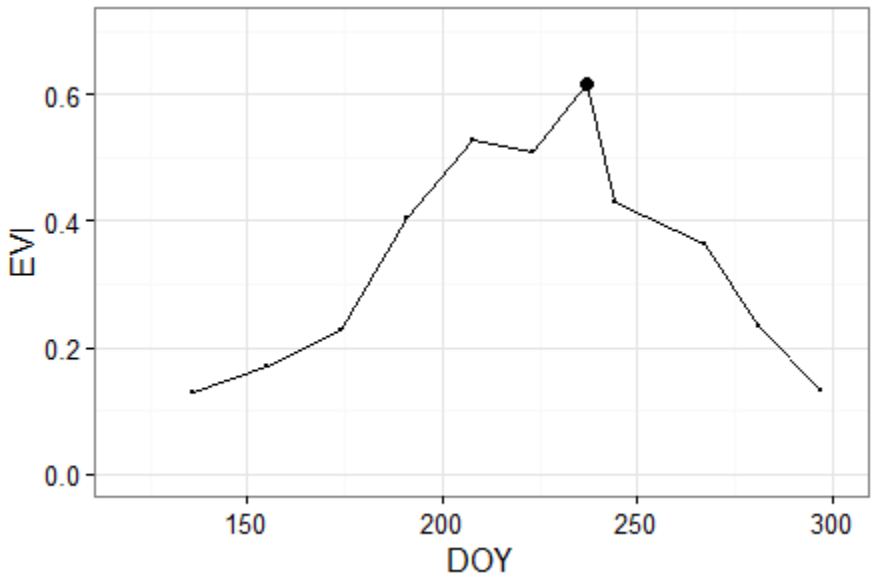

Figure 1.9. Temporal biomass variation as estimated by EVI for Site I. Peak value highlighted by a bold point (DOY 237).

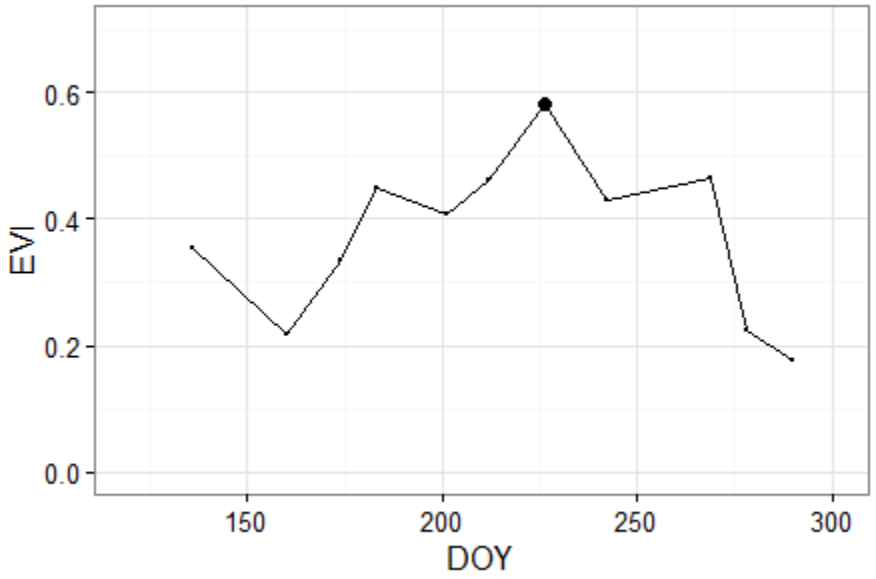

Figure 1.10. Temporal biomass variation as estimated by EVI for Site II. Peak value highlighted by a bold point (DOY 226).

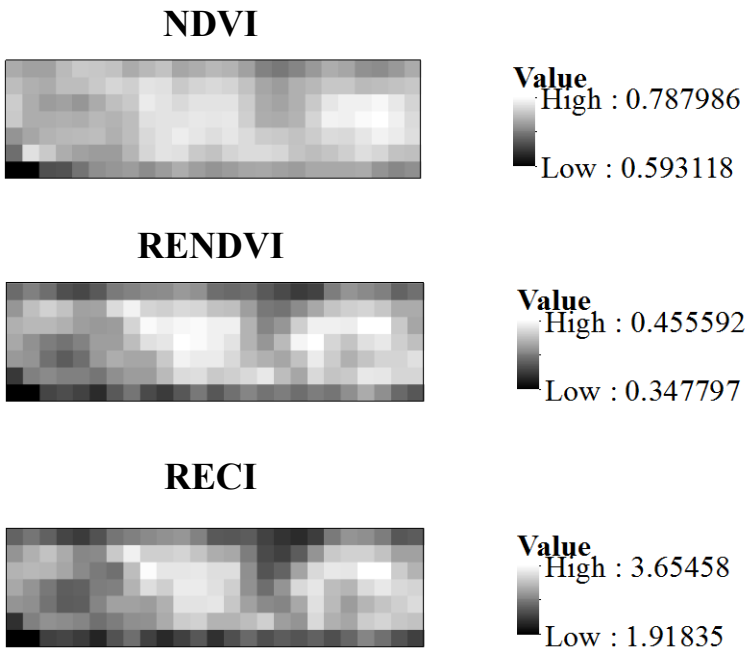

Figure 1.11. Normalized Difference Vegetation Index (NDVI), Red-edge NDVI (RENDVI) and Red-edge Chlorophyll Index (RECI) showing the spatial variability of the biomass for Day of Year 242 for Site I.

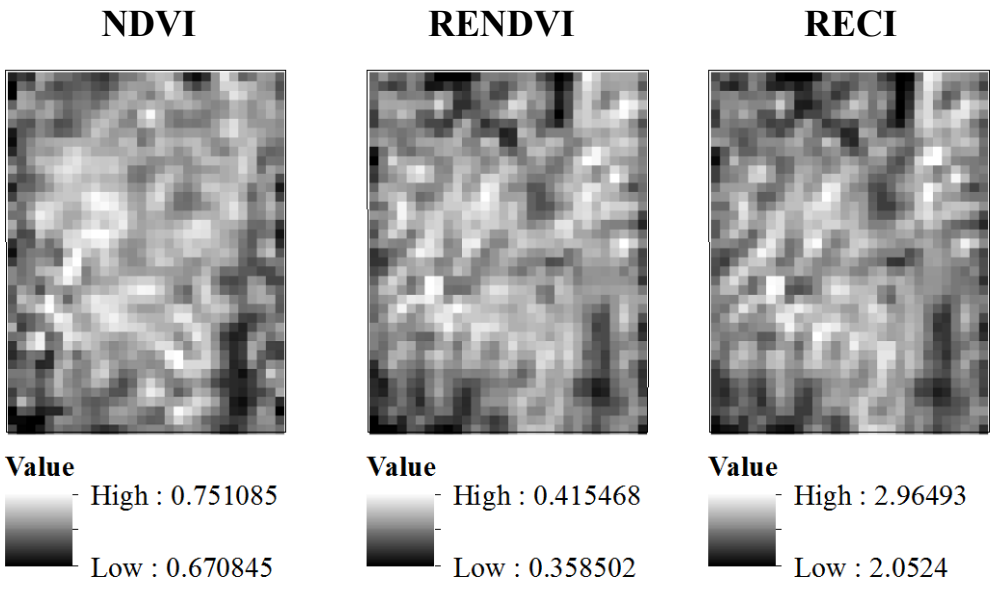

Figure 1.12. Normalized Difference Vegetation Index (NDVI), Red-edge NDVI (RENDVI) and Red-edge Chlorophyll Index (RECI) showing the spatial variability of the biomass for Day of Year 242 for Site II.

maize yield and NDVI, RECI or RENDVI for all imagery acquisition dates at Site I (Table 1.7) and II (Table 1.8). The DOY 221 was a cloudy day and the three indices had to be discarded due to a substantial cloud coverage of the ground. At Site I, RECI and RENDVI values for DOY 242 imagery (i.e. latest imagery acquired for the season) were the only ones that showed significant correlation with maize grain yield. At Site II all three indices were significant at the DOY 155, and only the RENDVI for the DOY 192.

Table 1.7. Day of Year, vegetation indices and corresponding correlations coefficient in relation to maize yield for Site I. Significant (p value < 0.05) correlation coefficients are reported and non-significant correlation are indicated with a hyphen (-).

DOY	Index†	Correlation
155	NDVI	-
	RECI	-
	RENDVI	-
164	NDVI	-
	RECI	-
	RENDVI	-
178	NDVI	-
	RECI	-
	RENDVI	-
192	NDVI	-
	RECI	-
	RENDVI	-
204	NDVI	-
	RECI	-
	RENDVI	-
242	NDVI	-
	RECI	0.72
	RENDVI	0.63

† NDVI, Normalized Difference Vegetation Index; RECI, Red-edge Chlorophyll Index; RENDVI, Red-edge Normalized Difference Vegetation Index

The significant dates identified in the best date model for the average of the entire soil profile were DOY 219, 226 and 237 for Site I, and none for Site II (neutron probe did not significantly explain yield at any date). Therefore, the imagery model was only calculated for Site I. The mentioned three NP dates were set to be consistently part of the output models, and the six available imagery dates, one index at a time, were tested for the improvement of the best date

model. Outputs from the automated model selection for NDVI, RECI and RENDVI are shown on table 1.9.

Table 1.8. Day of Year, vegetation indices and corresponding correlations coefficient in relation to maize yield for Site II. Significant (p value < 0.05) correlation coefficients are reported and non-significant correlation are indicated with a hyphen (-).

DOY	Index†	Correlation
155	NDVI	0.47
	RECI	0.59
	RENDVI	0.55
164	NDVI	-
	RECI	-
	RENDVI	-
178	NDVI	-
	RECI	-
	RENDVI	-
192	NDVI	-
	RECI	-
	RENDVI	0.47
204	NDVI	-
	RECI	-
	RENDVI	-
242	NDVI	-
	RECI	-
	RENDVI	-

† NDVI, Normalized Difference Vegetation Index; RECI, Red-edge Chlorophyll Index; RENDVI, Red-edge Normalized Difference Vegetation Index

For Site I, among the NDVI calculated for six dates, none of them was selected to improve the reduced model (SWC-only model), therefore the best model remained the same as the "best dates model" ($r^2 = 0.77$, AICc = 297.3). In agronomic terms, inclusion of NDVI in the soil water model did not improve model's ability to explain maize grain yield. On the contrary, results indicate that inclusion of NDVI values in the soil water model significantly (p value < 0.05) reduced the performance of the model. The RECI and RENDVI automated model selection included the indices of DOY 204 in both cases, and showed to be a significant (p value < 0.05) improvement to the SWC-only model. The wide range of values of RECI and sensitivity of

Table 1.9. Results from the automated model selection for the Imagery models. Selected variables of the best model for each index are indicated with an X. Numbers next to variables indicate the corresponding Day of the year.

NDVI† model										
NP¶ 219	NP 226	NP 237	NDVI 155	NDVI 164	NDVI 178	NDVI 192	NDVI 204	NDVI 242	r^2	AICc #
X	X	X	-	-	-	-	-	-	0.77	297.3

RECI‡ model										
NP 219	NP 226	NP 237	RECI 155	RECI 164	RECI 178	RECI 192	RECI 204	RECI 242	r^2	AICc
X	X	X	-	-	-	-	X	-	0.84	294.9

RENDVI§ model										
NP 219	NP 226	NP 237	RENDVI 155	RENDVI 164	RENDVI 178	RENDVI 192	RENDVI 204	RENDVI 242	r^2	AICc
X	X	X	-	-	-	-	X	-	0.83	296.4

† Normalized Difference Vegetation Index Day of year
‡ Red-edge Chlorophyll Index Day of year
§ Red-edge Normalized Difference Vegetation Index Day of year
¶ Neutron probe Day of the year
# corrected Akaike Information Criteria

RENDVI over NDVI is noticeable in Figures 1.11 and 1.12, where lower contrast is observed for the latter index. These differences in the contrast levels, wide-range and sensitivity for respective indices are a potential explanation to the better performance of these indices. The NDVI fails to explain maize biomass variability, probably due to saturation of this index at high leaf area index values as previously suggested (Myneni et al., 1997). The NDVI values have a wider range than RENDVI, however, narrower than RECI. Even though NDVI showed higher variability, its ability to describe biomass was worse than RENDVI.

For Site I, the highest correlations between vegetation indices and grain yield was on DOY 242. However, when remote sensing data was coupled with the best dates model, the best model was observed with indices for DOY 204. This shift in the optimal date of acquisition of vegetation indices to an earlier DOY may be due to a collinearity between the index of the DOY 242 and

SWC readings. To test for this possibility, correlations between NP readings from the best dates model and each vegetation index were calculated (Table 1.10).

Table 1.10. Neutron probe Day of Year, vegetation indices Day of Year and correlation between the neutron probe values averaged for entire soil profile to 150 cm and vegetation indices for Site I. Significant (p value < 0.05) correlation coefficients are indicated and non-significant correlation are indicated with a hyphen (-).

Neutron Probe	NDVI†		RECI‡		RENDVI§	
DOY	DOY 204	DOY 242	DOY 204	DOY 242	DOY 204	DOY 242
219	-	0.70	-	0.68	-	0.66
226	-	0.55	-	0.59	-	0.53
237	-	0.68	-	0.75	-	0.69

† Normalized Difference Vegetation Index
‡ Red-edge Chlorophyll Index
§ Red-edge Normalized Difference Vegetation Index

Significant correlations between neutron probe reading at DOY 219, 226 and 237 and all vegetation indices of DOY 242 were observed (Table 1.10). No significant correlation was found between neutron probe readings and vegetation indices of DOY 204 (Table 1.10). These results suggest that image acquisition later in the season would not provide new valuable information to the reduced model of yield estimation, which was based on the SWC-only. Indices acquired at DOY 242 are likely to add information already provided by the neutron probe measurements prior to DOY 242. However, this phenomenon was not observed for DOY 204, and the inclusion of RECI and RENDVI of DOY 204 outperformed the reduced model (ANOVA test, *p* value < 0.05). RECI was somewhat better than the RENDVI, with a slightly higher r^2 (0.84 and 0.83) and a smaller AICc (294.9 and 296.4). Since vegetation indices are a numerical estimate of the biomass spatial variability, they provide an estimation of the plant size, which is related to their soil water uptake capacity (Hupet and Vanclooster, 2002). Images acquired on DOY 204 and 242 corresponded to maize growth stages of V9 (9-leaf) and R3 (milk stage) at Site I. Therefore, the

earlier characterization of the biomass combined with the later soil water readings provided the best inputs for the maize yield assessment model.

As estimated by EVI at Site I, the DOY 242 corresponded to peak growth stage of the crop. Imagery acquired at the peak of biomass might be the optimal timing to characterize the relationship between the vegetation indices and yield. Biomass variability during the critical growth stage is a better yield predictor than the entire growing period (Unganai and Kogan, 1998). At this stage, the crop has acquired most of the resources that define its yield potential (Andrade and Sadras, 2000). Previous studies showed that the vegetation indices that had the highest correlation with yield are those close to the period bracketing flowering (Teal et al., 2006). Mahey et al. (1993) found a linear correlation between wheat yield and NDVI at maximum vegetation cover, and Unganai and Kogan (1998) reported that maize yield was significantly correlated with NDVI during the grain filling stage. The early correlations at Site II may perhaps be attributed to the soil background color and its association with SWC and organic matter levels, which are strongly correlated with yield (Chen et al., 2000). Figure 1.10, illustrate that the vegetation cover was minimum at DOY 160. Therefore, in addition to sparse biomass, satellite imagery would capture spatial patterns of soil organic matter, which is related to yield patterns. Bhatti et al. (1991) used Landsat Thematic Mapper images of bare soil to estimate organic matter content, and reported an excellent agreement with wheat yield. The absence of significant correlations at later crop growth stages may be due to a lack of imagery in proximity of the peak biomass growth (around DOY 226). Additionally, the tillage treatments at Site II, may have created additional unrelated variance in the relationship between vegetation indices and maize yield.

The best imagery models (built from the SWC model) to estimate yield, included vegetation indices explaining the maize biomass variability before the critical growth stages. The

first important component found in this study was the neutron probe readings acquired around the reproductive stage (DOY 219, 226 and 237), successfully described the soil water availability during the critical growth period. The second component was a RECI or RENDVI image of the crop before tasseling (DOY 204), which corresponded to the V9 growth stage of maize. At this stage, maize already had nine expanded leaves and was at the beginning of the most resource-demanding period of its lifecycle. Root depth, leaf area and water use increase rapidly during this period, reaching peak daily water use rates during pollination. A water stress during this period would have the greatest impact on the crop yield (Kranz et al., 2008). Therefore, an image acquired at V9 (9-leaf) growth stage of maize is a snapshot of the plant's potential to use all of the available resources during the upcoming critical growth period, which defines most of the grain yield. The NDVI was not able to describe the higher level of leaf area index reached by maize compared to other crops. Maize leaf structure is described as erectophile, which means that leaves have the ability to turn away from neighbors by growing in a more erect position (Maddonni et al., 2002). This characteristic allows maize to grow leaves with lower levels of overlap, then being able to intercept higher quantities of radiation per ground surface by a higher LAI. This was the case in our study, where the water provided by irrigation was sufficient enough to allow for the crop to express its potential. Likewise, Chen et al. (2006) found that fields in Western Mexico exhibited saturated NDVI values 30 days after planting. Asrar et al. (1984) reported a low sensitivity of NDVI in predicting wheat LAI above 6 $m^2 m^{-2}$ due to small changes in canopy reflectance. The better performance of RECI and RENDVI indices to explain higher biomass amounts may be due to the inclusion of the red edge band instead of the red band in the NDVI. While the former band capitalizes on the sensitivity of the vegetation red edge response to small changes in LAI, the latter is located in the main absorption and reflectance peaks (Gitelson and Merzlyak, 1994). The red

edge band is spectrally located between the red and NIR band, where the reflectance highly increases from the red portion towards the NIR plateau for green vegetation (Schuster et al., 2012). Viña et al. (2011) tested the performance of NDVI, RECI and MERIS Terrestrial Chlorophyll Index (MTCI), which also includes the red edge band, to estimate maize and soybean LAI. The RECI and MTCI exhibited more sensitivity to moderate to high LAI than the widely used NDVI. Depending on the development, growth, type of crop and the minimum requirements of the variability assessment, the widely used NDVI may not always be the best index. Indices, such as those including the red edge band in their formulation, could be a potential replacement to NDVI in scenarios where the LAI values are high and NDVI saturates.

The imagery model, which is a combination of soil water measurements with remote sensing data, provides some new insights on how to develop high frequency soil water maps. Frequent maps of the vegetation cover as estimated by remote sensing could provide useful information of the plant's water status of the entire field. Such maps could be used to address the high temporal variability previously reported in the SWC at the soil surface (Hupet and Vanclooster, 2002; Longchamps et al., 2015). Soil moisture probes could be used to acquire data on SWC variability at deeper soil depths which tends to be relatively stable (Longchamps et al., 2015). Combining crop imagery with deep soil moisture probe data may render possible the estimation of SWC of the entire root zone soil profile (0 - 100 cm). The advent of new technologies (e.g. drones, high-end generation satellites), makes high temporal and/or spatial resolution imagery of fields, accessible and easier than ever. In addition, this information could be coupled with soil water management zones, which consists of different levels of available water-holding capacities across the field (Hedley and Yule, 2009). In sum, inter and intra zones variability could be more precisely described, representing valuable information for an optimal irrigation water management

along the crop growing season. Nonetheless, investigation on how to precisely combine all the different sources of water information has to be further studied.

CONCLUSION

In this study, grain yield across a variable rate irrigated maize field was shown to be related with the SWC, as measured by NP readings. No relationship was found for the furrow irrigated field, probably due to the higher SWC not limiting maize grain yield. When water was the main factor controlling grain yield, the importance of the SWC values in space and depth varied across the crop growing season. From the correlation analysis between single NP readings and yield values, there was a trend consisting of higher correlation after tasseling. Similarly, automated model selection chose NP reading dates spread around reproductive growth stages to best assess maize grain yield. During this period, deeper SWC readings had the strongest relationship with crop yield, and may be the most limiting factor defining yield. However, if the goal is to characterize water requirements apart from the critical growth stages, the surface readings explained the maize yield most of the time. To enhance the maize yield prediction by SWC, vegetation indices were also included in an attempt to describe the plant biomass, which is highly related with the plant water uptake. The RECI and RENDVI proved to be significant additions to the SWC-only model, improving the grain yield assessment. The NDVI failed to improve the SWC-only model, suggesting that in order to account for subtle differences in biomass, the red-edge-based vegetation indices may be a better solution. Results from this study showed that different sources of information could be combined to obtain more accurate models relating soil water content and maize yield. Further, the incorporation of soil water management zones could be of great interest in order to develop site-specific models, that is, to account for spatial variability

of the soil's available water-holding capacity. Combined with newer remote sensing technologies (higher spatial and temporal resolution), an enhanced characterization of the soil water status could be performed. All sources of information together, properly integrated, could become a powerful tool for an optimal irrigation management.

REFERENCES

Andrade, F.H. and V.O. Sadras. 2000. Bases para el manejo del maíz, el girasol y la sojaINTA, Buenos Aires (Argentina). EEA Balcarce.

Ashcroft, P., J. Catt, P. Curran, J. Munden and R. Webster. 1990. The relation between reflected radiation and yield on the Broadbalk winter wheat experiment†. REMOTE SENSING 11: 1821-1836.

Asrar, G., M. Fuchs, E. Kanemasu and J. Hatfield. 1984. Estimating absorbed photosynthetic radiation and leaf area index from spectral reflectance in wheat. Agronomy journal 76: 300-306.

Bhatti, A., D. Mulla and B. Frazier. 1991. Estimation of soil properties and wheat yields on complex eroded hills using geostatistics and thematic mapper images. Remote Sensing of Environment 37: 181-191.

Biswas, A. and B.C. Si. 2011. Scales and locations of time stability of soil water storage in a hummocky landscape. Journal of Hydrology 408: 100-112.

Burnham, K.P. and D.R. Anderson. 2003. Model selection and multimodel inference: a practical information-theoretic approachSpringer Science & Business Media.

Calviño, P.A., F.H. Andrade and V.O. Sadras. 2003. Maize yield as affected by water availability, soil depth, and crop management. Agronomy Journal 95: 275-281.

Chen, F., D.E. Kissel, L.T. West and W. Adkins. 2000. Field-scale mapping of surface soil organic carbon using remotely sensed imagery. Soil Science Society of America Journal 64: 746-753.

Chen, P.-Y., G. Fedosejevs, M. Tiscareno-Lopez and J.G. Arnold. 2006. Assessment of MODIS-EVI, MODIS-NDVI and VEGETATION-NDVI composite data using agricultural measurements: an example at corn fields in western Mexico. Environmental monitoring and assessment 119: 69-82.

Condon, A., R. Richards, G. Rebetzke and G. Farquhar. 2004. Breeding for high water-use efficiency. Journal of Experimental Botany 55: 2447-2460.

da Silva, A.P., A. Nadler and B. Kay. 2001. Factors contributing to temporal stability in spatial patterns of water content in the tillage zone. Soil and Tillage Research 58: 207-218.

Delegido, J., J. Verrelst, C. Meza, J. Rivera, L. Alonso and J. Moreno. 2013. A red-edge spectral index for remote sensing estimation of green LAI over agroecosystems. European Journal of Agronomy 46: 42-52.

Djaman, K. and S. Irmak. 2012. Soil water extraction patterns and crop, irrigation, and evapotranspiration water use efficiency of maize under full and limited irrigation and rainfed settings. Transactions of the ASABE 55: 1223-1238.

Evett, S.R., R.C. Schwartz, J.A. Tolk and T.A. Howell. 2009. Soil profile water content determination: spatiotemporal variability of electromagnetic and neutron probe sensors in access tubes. Vadose Zone Journal 8: 926-941.

Famiglietti, J., J. Devereaux, C. Laymon, T. Tsegaye, P. Houser, T. Jackson, et al. 1999. Ground-based investigation of soil moisture variability within remote sensing footprints during the Southern Great Plains 1997 (SGP97) Hydrology Experiment. Water Resources Research 35.

FAO. 2015. Statistical Pocketbook World food and agriculture. FAO.

Fipps, G. 1995. Soil Moisture ManagementTexas Agricultural Extension Service, Texas A&M University System, College Station.

Gao, X., A.R. Huete, W. Ni and T. Miura. 2000. Optical–biophysical relationships of vegetation spectra without background contamination. Remote Sensing of Environment 74: 609-620.

Gao, X., P. Wu, X. Zhao, J. Wang and Y. Shi. 2014. Effects of land use on soil moisture variations in a semi- arid catchment: implications for land and agricultural water management. Land Degradation & Development 25: 163-172.
Gitelson, A. and M.N. Merzlyak. 1994. Quantitative estimation of chlorophyll-a using reflectance spectra: experiments with autumn chestnut and maple leaves. Journal of Photochemistry and Photobiology B: Biology 22: 247-252.
Gitelson, A. and M.N. Merzlyak. 1994. Spectral reflectance changes associated with autumn senescence of Aesculus hippocastanum L. and Acer platanoides L. leaves. Spectral features and relation to chlorophyll estimation. Journal of Plant Physiology 143: 286-292.
Gitelson, A.A., Y.J. Kaufman and M.N. Merzlyak. 1996. Use of a green channel in remote sensing of global vegetation from EOS-MODIS. Remote Sensing of Environment 58: 289-298.
Gitelson, A.A., Y.J. Kaufman, R. Stark and D. Rundquist. 2002. Novel algorithms for remote estimation of vegetation fraction. Remote Sensing of Environment 80: 76-87.
Gitelson, A.A. and M.N. Merzlyak. 1997. Remote estimation of chlorophyll content in higher plant leaves. International Journal of Remote Sensing 18: 2691-2697.
Gitelson, A.A., A. Viña, T.J. Arkebauer, D.C. Rundquist, G. Keydan and B. Leavitt. 2003. Remote estimation of leaf area index and green leaf biomass in maize canopies. Geophysical Research Letters 30.
Hanks, R. 1983. Yield and water-use relationships: An overview. Limitations to efficient water use in crop production: 393-411.
Hanson, B. and K. Kaita. 1997. Response of electromagnetic conductivity meter to soil salinity and soil-water content. Journal of irrigation and Drainage Engineering 123: 141-143.
Hawley, M.E., T.J. Jackson and R.H. McCuen. 1983. Surface soil moisture variation on small agricultural watersheds. Journal of Hydrology 62: 179-200.
Hedley, C.B. and I.J. Yule. 2009. Soil water status mapping and two variable-rate irrigation scenarios. Precision Agriculture 10: 342-355.
Henninger, D., G. Petersen and E. Engman. 1976. Surface soil moisture within a watershed—variations, factors influencing, and relationship to surface runoff. Soil Science Society of America Journal 40: 773-776.
Holzman, M., R. Rivas and M. Piccolo. 2014. Estimating soil moisture and the relationship with crop yield using surface temperature and vegetation index. International Journal of Applied Earth Observation and Geoinformation 28: 181-192.
Howell, T., J. Steiner, A. Schneider, S. Evett and J. Tolk. 1997. Seasonal and maximum daily evapotranspiration of irrigated winter wheat, sorghum, and corn—Southern High Plains. Transactions of the ASAE 40: 623-634.
Howell, T.A. 2001. Enhancing water use efficiency in irrigated agriculture. Agronomy journal 93: 281-289.
Huete, A., K. Didan, T. Miura, E.P. Rodriguez, X. Gao and L.G. Ferreira. 2002. Overview of the radiometric and biophysical performance of the MODIS vegetation indices. Remote sensing of environment 83: 195-213.
Huete, A., C. Justice and W. van Leeuwen. 1999. MODIS vegetation index (MOD13) algorithm theoretical basis document. Greenbelt: NASA Goddard Space Flight Centre, http://modarch. gsfc. nasa. gov/MODIS/LAND/# vegetation-indices.
Hupet, F. and M. Vanclooster. 2002. Intraseasonal dynamics of soil moisture variability within a small agricultural maize cropped field. Journal of Hydrology 261: 86-101.

Johl, S.S. 2013. Irrigation and Agricultural Development: Based on an International Expert Consultation, Baghdad, Iraq, 24 February-1 March 1979Elsevier.
Knipling, E.B. 1970. Physical and physiological basis for the reflectance of visible and near-infrared radiation from vegetation. Remote Sensing of Environment 1: 155-159.
Kranz, W.L., S. Irmak, S.J. Van Donk, C.D. Yonts and D.L. Martin. 2008. Irrigation management for corn. Neb Guide, University of Nebraska, Lincoln.
Kumar, R. and L. Silva. 1973. Light ray tracing through a leaf cross section. Applied Optics 12: 2950-2954.
Lichtenthaler, H.K. 1987. Chlorophyls and carotenoids: Pigments of photosynthetic biomembranes. Methods in enzimology 148 (34): 350-382. Academic Press.
Longchamps, L., R. Khosla, R. Reich and D. Gui. 2015. Spatial and Temporal Variability of Soil Water Content in Leveled Fields. Soil Science Society of America Journal 79: 1446-1454.
Lull, H.W. and K.G. Reinhart. 1955. Soil-moisture measurementSouthern Forest Experiment Station, Forest Service, US Forest Service.
Maddonni, G.A., M.a.E. Otegui, B. Andrieu, M. Chelle and J.J. Casal. 2002. Maize leaves turn away from neighbors. Plant Physiology 130: 1181-1189.
Mahey, R., R. Singh, S. Sidhu, R. Narang, V. Dadhwal, J. Parihar, et al. 1993. Pre-harvest state level wheat acreage estimation using IRS-IA LISS-I data in Punjab (India). International Journal of Remote Sensing 14: 1099-1106.
Martin, D., T. Smith, W. Kranz, S. Irmak, S. van Donk and J. Shanahan. 2014. Soil Water Management. Crop Insights 24.
Mohanty, B., J. Famiglietti and T. Skaggs. 2000. Evolution of soil moisture spatial structure in a mixed vegetation pixel during the Southern Great Plains 1997 (SGP97) Hydrology Experiment. Water Resources Research 36: 3675-3686.
Moore, I., G. Burch and D. Mackenzie. 1988. Topographic effects on the distribution of surface soil water and the location of ephemeral gullies. Transactions of the ASAE (USA).
Muñoz-Carpena, R., S. Shukla and K. Morgan. 2004. Field devices for monitoring soil water contentUniversity of Florida Cooperative Extension Service, Institute of Food and Agricultural Sciences, EDIS.
Myneni, R.B. and F.G. Hall. 1995. The interpretation of spectral vegetation indexes. Geoscience and Remote Sensing, IEEE Transactions on 33: 481-486.
Myneni, R.B., R. Ramakrishna, R. Nemani and S.W. Running. 1997. Estimation of global leaf area index and absorbed PAR using radiative transfer models. Geoscience and Remote Sensing, IEEE Transactions on 35: 1380-1393.
Nguy-Robertson, A., A. Gitelson, Y. Peng, A. Viña, T. Arkebauer and D. Rundquist. 2012. Green leaf area index estimation in maize and soybean: combining vegetation indices to achieve maximal sensitivity. Agronomy Journal 104: 1336-1347.
Nielsen, D.R., J.W. Biggar and K.T. Erh. 1973. Spatial variability of field-measured soil-water propertiesUniversity of California, Division of Agricultural Sciences.
Pagliai, M., N. Vignozzi and S. Pellegrini. 2004. Soil structure and the effect of management practices. Soil and Tillage Research 79: 131-143.
Pan, Y.X. and X.P. Wang. 2009. Factors controlling the spatial variability of surface soil moisture within revegetated- stabilized desert ecosystems of the Tengger Desert, Northern China. Hydrological Processes 23: 1591-1601.

Pinty, B., C. Leprieur and M.M. Verstraete. 1993. Towards a quantitative interpretation of vegetation indices Part 1: Biophysical canopy properties and classical indices. Remote Sensing Reviews 7: 127-150.
R Core Team. 2016. R: A language and environment for statistical computing. R Foundation for Statistical Computing, Vienna, Austria. 2016. ISBN 3-900051-07-0.
Rouse, J., R. Haas, J. Schell and D. Deering. 1974. Monitoring vegetation systems in the Great Plains with ERTS. NASA special publication 351: 309.
Schuster, C., M. Förster and B. Kleinschmit. 2012. Testing the red edge channel for improving land-use classifications based on high-resolution multi-spectral satellite data. International Journal of Remote Sensing 33: 5583-5599.
Sharp, R. and W. Davies. 1985. Root growth and water uptake by maize plants in drying soil. Journal of Experimental Botany 36: 1441-1456.
Sheets, K.R. and J.M. Hendrickx. 1995. Noninvasive soil water content measurement using electromagnetic induction. Water resources research 31: 2401-2409.
Steduto, P. 1996. Water use efficiency. Sustainability of Irrigated Agriculture. Springer. p. 193-209.
Steduto, P., T.C. Hsiao, D. Raes and E. Fereres. 2012. Crop yield response to waterFood and Agriculture Organization of the United Nations Rome.
Stone, J., D. Kirkham and A. Read. 1955. Soil moisture determination by a portable neutron scattering moisture meter. Soil Science Society of America Journal 19: 419-423.
Tanner, C. and T. Sinclair. 1983. Efficient water use in crop production: research or re-search? Limitations to efficient water use in crop production: 1-27.
Teal, R., B. Tubana, K. Girma, K. Freeman, D. Arnall, O. Walsh, et al. 2006. In-season prediction of corn grain yield potential using normalized difference vegetation index. Agronomy Journal 98: 1488-1494.
Teuling, A.J. and P.A. Troch. 2005. Improved understanding of soil moisture variability dynamics. Geophysical Research Letters 32.
Unganai, L.S. and F.N. Kogan. 1998. Drought monitoring and corn yield estimation in Southern Africa from AVHRR data. Remote Sensing of Environment 63: 219-232.
Vachaud, G., A. Passerat de Silans, P. Balabanis and M. Vauclin. 1985. Temporal stability of spatially measured soil water probability density function. Soil Science Society of America Journal 49: 822-828.
Viña, A., A.A. Gitelson, A.L. Nguy-Robertson and Y. Peng. 2011. Comparison of different vegetation indices for the remote assessment of green leaf area index of crops. Remote Sensing of Environment 115: 3468-3478.
Walthall, C., W. Dulaney, M. Anderson, J. Norman, H. Fang and S. Liang. 2004. A comparison of empirical and neural network approaches for estimating corn and soybean leaf area index from Landsat ETM+ imagery. Remote Sensing of Environment 92: 465-474.
Wang, L. and J.J. Qu. 2009. Satellite remote sensing applications for surface soil moisture monitoring: A review. Frontiers of Earth Science in China 3: 237-247.
Wiegand, C., A. Richardson, D. Escobar and A. Gerbermann. 1991. Vegetation indices in crop assessments. Remote Sensing of Environment 35: 105-119.

CHAPTER 2

APPARENT ELECTRICAL CONDUCTIVITY TO CHARACTERIZE SOIL WATER CONTENT

INTRODUCTION

Current water usage for the purpose of crop production is not sustainable (Postel, 2000). Water scarcity is intensifying due to more frequent drought events and increased demand of the urban and industrial areas which are exacerbating groundwater shortage (Turral et al., 2011). While 80% of the world's farmland is rainfed, almost 40% of the total supply of food and fiber is produced by irrigated agriculture (Turral et al., 2011). Of the world's total freshwater naturally available from the hydrologic cycle, almost 70% is withdrawn by irrigated agriculture (AQUASTAT, 2002). On average, the irrigation efficiency is 38% worldwide (FAO., 2002). With united efforts and use of applicable technology, it may be possible to expand one-third of the irrigated harvest area by increasing water use efficiency, which is key to prospective food security (FAO., 2002). Satisfying the increasing demand of a growing global population for food, water, and material goods while at the same time being sustainable requires new approaches to using and managing fresh water (Postel, 2000). Thereby the development and commercial incorporation of more precise, productive irrigation systems to provide higher, more stable, and sustainable yields is paramount to meet the demand of our constantly expanding population.

Inefficient water management on irrigated agricultural land has resulted in 30% of all irrigated land suffering some degree of waterlogging and salinization (FAO., 2002). Large amounts of water are wasted when applied to soil with no crops or when in excess of the uptake needed by the plants. Waterlogging and salinization alone represent a significant threat to the

world's crop productivity capacity (Alexandratos, 1995). FAO (2002) has estimated that 1-2 percent of the existing irrigated land is being degraded every year. Despite this evidence, not only will irrigated land continue to be used, but is likely to expand in area. Improving irrigation efficiency is a key goal for the future (FAO., 2002). Better irrigation practices require more accurately matching the water supply with the crop demands. This decreases the water wastage, decreases production costs, increases farm profit, and lowers undesirable effects (FAO., 2002).

Center-pivot irrigation, sometimes called circle irrigation or waterwheel, is a method of crop irrigation in which equipment rotates around a central pivot point and crops are watered using sprinklers (Omary et al., 1997). Currently, the majority of center pivot irrigation systems apply water at uniform rates to entire fields. However, most fields exhibit spatial heterogeneity for several soil characteristics that influence soil water content (SWC), such as soil type and topography (Groeteke et al., 2014). Common agricultural practice is to adjust the irrigation rate for the driest zone of the field, ensuring that no part of the field is under-irrigated (Peters et al., 2013). This results in suboptimal utilization of water on the other parts of the field, thereby wasting water.

Best irrigation practices aim to maintain SWC between field capacity (FC), where no more water can be absorbed by the soil, and management allowable depletion where SWC is half way between FC and permanent wilting point (Peters et al., 2013). If these limits are exceeded, under or over watering occurs. The outcome of both scenarios may result in stress that can reduce crop yield (Martin et al., 2014). The permanent wilting point (PWP) is the SWC level at which the plant cannot extract water and thus is subject to permanent damage. While the consequences of under-watering are well recognized, the consequences of over-watering may sometimes be underestimated. Over watering leads to leaching of mobile nutrients in soil, drainage issues,

waterlogging, and salinization of patches by evaporation of water that leaves its salt content next to the soil surface (Martin et al., 2014). Likewise, an increase in the abundance of algae (algal bloom) and aquatic plant could be generated by fertilizers washed into the groundwater or surface water, known as eutrophication (Smith et al., 1999). This phenomenon degrades freshwater systems worldwide by reducing water quality and altering ecosystem structure and function (Dodds et al., 2008). The negative consequences of under- and over-watering are well understood by the scientific community, but the way to maintain SWC at the optimal level at every location of the field still requires investigations.

Available water-holding capacity (AWC) is the maximum amount of water accessible to crops in the root zone, held between FC and PWP (Schmitz and Sourell, 2000). The FC and PWP change with soil properties, hence a precise delineation of field areas possessing homogenous characteristics (i.e. site specific management zones (Fleming et al., 1999; Khosla et al., 2002)) is key for precise irrigation management (Hedley et al., 2009). Differences in AWC require different irrigation frequencies, thus emphasizing the need for a detailed soil maps characterizing the variability in SWC to more efficiently manage irrigation. Hence there is a vast potential for improvement in water management, and more knowledge and irrigation techniques are demanded.

Site-specific management zones (SSMZ) are described as homogeneous regions within fields that have similar edaphic properties limiting crop yield. In the case of SSMZ for precision irrigation, these are the soil hydraulic properties which define the optimal soil water parameters for each region (Hedley et al., 2009). The adoption of SSMZ for irrigation has been demonstrated to be an effective practice to increase irrigation efficiency, defined as the amount of water used by the plant divided by the total amount of water applied (Evans and Sadler, 2008). Research has indicated a significant improvement in the water use per unit of dry matter produced for potatoes,

maize, and pasture with the application of SSMZ (Hedley and Yule, 2009). Sadler et al. (2002) explained the spatial response of maize to irrigation rates in fields that present different soil types. Precision Irrigation (PI) or Variable Rate Irrigation (VRI) systems provide the possibility of varying the amount of water applied across the field (Groeteke et al., 2014). Thereby, PI presents an opportunity to improve water use efficiency by targeting optimal water rates needed within each zone (SSMZ for irrigation). Furthermore, PI has the potential to lessen contamination of groundwater through a reduction of chemical leaching, increase the harvestable area by limiting waterlogging, and decrease incidence of crop diseases (Sadler et al., 2005). Hedley et al. (2009) demonstrated the potential of VRI to address the soil hydraulic spatial variability and reported water savings up to 26.3% on a 53-ha maize field with little variability (161 – 164 mm m^{-1}) in AWC. Sadler et al. (2005) reported water savings up to 50% with precision irrigation techniques.

Currently, variable rate irrigation strategies are extensively based on apparent soil electrical conductivity (EC_a) surveys (Hedley and Yule, 2009; LaRue, 2011; Martin et al., 2014). Measuring EC_a is a quick, non-invasive, and reliable measurement that is commonly employed to characterize the spatio-temporal variability of a variety of edaphic properties (Corwin and Lesch, 2005). Previous studies directly divide fields into high, medium, and low EC_a zones to assess the SWC variability (Fleming et al., 2000; Hedley et al., 2009). Commercial agricultural retailers use this approach broadly. Peralta et al. (2013) suggest that using more than three zones does not increase the available information on various soils. However, the determination of the optimal number and boundaries for the classification is not straightforward. There are complex interactions between soil factors that may affect the soil hydraulic properties, thus the number of zones definition should be tailor-made for each field.

The EC_a is influenced by a combination of physical and chemical properties including soluble salts, clay content and mineralogy, cation exchange capacity (CEC), bulk density, organic matter, soil temperature, and SWC (Corwin et al., 2003; Peralta and Costa, 2013). However, the most commonly cited factors influencing EC_a are clay, salinity, and SWC (McNeill, 1980). The spatial variability of SWC and apparent soil electrical conductivity have been extensively studied and strong correlations between both variables has been found in several cases (Brevik et al., 2006). Sheets and Hendrickx (1995) found that noninvasive electromagnetic induction is linearly related to total SWC in soils with low concentrations of dissolved electrolytes (non-saline). Also in non-saline soils, Waine et al. (2000) found that at field capacity AWC is the dominant factor influencing EC_a. The soil properties that most influence EC_a vary depending on the particular field being studied (Corwin and Lesch, 2003). Furthermore, research has shown that a single study area can include different EC_a controlling factors (Paine et al., 1998). To characterize SWC, commercial agricultural retailers are directly employing soil EC_a measurements without accounting for possible influence of other soil properties. An accurate characterization of in-field SWC spatial variability is pivotal for management of water using precision irrigation systems and potential interactions with other variables should not be ignored.

Review of the current literature indicates that the level of efficiency of SWC characterization by EC_a has not been properly studied at the field scale. We hypothesize that accounting for soil properties can improve the relationship between SWC and EC_a. The objectives of this study are (1) to assess how consistently EC_a derived management zones characterize SWC at field scale and (2) to determine whether soil properties coupled with apparent soil electrical conductivity could further improve the characterization of SWC.

MATERIALS AND METHODS

Study sites

This study was conducted during 2012 over two fields located in northeastern Colorado. Site I was located at the Agricultural Research Development & Education Center (ARDEC) on field number 3100, located in Fort Collins, CO (40°39''57.4 N, 104°59'53.1" W). This site was 4.8 hectares in size, corresponds to the south portion of a pivot irrigation system. Site II was located near Iliff, CO (40°46'05.2" N, 103°2'32.7" W) and was 11 hectares in size.

The soil at Site I is a Kim loam (1-3% slopes), fine-loamy, mixed, active, mesic Ustic Torriorthents, and Nunn clay loam (0-1% slopes), fine, smectitic, mesic Aridic Argiustolls (Soil Survey Staff, 1980). Based on corresponding soil samples, the texture was classified as sandy clay loam. The field was precision leveled (FieldLevel II, Trimble Navigation, Sunnyvale, CA) in 2012 and the slope is 0.9% in a single plane gradient. Site I was under a continuous maize (*Zea mays* L.) cropping system for the past 10 years under conventional tillage (20-cm deep disk tillage in the fall and 20-cm deep disk tillage, 30-cm deep plowing, and 10-cm deep roller arrow in the spring). In the year 2012, maize was planted on the entire field.

Soil at Site II is classified as Loveland clay loam (0-1%), fine-loamy over sandy, mixed, superactive, calcareous, mesic Fluvaquentic Endoaquolls, and Nunn clay loam (0-1%), fine, smectitic, mesic Aridic Argiustolls) (Soil Survey Staff, 1977). The texture was classified as clay loam based on the corresponding soil samples. Site II had a history of a diverse rotation, including canola (*Brassica rapa* var. Maverick), maize, soybean (*Glycine max* L.), triticale (X *Triticosecale* Wittmack), wheat (*Triticum aestivum* L.) and fallow. This field has been a research site since the year 2007. In 2012, the field was strip-tilled and planted to maize.

Colorado Agricultural Meteorological Network (CoAgMet) provided weather information. Weather stations were merely 1.5 km and 0.5 km away from the center of Site I and Site II, respectively. For the study year (2012), Colorado registered temperatures marginally above the twenty-year historic average.

For Site I, the average annual precipitation (1995-2015) was 272.9 mm. During 2012, the average annual precipitation was 148.6 mm with monthly averages below historical records. See Figure 2.1 and 2.2 for historic monthly temperatures and precipitation at Site I for the last two decades and 2012, respectively. In summary, for most of the months when the experiment was performed (April to September), weather conditions were drier than average at Site I.

For Site II, the average annual precipitation (2008-2015) was 431.3 mm. Annual rainfall for 2012 was 275.6 mm. See Figure 2.3 and 2.4 for historic monthly temperature and precipitation for the last eight years and 2012 at Site II, respectively. Overall, conditions at Site II were slightly

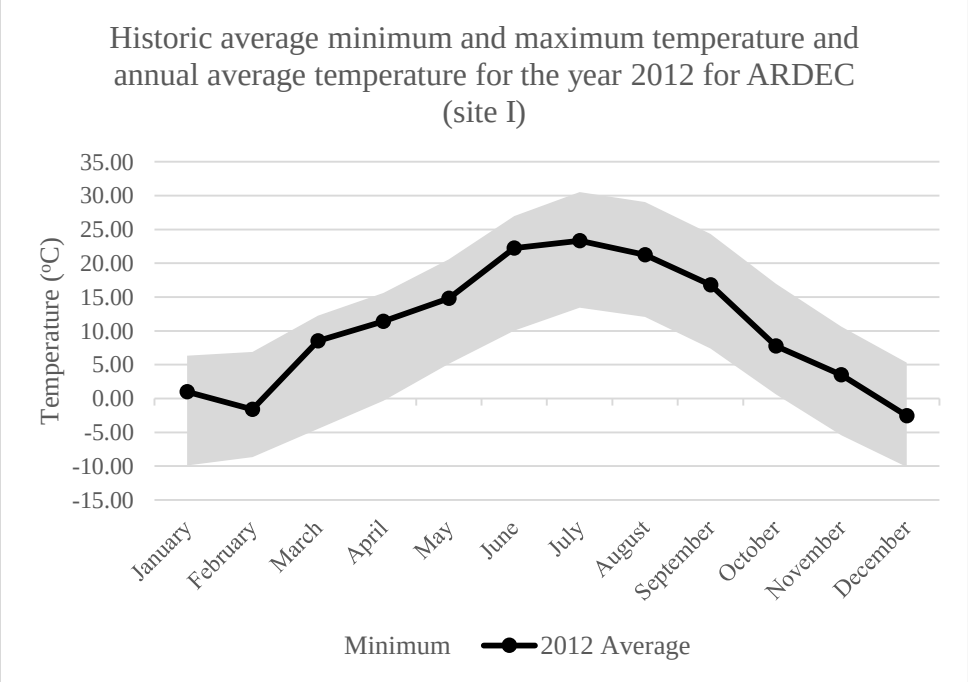

Figure 2.1. Monthly average temperature (ºC) registered at Site I location for the year 2012 (line) and monthly average of minimum and maximum temperature for the years 1995 to 2015 (gray area).

drier than normal for the period involving the experiment, with the exception of July when the monthly precipitation was 122.4 mm, 53.9 mm above average.

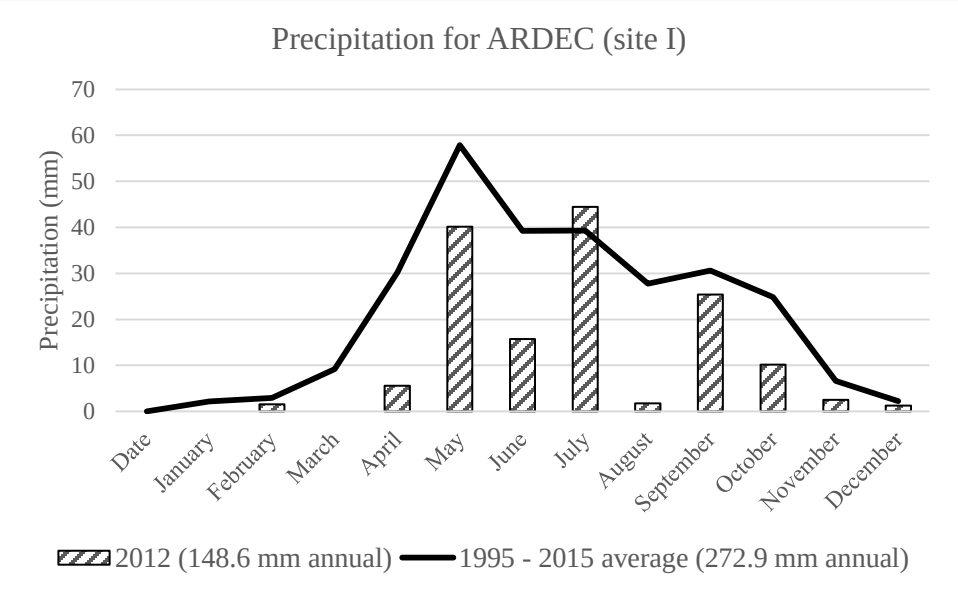

Figure 2.2. Monthly precipitation (mm) registered at Site I location for the year 2012 (bar plots) and historic monthly average precipitation recorded from 1995 to 2015 (line).

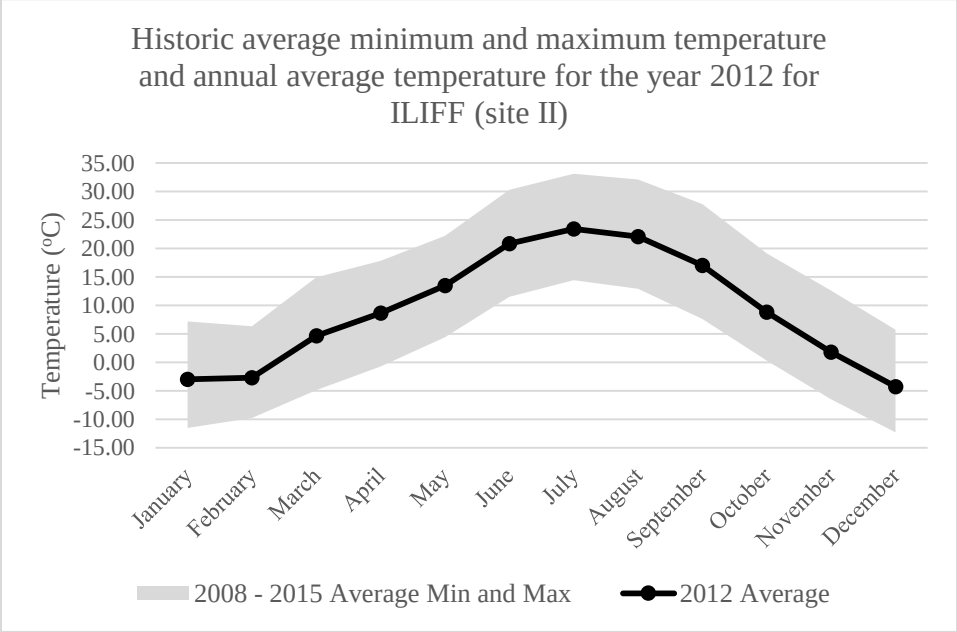

Figure 2.3. Monthly average temperature (ºC) registered at Site II location for the year 2012 (line) and monthly average of minimum and maximum temperature for the years 2008 to 2015 (gray area).

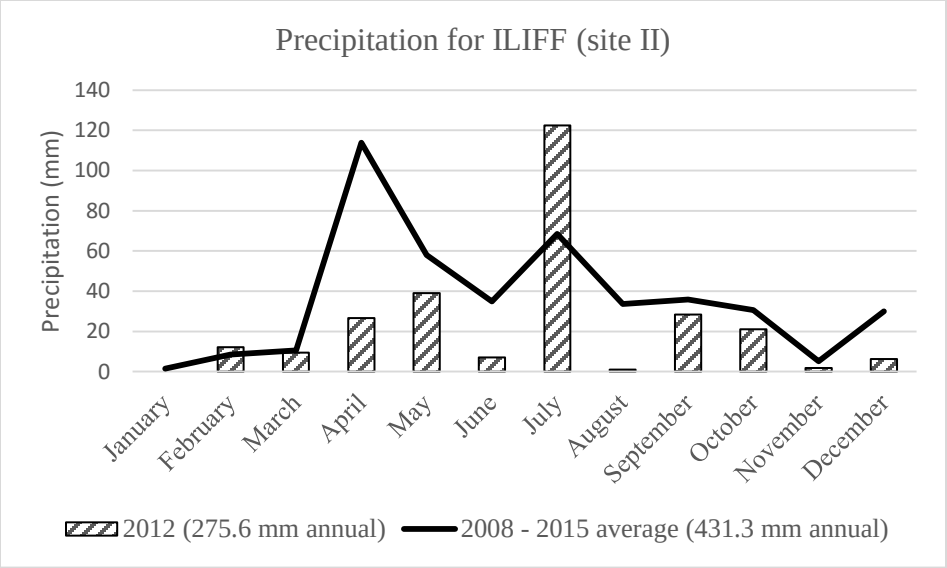

Figure 2.4. Monthly precipitation (mm) registered at Site II location for the year 2012 (bar plots), and historic monthly average precipitation recorded from 2008 to 2015 (line).

Experimental Procedure

Soil water data collection

Soil water data were collected utilizing a neutron probe (Model 503 DR Hydroprobe, CPN International, Martinez, CA). A total of 41 neutron probe access tubes were installed at Site I, distributed in a systematic unaligned (for both x and y axes) pattern (Figure 2.5). A total of 31 neutron probe access tubes were installed at Site II, also distributed in a systematic unaligned except for certain tubes that were aligned in a systematic pattern (Figure 2.6). Every access tube was geo-located using a differential-corrected Trimble™ Ag 114 global positioning system (DGPS) unit. Soil water data were collected at five soil depths (15, 45, 75, 105, and 135 cm). For Site I, data were acquired 13 times during the growing season, on a weekly basis, from June 1 to September 24, 2012. For Site II, data were acquired 9 times during the growing season, on a weekly basis, from June 14 to August 17, 2012. Counts from the probe were converted to volumetric SWC using a calibration curve. Neutron probe was calibrated against measured gravimetric soil water

and bulk density at both sites. The range of SWC was from 0.08 to 0.42 m^3 m^{-3}. The resulting calibration curve for Site I was:

$$\theta_v = -1.9863 + 3.5927 \times C_R$$

The calibration curve for Site II was:

$$\theta_v = -0.1655 + 0.2994 \times C_R$$

C_R is the ratio of neutron counts to the standard count acquired at the surface of an access tube with the probe still in the instrument. One standard count was acquired per site per acquisition date. Coefficients of the linear regression are site specific.

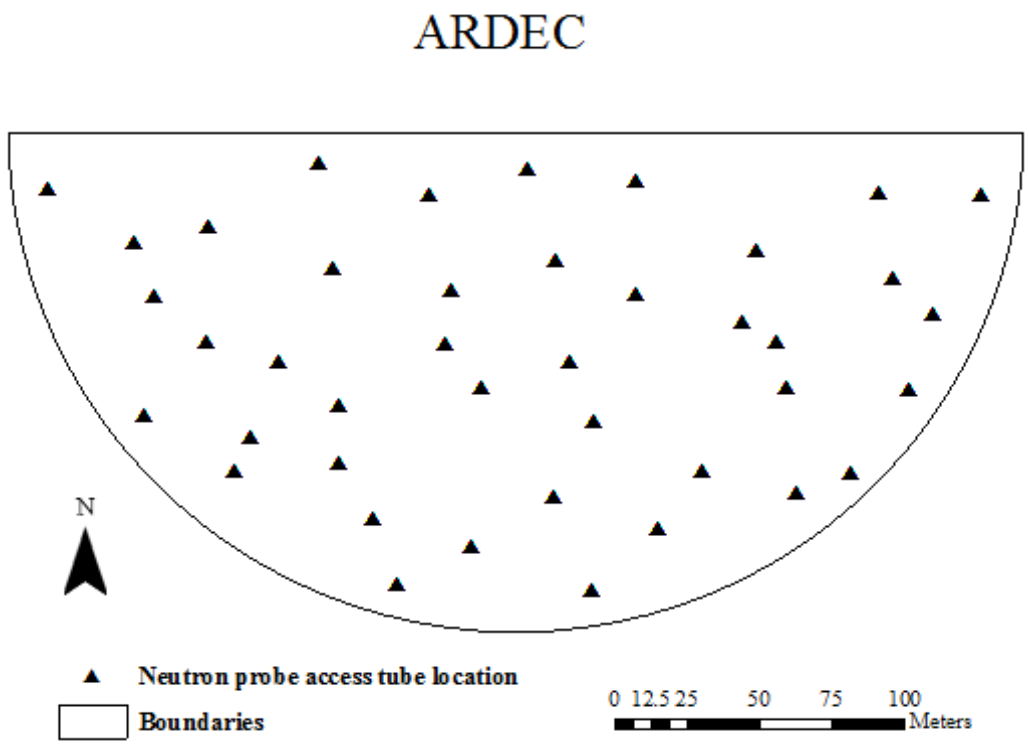

Figure 2.5. Map of ARDEC (Site I) showing the location of neutron probe access tubes.

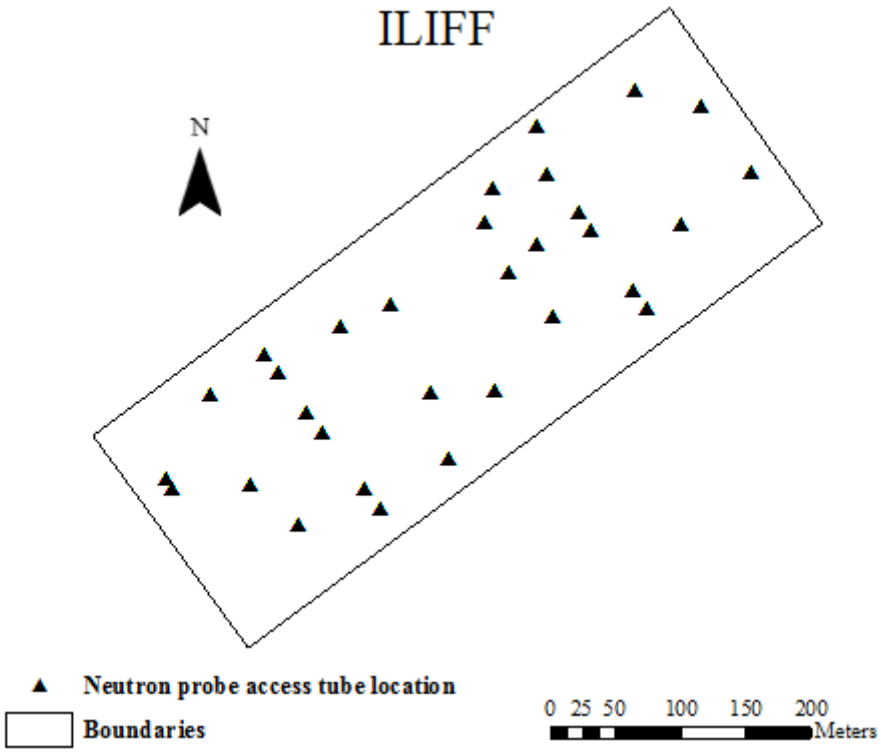

Figure 2.6. Map of ILIFF (Site II) showing the location of neutron probe access tubes.

Soil sampling and analysis

Soil samples were collected at two depths (0-20 and 20-60 cm) at both sites. Each sample location was geo-referenced with DGPS (Trimble Navigation Limited, Sunnyvale, CA). Samples consisted of five cores acquired randomly within a 2 m radius of the designated sample point. For Site I, soil samples were collected at 84 locations on April 8, 2012 and approximately evenly distributed on the entire surface under the pivot irrigation system (9.6 ha). For Site II, data were collected at 20 locations on April 30, 2012. Upon arrival at the laboratory, samples were air dried and sent to a commercial laboratory for chemical and physical analysis. Agvise laboratories (Benson, NE) performed routine soil tests and texture (clay, silt and sand). Soil tests included organic matter (%), soluble salts (dS m^{-1}) and CEC (meq $100g^{-1}$). Minimum, mean and maximum values of chemical and physical properties analyzed in each site are shown in Table 2.1.

Table 2.1. Soil samples collected at 0–60 cm soil depth with the minimum, mean and maximum values for Sand, Silt, Clay, pH, Organic matter, Soluble salts, Calcium, Magnesium and Cation Exchange Capacity.

	Depth	Descriptive	Sand	Silt	Clay	OM	Salts	CEC
	cm	statistics	----------%----------			%	dS m^{-1}	
Site I	0-60	min.	45.40	13.07	31.35	1.26	0.53	29.83
		mean	48.35	16.95	34.62	1.61	0.59	31.65
		max.	56.63	19.33	35.62	1.87	0.69	32.20
Site II	0-60	min.	33.00	20.00	33.00	2.60	0.95	27.53
		mean	37.73	23.70	38.57	3.03	1.47	32.23
		max.	46.33	25.33	43.67	3.40	1.83	35.13

Soil apparent electrical conductivity data collection

Sensor EM38MK2 (Geonics Limited., Mississauga, ON, Canada) was combined with DGPS and dataloggers mounted on an all-terrain vehicle was used to acquire high-resolution EC_a. The EM38 was in vertical mode and collected datasets at two depths. The depths corresponded to a "deep" reading at 150 cm, and a "shallow" reading at 75 cm. For maneuverability, the vehicle traveled in the direction of crop rows in a series of parallel transects spaced at 8 to 12 m intervals. At Site I, soil EC_a was mapped on June 3, 2015. The total number of observations at Site I was slightly below 2900, approximately one observation at every two meters. At Site II, soil EC_a was measured on March 20, 2013. The total number of observations was slightly over 2000 (approximately one observation every ten meters), which resulted in a roughly equidistant grid of EC_a observations.

Statistical Analysis

Preprocessing and interpolation of EC_a

The EC_a data was cleaned to remove points outside the area of interest, variations induced by traffic patterns (Corwin and Lesch, 2005), and filtered for measurement errors (outliers). Parameters for interpolation were automatically calculated for each EC_a depth and site. The EC_a

raster maps were produced with ArcGIS 10.2.2 (Environmental System Research Institute, Redlands, CA) using Empirical Bayesian Kriging, which determined optimal semi-variograms, number of neighbors, nugget, sill, and range. This kriging method uses local models to capture small scale effects instead of the common approach of using one model to fit the entire data.

EC_a classification

Management Zone Analyst (MZA) software was used to optimize the number of zones determination (Fridgen et al., 2004). The MZA provides two performance indices, called fuzziness performance index (FPI) and normalized classification entropy (NCE). These indices are calculated for a range of clusters, to assist in the determination of the number of management zones for each field. The FPI models the amount of membership sharing that occurs between classes, i.e. measures the degree of separation between zones. The NCE models the amount of disorganization created by dividing a data set into classes. The software calculates descriptive statistics of input variables before the clustering analysis. Fuzzy *c*-means (also known as *k*-means) clustering algorithm is used to partition data observations in feature space into *c* clusters (from two to six). Generally, the optimal number of clusters occurs when both FPI and NCE indices values are at a minimum with the least number of clusters used. In addition to the suggested optimal number of zones defined by MZA, three zones maps were calculated for every EC_a reading for comparison with the approach of the commercial agricultural retailers. The EC_a zone maps were obtained from the EC_a krigged values, using the Iso-Cluster Unsupervised Classification tool from the Spatial Analyst toolbox in ArcGIS 10.2.2. This tool uses *k*-means as the clustering approach. This means that the outputs from MZA are compatible with the ArcGIS software classification tool.

EC_a to assess SWC

The EC_a zones derived from the deep EC_a reading (0-1.5 m) were evaluated with the average SWC for the soil depth down to 1.35 m, and the EC_a zones derived from the shallow EC_a reading (0–0.75 m) were evaluated with the average SWC for the soil depth down to 0.75 m. Statistical analysis was performed using the R statistical software (R Core Team, 2016). Linear mixed models were used to explain the relationship between SWC values and EC_a derived management zones. The advantage of this method over the classic linear models is that it accounts for random effects in addition to the usual fixed effects (McCulloch and Neuhaus, 2001). In this study, the random effects are the individual model differences of the soil water measurements and the EC_a relationships at the different NP locations. Soil characteristics not included in the model could be adding different effects at each location, which would be repeated across dates. Linear mixed models can account for these individual differences by assuming different random intercepts for each location, and considering for the different dates as repeated measurements on the same locations. The function "lmer" from the "lme4" package (Bates et al., 2015) of the R statistical software was used to create the linear mixed models.

An analysis of variance (ANOVA) was used to determine significant differences on the soil water measurements among the different EC_a zones as treatments. ANOVA was performed with the function "anova" from the package "stats" (R Core Team, 2016). The total number of scenarios to be analyzed were the result of the combination of the different EC_a zone maps, for each EC_a reading depth, at both locations. Separation of the mean SWC among the EC_a zones was performed using least squares means with the function "lsmeans" from the "lsmeans" package (Russell V, 2016).

Soil EC_a coupled with soil properties

To evaluate any increase in the SWC estimation accuracy, krigged EC_a values (before classification) were combined with organic matter, soluble salts, cation exchange capacity and clay content as SWC predictors. Analysis included only the EC_a readings at measurement depths that were significant in the previous analysis. Optimal soil properties parameters for kriging were calculated using the same approach as with EC_a (i.e. Empirical Bayesian Kriging). Interpolation of the soil attributes was performed at Site I, but the low and clustered soil sampling density was insufficient for kriging requirements at Site II.

The "dredge" function, from the "MuMIn" package for R statistical software (Barton, 2016), was used to test addition of soil properties as explanatory variables to the krigged EC_a values. The input of this function is a linear model containing all the predictors to be tested, i.e. "full model". This approach returns linear regression models as outputs. However, as previously indicated linear models do not account for random effects as with linear mixed models. Therefore, NP measurement from a single date had to be provided as response variable. In order to increase the potential of getting a significant model, the lowest NP reading values registered at each location at any date were selected as the response for the "full model". The basis on why the above-mentioned NP readings would be the best to characterize the different zones was based on the findings by Hupet and Vanclooster (2002) and Famiglietti et al. (1999). A negative correlation between the standard deviation and the mean value of the SWC, implies that with lower SWC there is a higher contrast between NP values. Linear models were created with the function "lm" from the R package "stats" (R Core Team, 2016). The ratio of the sample size to the number of predictors was less than 40. Hence, the corrected version of the Akaike Information Criteria (AICc) guided selection of the preferred model (Burnham and Anderson, 2003). All possible combinations

of soil properties with the krigged EC_a values (locked as the base predictor), were tested for an improvement in the assessment of the neutron probe readings (direct soil water estimation). If any soil properties improved the SWC prediction, the corresponding krigged soil property (or various properties) layer was combined with the krigged EC_a layer to delineate new soil water management zones. The measured soil properties (organic matter, soluble salts, cation exchange capacity and clay content) each has a unique scale of measure, hence the ECa values along with other significant data layers were normalized prior to combination and classification process. Normalization was calculated using ArcGIS 10.2.2., and it consists of subtracting the mean and then dividing by the standard deviation.

RESULTS AND DISCUSSION

EC_a interpolated maps

At the neutron probe access tube locations in Site I, the mean value of deep EC_a was 70.92 mS m^{-1}, and ranged from 64.29 to 81.13 mS m^{-1}. The mean value of shallow EC_a was 20.49 mS m^{-1}, and ranged from 15.84 to 30.33 mS m^{-1}. Also at the neutron probe access tube locations in Site II, the mean value of deep EC_a was 37.38 mS m^{-1}, and ranged from 24.11 to 69.61 mS m^{-1}. The mean value of shallow EC_a was 24.36 mS m^{-1}, and ranged from 16.05 to 38.3 mS m^{-1}. Figure 2.7 shows krigged EC_a surface of the entire field based on the EC survey for the two depths (1.5 m and 0.75 m) at Site I and Site II. Straight lines with higher EC_a values (parallel to the shorter sides of Site II) were the result of repeated vehicle transit on those parts of the field. Corwin and Lesch (2005) found that soil compaction can induce higher conductivity values. However, all NP locations were outside of that area.

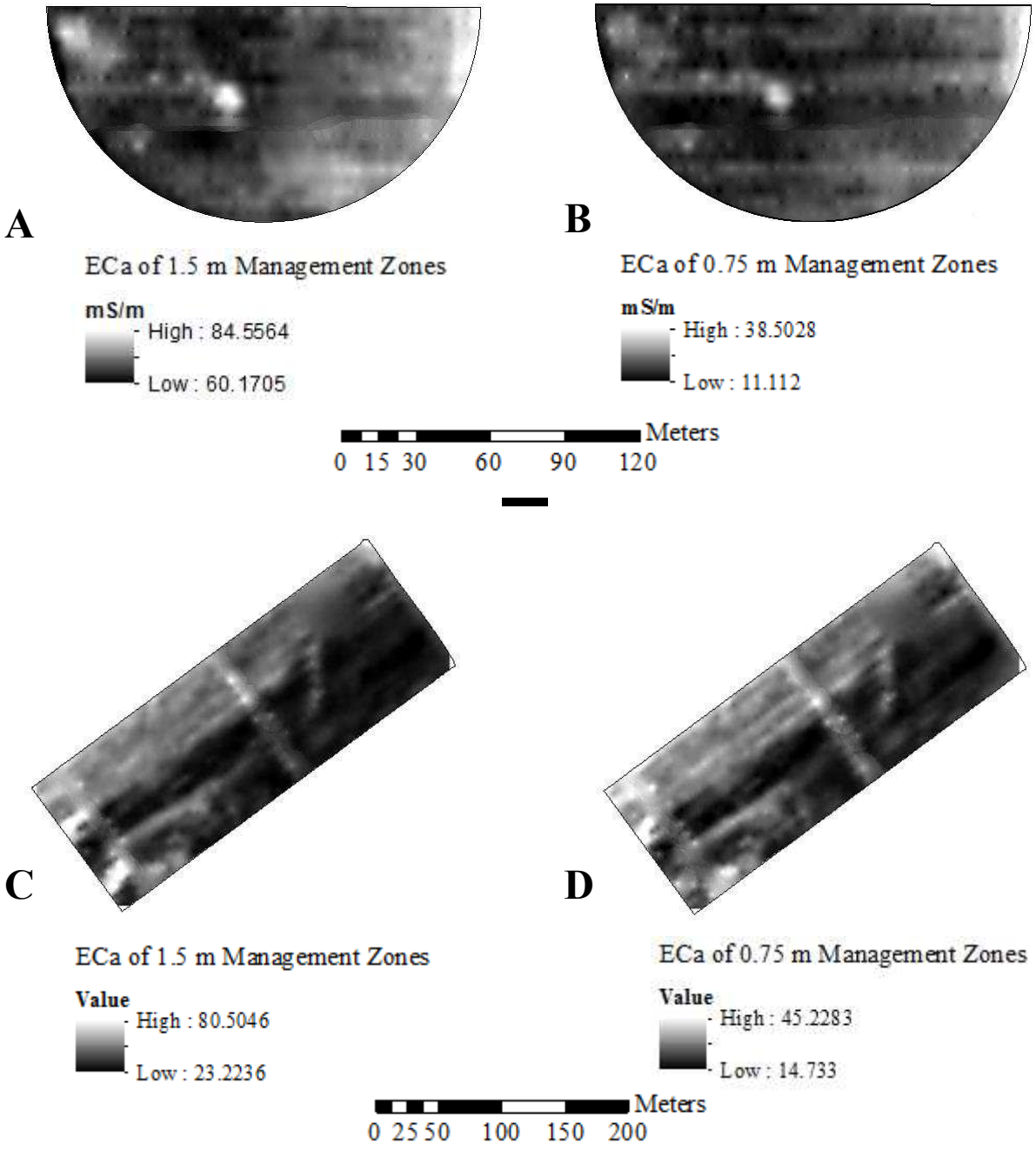

Figure 2.7. A and B represents EC_a maps of 1.5 and 0.75 m depth for Site I. C and D represents EC_a maps of 1.5 and 0.75m depth for Site II.

EC_a derived management zones maps

The MZA software was used to calculate fuzziness and entropy indices for both depths of measured EC_a at Site I (Figure 2.8 and 2.9), and Site II (Figure 2.10 and 2.11). The optimal number of zones for Site I were two and four at EC_a measurement depths of 1.5 m and 0.75 m, respectively. The optimal number of zones for Site II were two at EC_a measurement depth of 1.5 m, and from

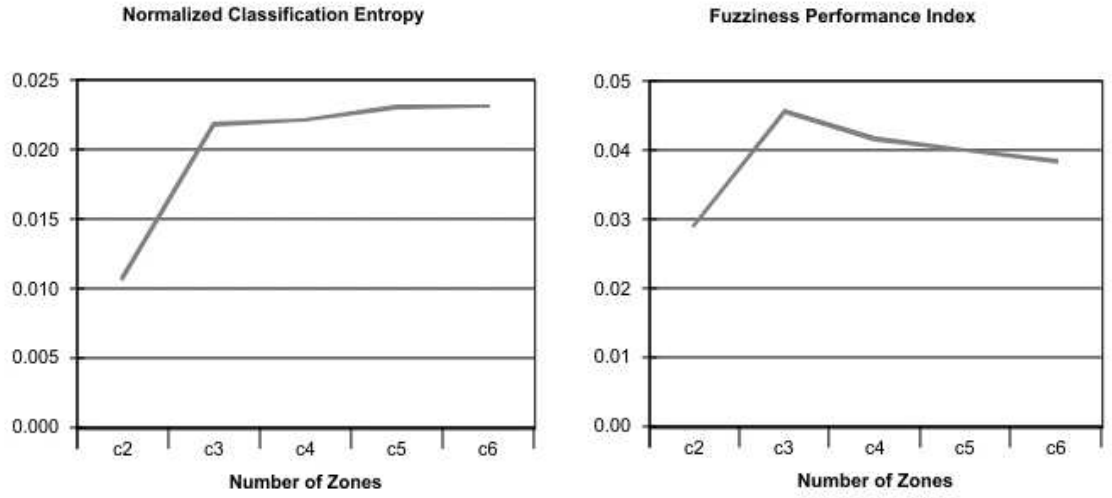

Figure 2.8. Site I MZA software output for the Normalized Classification Entropy and Fuzziness Performance Index of the EC_a of 1.5 m depth classification in two to six clusters.

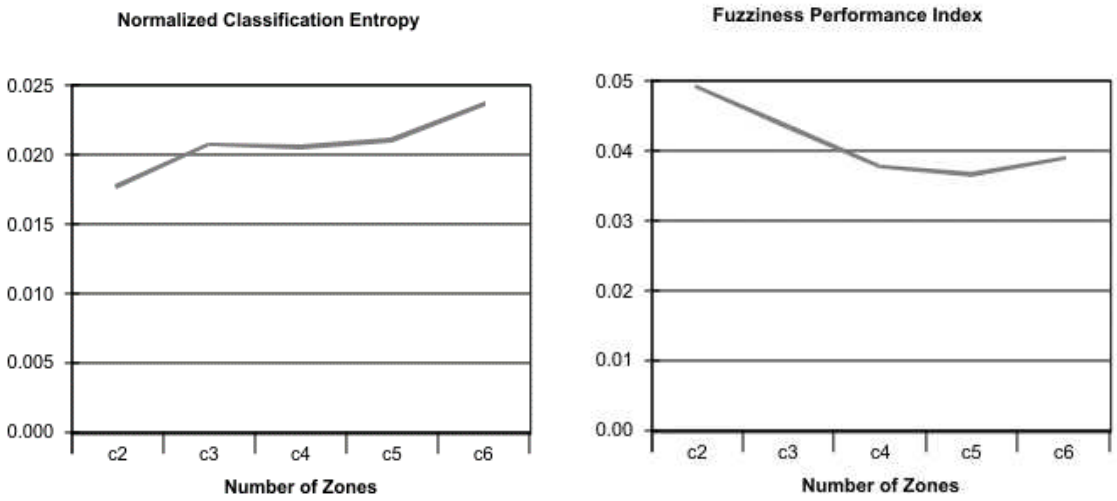

Figure 2.9. Site I MZA software output for the Normalized Classification Entropy and Fuzziness Performance Index of the EC_a of 0.75 m depth classification in two to six clusters.

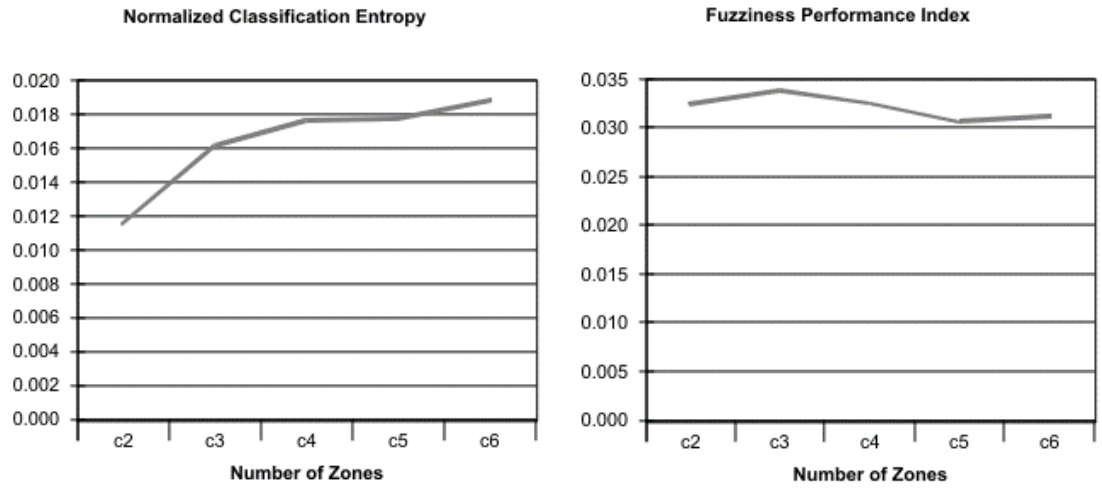

Figure 2.10 Site II MZA software output for the Normalized Classification Entropy and Fuzziness Performance Index of the EC_a of 1.5 m depth classification in two to six clusters.

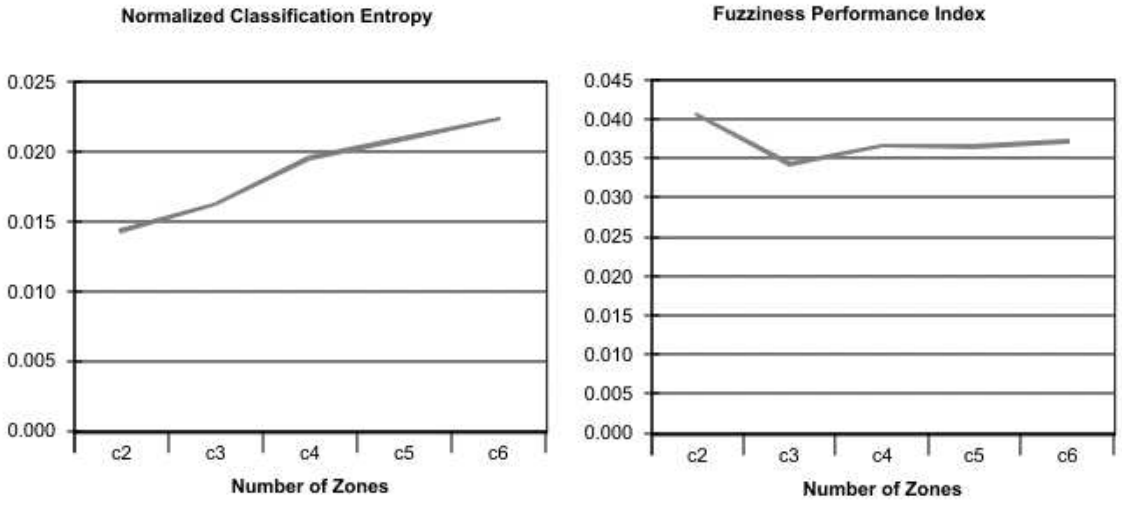

Figure 2.11. Site II MZA software output for the Normalized Classification Entropy and Fuzziness Performance Index of the EC_a of 0.75 m depth classification in two to six clusters.

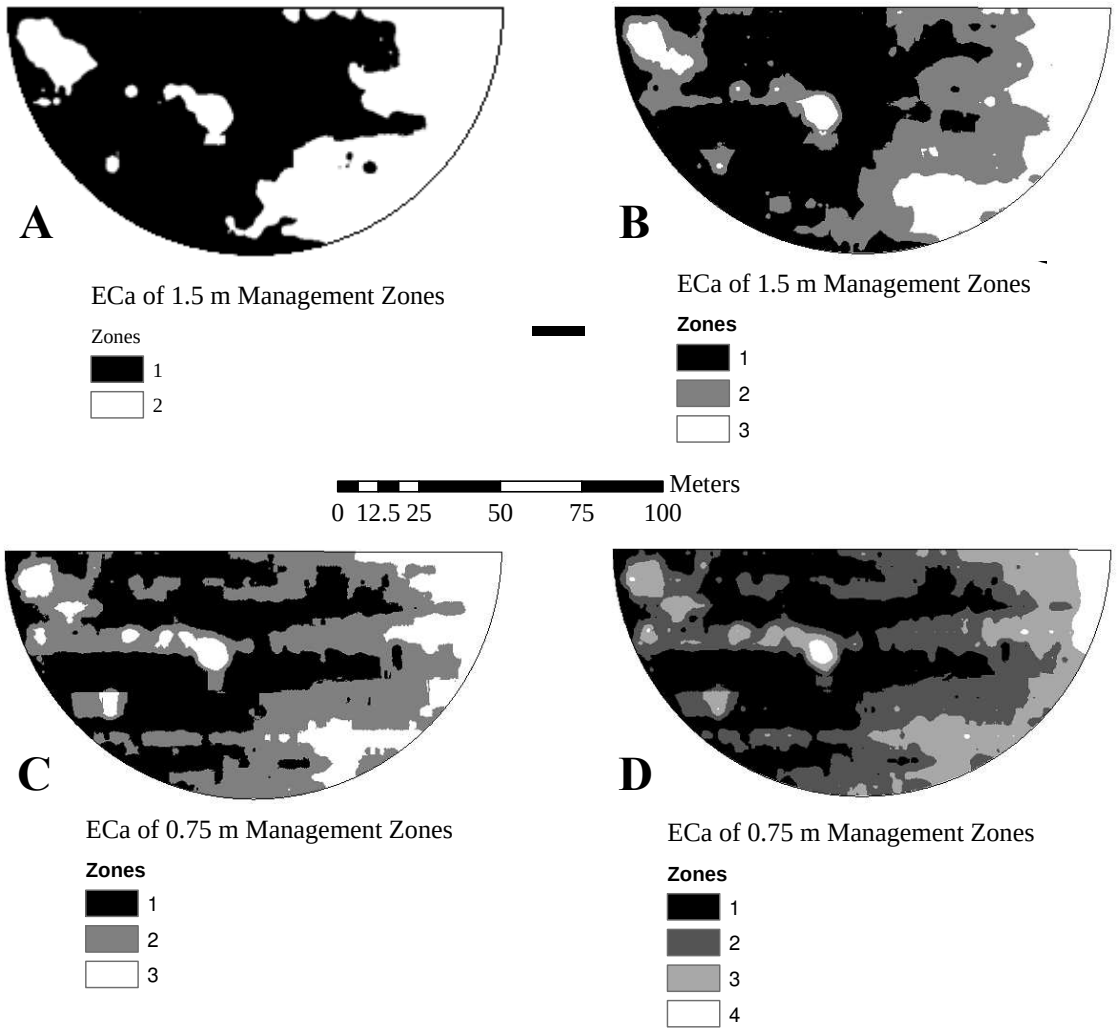

Figure 2.12. Site I management zones derived by EC_a measurements at 1.5 m soil depth presented in sub-figure A and B and zones derived by EC_a measurements at 0.75 m soil depth in sub-figure C and D.

two to three (i.e. divergent entropy and performance values) at EC_a measurement depth of 0.75 m. For EC_a measurement depth of 0.75 m, it appears that three zones may be a better option since there is a modest increase in entropy however, at the same time there is a decrease in fuzziness, as compared with that of two zones. Nonetheless, two zones were calculated based on the software recommendation to select the lowest number of zones when the sum of both indices are close. As previously mentioned, to emulate the commercial approach, three zones were also calculated for each EC_a depth. Overall, for each site and EC_a reading depth, two EC_a derived management zone

maps were calculated, thereby generating a total of eight zonal maps. Figures 2.12 and 2.13 depict EC_a derived management zones for both EC_a depths at Site I and II.

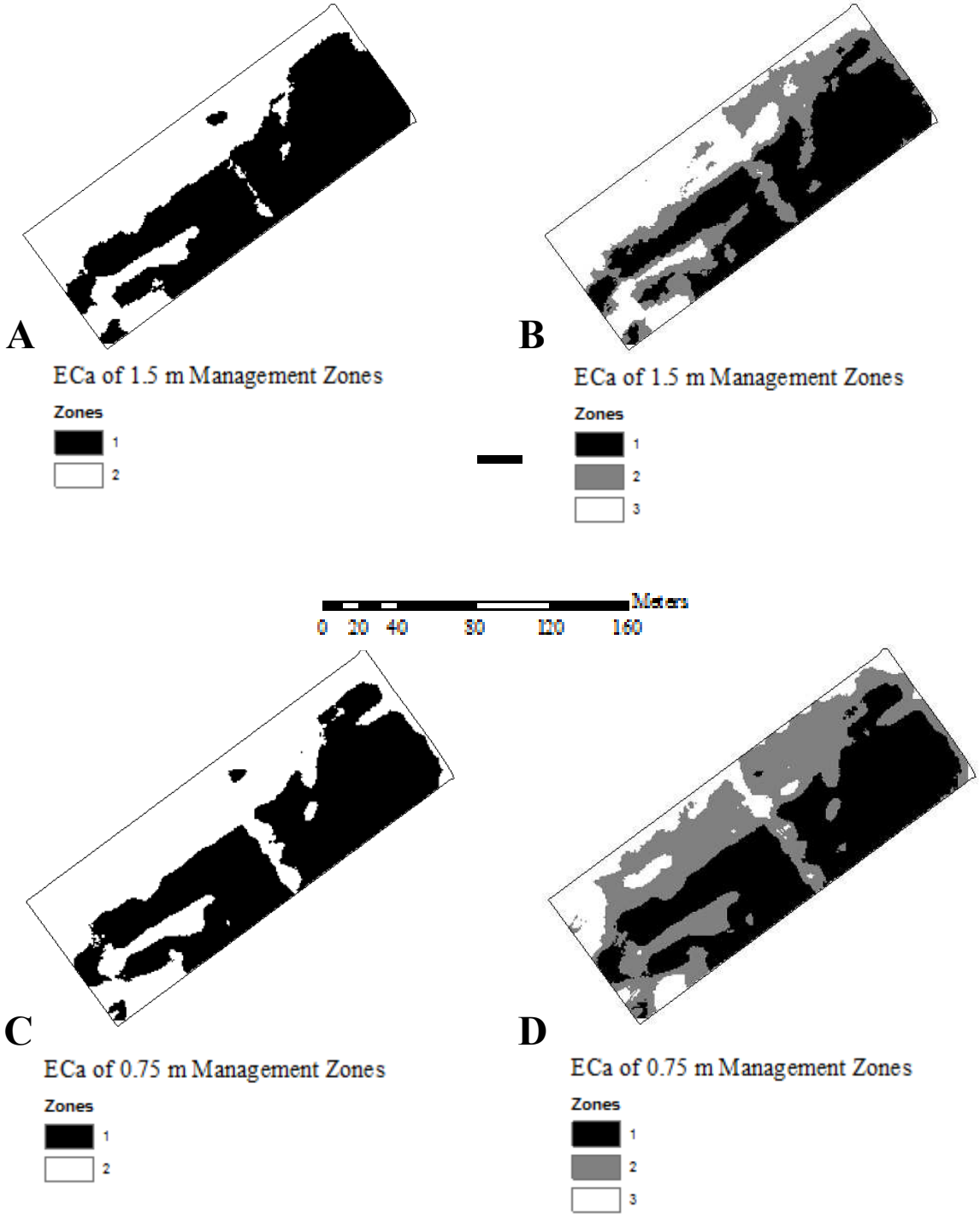

Figure 2.13. Site II management zones derived by EC_a measurements at 1.5 m soil depth presented in sub-figure A and B and zones derived by EC_a measurements at 0.75 m soil depth in sub-figure C and D.

EC_a derived management zones to assess SWC

Across all dates and depths of soil moisture measurements, the volumetric SWC ranged from 0.09 to 0.45 $m^3\ m^{-3}$ at Site I, and from 0.01 to 0.46 $m^3\ m^{-3}$ at Site II. Figure 2.14 to 2.15 show the average SWC of the different EC_a-zones for both shallow and deep EC_a measurements for Site I and II, respectively.

In order to detect statistical differences in SWC and EC_a derived zones, least-squares means of SWC across each EC_a management zones maps were calculated (p value < 0.05; Figures 2.16 and 2.17). At Site I, only the deep EC_a-zones explained differences in SWC (p value < 0.05). The two-zone map performed better than three-zone map, because when three zones were created, there was not a significant difference between zone 2 and zone 3 SWC (p value = 0.1139). At Site II, regardless of the depth of data acquisition, EC_a maps with two zones succeeded to explain SWC variations (p value < 0.05). As compared to Site I results of deep EC_a that led to the classification into three zones, similar observations were made at Site II. The creation of a third zone was not statistically different from the rest (i.e. Zone 2 with Zone 1 and 3 for the deep EC_a reading, and Zone 3 with Zone 1 and 2 for the shallow EC_a reading).

These results showed that with an inappropriate number of zones, there could be a confounded characterization of the spatial variability of SWC due to the creation of an extra management zone. The MZA-suggested quantity of zones resulted in the best SWC characterization throughout the growing season. For that reason, MZA software appears to be a useful tool to determine the number of zones to be delineated for precision irrigation purposes. Likewise, Hezarjaribi and Sourell (2007) used a similar software to successfully determine the accurate number of EC_a zones to characterize SWC.

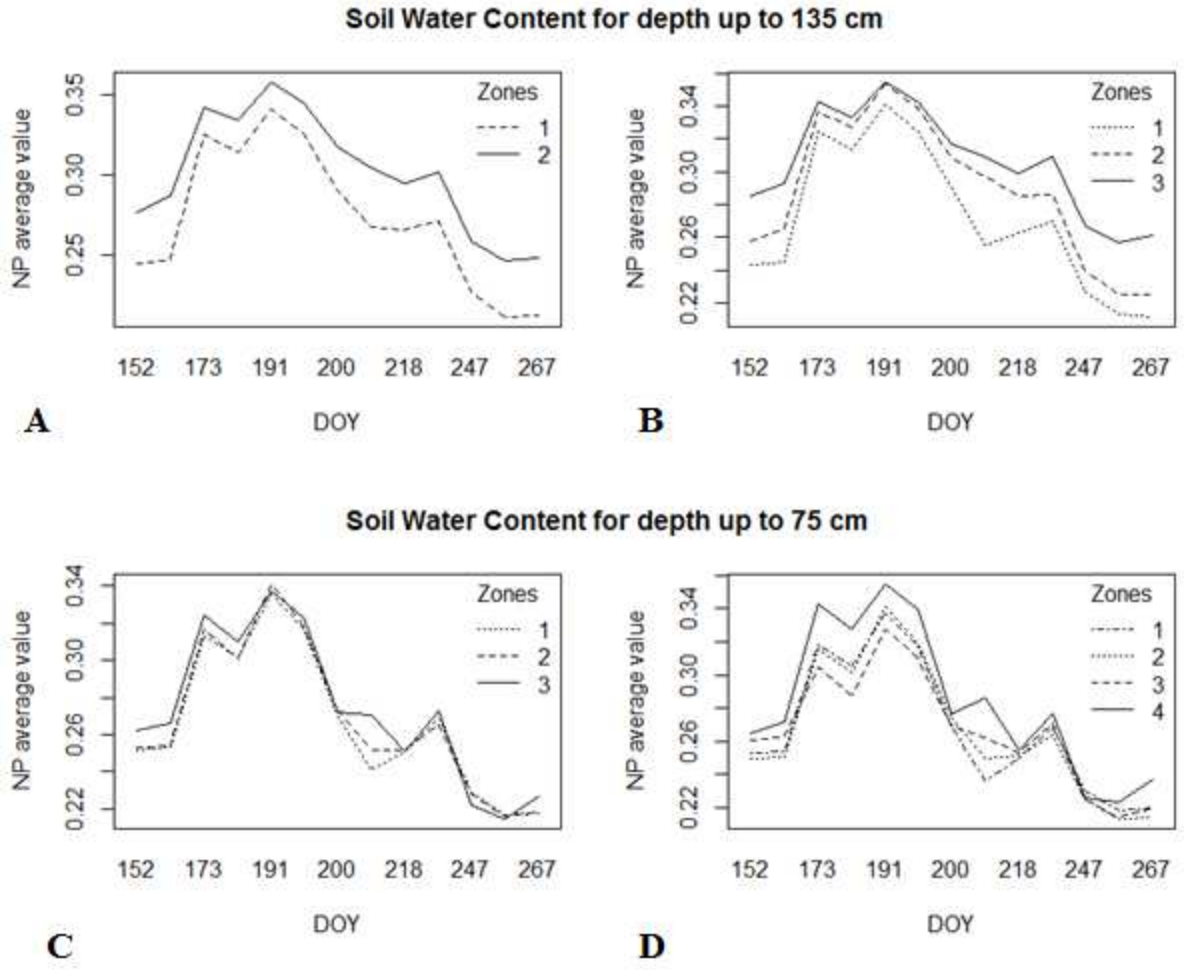

Figure 2.14. Site I temporal average SWC variation throughout the crop season for two (A) and three (B) zones of EC_a 1.5 m, and for three (C) and four (D) zones of EC_a 0.75 m.

In this study, only the deep EC_a-derived zones show significant differences in SWC at Site I, but both deep and shallow depths showed SWC differences at Site II. This indicates that there exists a field specificity for the interpretation of the EC_a and SWC relationship. At both locations, forcing the classification from two to three zones seems to create a transitional zone that overlaps values from other zones, thus not representing a logical soil water management zone. This means that values of the neutron probes within the transitional zone were similar to another zone and an

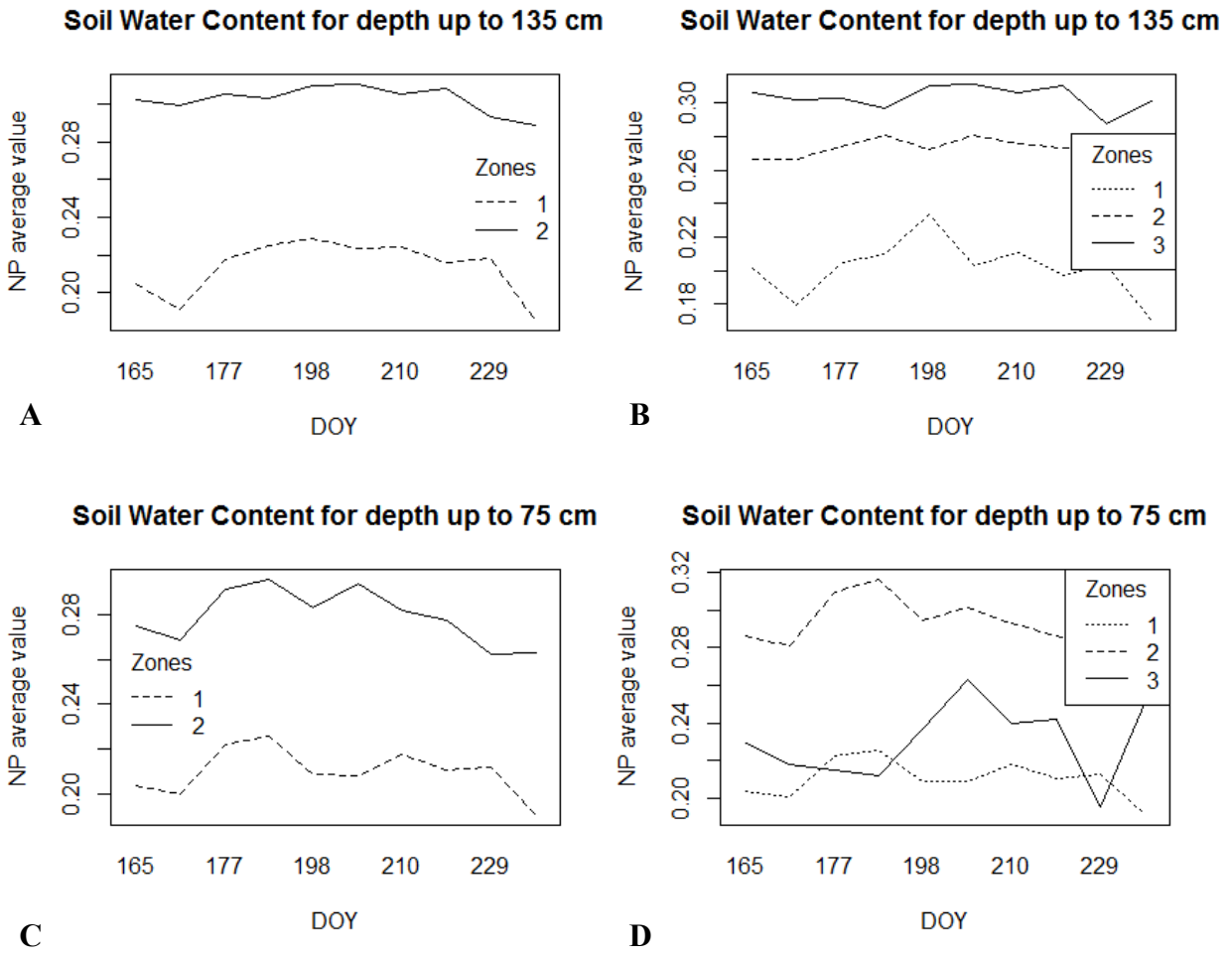

Figure 2.15. Site II temporal average SWC variation throughout the crop season for two (A) and three (B) zones of EC_a 1.5 m, and for two (C) and three (D) zones of EC_a 0.75 m.

equivalent water management for both would be more logical. Overall, the MZA-recommended number of EC_a management zones described SWC well in most cases as reflected by the successful results obtained for the deep ECa reading for Site I, and both depths at Site II. The exception to this observation was with the shallow EC_a readings at Site I, where both classifications failed to describe the variations in NP reading (Figure 2.16, EC_a of 0.75 m).

In general, the lowest quantity of zones from the shallow EC_a readings showed higher fuzziness indices values. This suggest that the shallow sensing seemed to be have higher noise (i.e. soil properties affecting EC_a other than SWC) to signal ratio compared to the deeper configuration.

Even though Hezarjaribi and Sourell (2007) also reported a higher sensitivity of the shallow EC_a measurements to near-surface material, the depth that best fitted their field was also the shallow EC_a reading. Overall, results from this study suggest that the EC_a relationship with SWC depends not only on the horizontal nature of the field characteristics, but on its variability in soil depth as well.

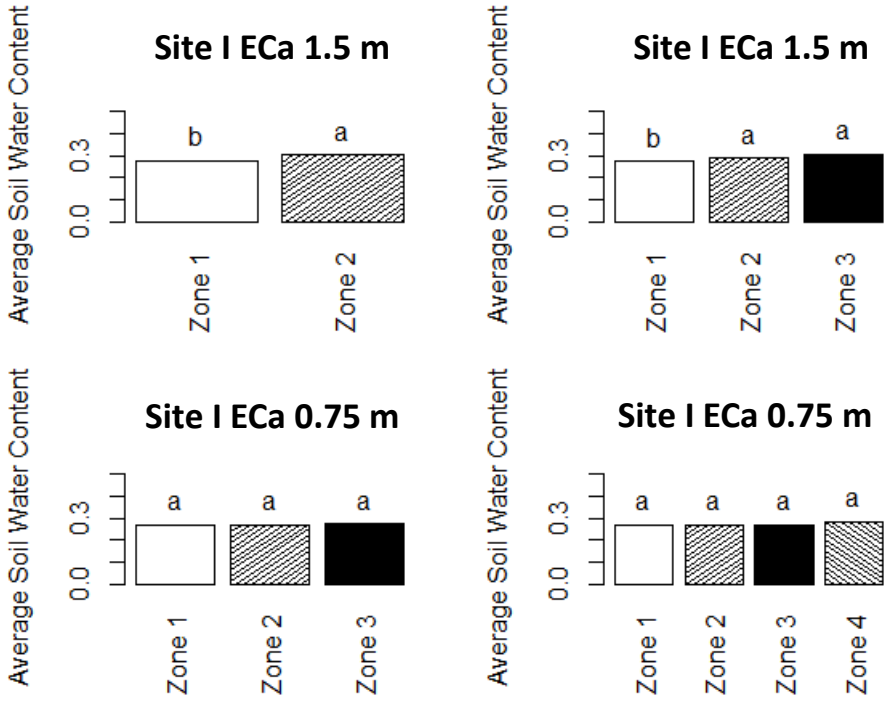

Figure 2.16. Mean SWC across EC_a derive management zones for Site I. Different letters are significantly different (p value < 0.05).

Prior studies showed significant correlation between SWC and EC_a, and the estimation of AWC using regression models (Hedley and Yule, 2009; Hezarjaribi and Sourell, 2007). Likewise, Sheets and Hendrickx (1995) demonstrated the feasibility of the EC_a simple linear models to assess SWC over time. However, review of literature indicated no previous detailed studies examining the quality of the SWC assessment by EC_a derived management zones. Results from this study

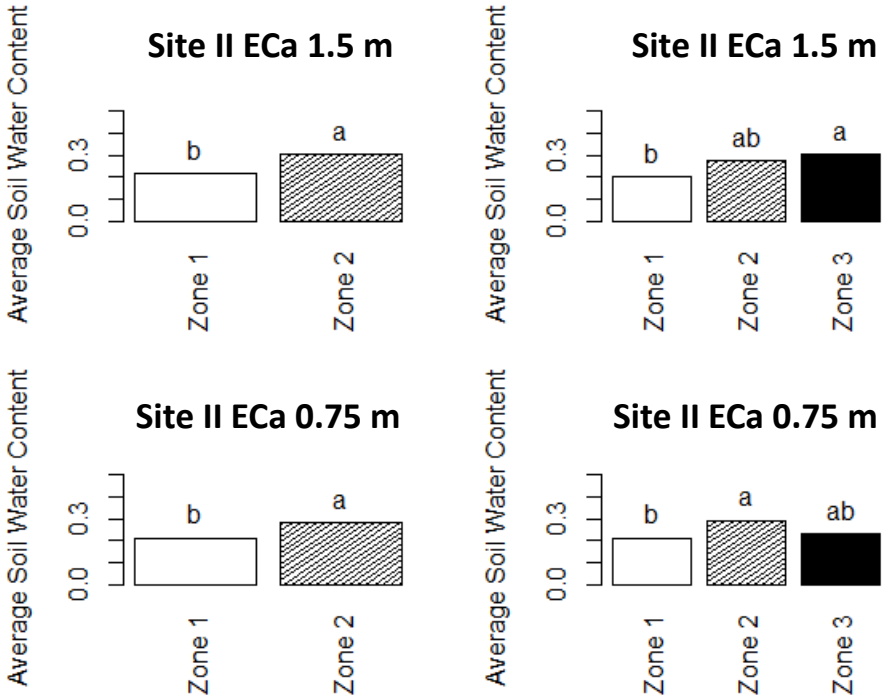

Figure 2.17 Mean SWC across EC_a derive management zones for Site II. Different letters are significantly different (p value < 0.05).

suggested that the EC_a measurements could provide useful information to characterize in-field SWC variability, consistently throughout the season. Nonetheless, EC_a derived management zones maps should be tailor-made, i.e. site-specific because one zone delineation procedure may not be suitable for all fields. A combination of factors could influence EC_a to varying degrees across different fields, and EC_a maps interpretation could be rather complex (Corwin and Lesch, 2003). Selecting a number of zones for the EC_a derived maps, regardless of the field characteristics, could lead to an inaccurate variable rate irrigation management.

EC_a coupled with soil properties to enhance the assessment of SWC

The spatial distribution and intensity of the soil sampling at Site I reached the kriging interpolation requirements (i.e. spatial auto-correlation), but not at Site II. At this location, samples were taken only on the southwestern part of the field, and were acquired at a distance larger than

the range estimated by the semi-variograms. For Site I, the deep EC_a map of two zones was the best to explain the differences in SWC across NP locations. Therefore, the "full model" consisted of the krigged EC_a values of 1.5 m depth combined with the soil properties as predictors in the automated model selection. Results of the automated model selection are shown in Table 2.2.

Table 2.2. Automated model selection output for the first five models by rank. Full model consisted in the krigged EC_a values of 1.5 m depth combined with soil properties to explain SWC at Site I. Selected variables for each best model are indicated with an X.

Rank	EC_a 1.5 m	CEC†	Clay	OM‡	Salts	r^2	AICc§
1	X	-	-	X	X	0.69	-82.89
2	X	-	-	-	-	0.44	-80.62
3	X	-	-	-	X	0.55	-80.55
4	X	-	X	-	X	0.64	-80.3
5	X	-	-	X	-	0.53	-79.88

† Cation exchange capacity
‡ Organic Matter
§ corrected Akaike Information Criterion

By combining soil properties with the base model, SWC assessment was improved (*p* value < 0.05). The best model as indicated by the lowest AICc value, included organic matter and salt content. The second best was the simplest model (base model), which utilized only the krigged EC_a values of 1.5 m depth as the predictor of the SWC. The third and fourth models selected salt content as part of the model predictors, making the salt content the most consistent variable across the top five models. The first model (krigged EC_a values of the 1.5 m depth, O.M. % and salt content) explained SWC significantly better than the best next model (only krigged EC_a values of the 1.5 m depth) (r^2 = 0.69 and 0.44, respectively). Results from this study suggest that organic matter and salt content should be incorporated at Site I (Figure 2.18), even with low organic matter values and salt concentration levels that are below yield-impacting levels as observed in that field. Management zone boundaries using only EC_a or using EC_a plus organic matter and salinity are juxtaposed in Figure 2.19. Changes in boundaries of the "EC_a coupled with Soil properties"

management zones resulted in an area disagreement of 8.16 % against the only EC_a management zones. There was a perfect agreement in SWC classes between the two sets of zones at the location of the NP access tubes. Hence, further testing for these new zones accuracy is not logical with the NP distribution existing in our study. Additional SWC sampling would be necessary to study the differences, specifically on the areas where the zones disagree.

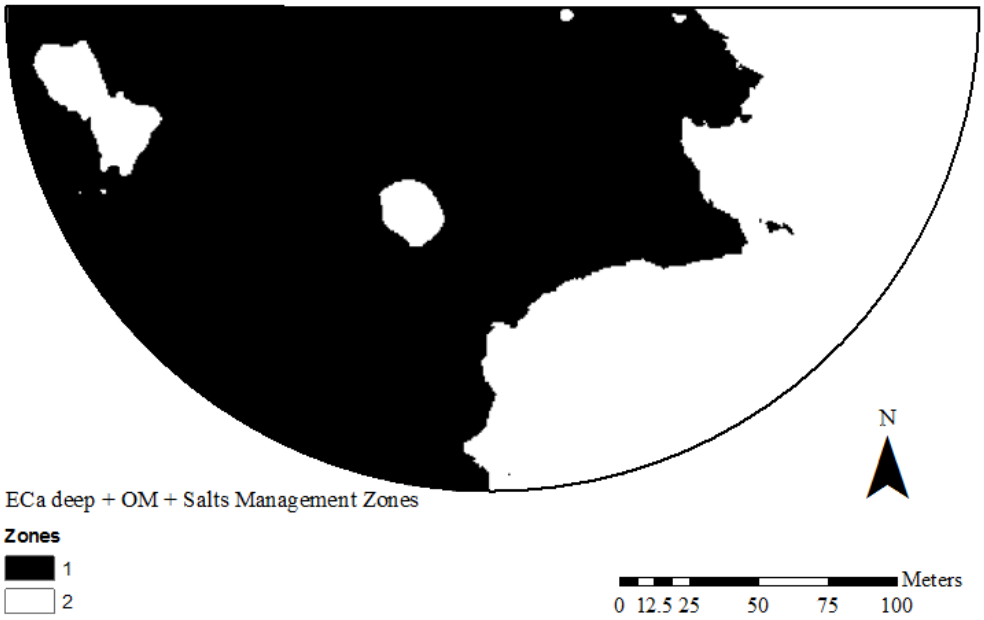

Figure 2.18. Management zone map delineated using ECa measured up to 1.5 m depth in addition to organic matter and soil salinity for Site I.

Researchers and commercial retailers have widely made use of the robust correlation between EC_a and SWC to create soil water management zones (Groeteke et al., 2014; Hedley et al., 2010). However, EC_a is influenced by a combination of physical and chemical properties including soluble salts, clay content and mineralogy, cation exchange capacity (CEC), bulk density, organic matter, soil temperature, and SWC (Corwin and Lesch, 2005).

ANOVA results showed that including organic matter and salt content significantly improved the estimation of SWC by EC_a. Organic matter increases the soil's water retention by its adsorption and absorption capacity, and by providing greater pore space (Gupta et al., 1977). Even

though the field's organic matter content in Colorado was relatively low (1.6 %) as compared with the range of Northern Great Plains of the United States (4 to 7%) (Overstreet and DeJong-Huges, 2009), it was included as a part of the equation between EC_a and SWC. The organic matter contribution to the model could potentially be greater in fields with higher organic matter percentage. Therefore, depending on the field, accounting for the soil organic matter could be of value when explaining the SWC by EC_a.

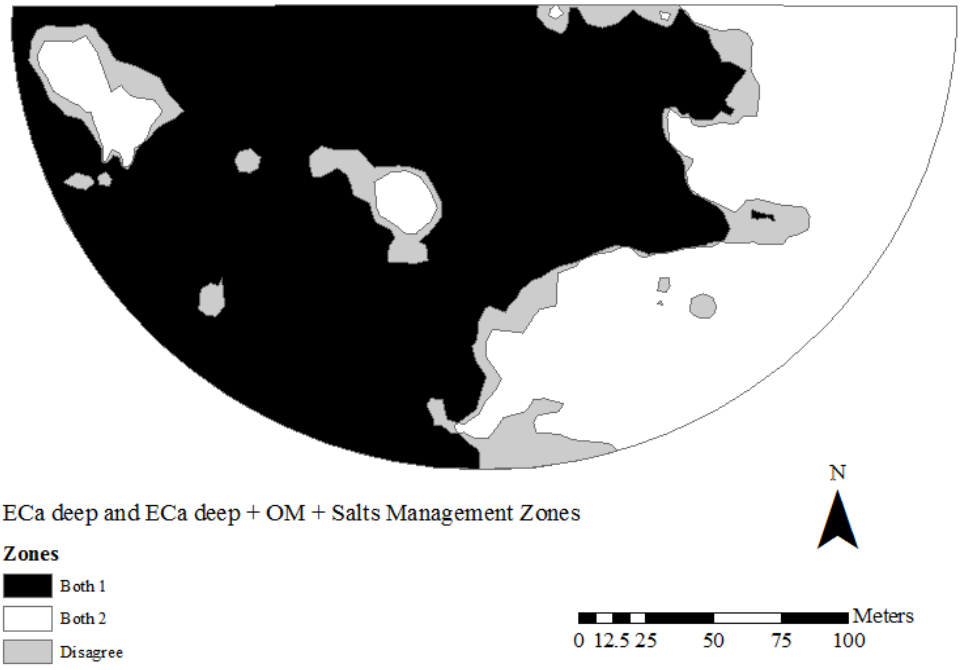

Figure 2.19. Comparison of management zones delineated with using ECa measured up to 1.5 m depth and management zones delineated using ECa measured up to 1.5 m depth in addition to organic matter and soil salinity for Site I. Differences are presented in the two techniques are presented as gray color referred to as "disagree" in the legend.

The spatial distribution of the soil properties influencing EC_a may be different from SWC's spatial distribution, making the EC_a interpretation more difficult. For example, high pH, salt or sodium levels are commonly heterogeneously distributed across the fields (Waskom et al., 2003). A typical feature of salt-affected soils is the inherent spatial variability in short distances (Isla et al., 2003). This means that the EC_a value could be affected by the salt content at some locations of

the field but not in the rest of the field, and thereby confounding the SWC estimation. Numerous studies relating SWC and EC_a have been conducted under non-saline conditions (Hedley et al., 2010; Hedley et al., 2004; Sudduth et al., 2005; Waine et al., 2000). The thresholds that define non-saline conditions are reported with respect to each specific crop (Maas and Hoffman, 1977). In addition, a soil is diagnosed as non-saline if the average of the samples is below a certain threshold, regardless of the variance. Consequently, most studies were performed without accounting for the potential effect of the low salinity levels on the EC_a. The soil salinity threshold for maize potential yield decrease is 1.7 dS m^{-1} (Ayers and Westcot, 1985), and the salt content values at Site I did not exceed the value 0.7 dS m^{-1} at any sampling location. Although this may suggest that soil salt concentration did not affect yield in this study, results showed that it did affect the EC_a and SWC relationship, even with the low salt content values for the study area. The high EM38MK2 sensitivity to the low salt content values in our study followed its original design purpose, the rapid above-ground measurement of soil salinity (Rhoades and Corwin, 1981).

Soil test for salinity is the best way for an accurate diagnosis (Waskom et al., 2003). However, conventional sampling techniques for salt content and organic matter could be time consuming, dense and expensive. For an accurate map prediction, the sample interval of a soil property should be at a distance of 0.4 times or less than the range of its spatial dependence (Kerry et al., 2010). For instance, in a 5.35 ha agricultural field, Shi et al. (2005) reported a soil salinity range from 133.7 to 169.1 m. This would mandate sampling at every 0.29 ha, while the common practice is that of one sample per ten hectares (Sosa, 2012). Benefits from improving the SSMZ for the purpose of precision irrigation by incorporating other soil properties have to be compared with the cost of sampling for those soil components. Therefore, the economic feasibility of this approach might not be convenient and new cost-effective methods should be developed to render

it feasible. Even though remote sensing has been proven to estimate superficial salinity (Mehrjardi et al., 2008; Yong-Ling et al., 2010) and organic matter content (Bhatti et al., 1991), yet they are not quantitatively precise enough (Yong-Ling et al., 2010). However, with the development of better techniques and the advent of better sources (e.g. satellites and drones), significant improvement has been achieved in the soil salinity estimation (Yong-Ling et al., 2010) making remote sensing a promising alternative to extensive sampling of the soil properties.

When "constructing" soil water management zones based on EC_a measurements, special attention should be given to those soil properties previously reported as influencing the EC_a. Such soil properties may not have an impact on yield, but may still can have an effect on the EC_a as was observed in this study. When the spatial distribution of a soil property does not follow the SWC spatial distribution, the proportional effect of the SWC on the EC_a varies in space. This would implicate a loss in SWC assessment accuracy by EC_a across the field, i.e. over and/or under estimation. In order to provide wider technical recommendations, it may be necessary to do further research on scenarios with different quantities of soil organic matter and soluble salts, as well as scenarios with different soil properties affecting the EC_a against SWC relationship.

The results from this study showed that EC_a derived management zones were able to explain the SWC variations along the season. However, it is worth noting that this was only true for the average SWC values within zones. Longchamps et al. (2015) reported the existence of dynamic water management zones throughout the season, that is to say a continuous variability in the SWC patterns in time. To address this finer scale in the SWC variability, hence achieve better VRI practices, more detailed information about the SWC status would be necessary. de Lara (2016) suggested the use of vegetation indices (i.e. Normalized Difference Vegetation Index, Red Edge Chlorophyll Index and Red Edge Normalized Difference Vegetation Index) for the real-time

assessment of the SWC within each EC_a derived water management zone. Combining the advent of new remote sensing technologies, such as drones and high-end satellites, with new precision irrigation technologies (capable of varying rates at every nozzle), the future of variable rate irrigation seems to be prosper. However, more research combining these different technologies for crop production is needed for an accurate management at the farmer level.

CONCLUSION

Variable rate irrigation (VRI) has been proven to be an effective practice to increase irrigation efficiency. Soil water management zones for irrigation are the platform with which VRI is currently being commercially applied, and EC_a has been widely used to obtain them. In this study, the Management Zones Analyst (MZA) software recommendations were more accurate than the fixed number of zones typically proposed by commercial retailers. The three of four combinations (two sites over two EC_a reading depths), the EC_a zones explained the SWC. In general, the deep EC_a readings (0 to 150 cm) outperformed the shallow EC_a readings (0 to 75 cm) to assess SWC across fields. The latter has a higher sensitivity for more superficial soil layers, which could be less related to the SWC depending on the local characteristics. For Site I, coupling krigged EC_a with organic matter and salt content data significantly improved the SWC assessment. Therefore, when creating EC_a plus organic matter and salt content derived zones, boundaries of the management zones differed from the map delimited only with EC_a. However, management zones for both approaches had the same NP access tubes spatial distribution, thereby further testing was not logical. In summary, EC_a derived management zones showed to be an effective method to characterize in-field SWC variability between zones throughout the season. The EC_a zones could potentially be used for precision irrigation (SSMZ for irrigation), which consists in applying

specific rates of water based on the requirements of each zone. However, the process of deriving the management zones from the EC_a should be tailor-made, given the variability in soil hydraulic properties existing across farms. Results suggested that to improve the accuracy on the creation of maps for precision irrigation management, EC_a should be combined with the soil properties significantly influencing the EC_a-SWC interaction. Nonetheless, the findings in this study were only valid for the average SWC within each ECa derived management zone. When studying the spatial SWC variability across maize fields, Longchamps et al. (2015) found dynamic water management zones. This suggested the need for updated SWC estimations to account for the temporal SWC variability within zones. Likewise, de Lara (2016) proposed the use of remote sensing as a feasible tool for the real-time assessment of the SWC during the crop season. Altogether, new technologies have to be combined and studied for the possibility of a more accurate precision irrigation at the field scale.

REFERENCES

Alexandratos, N. 1995. World agriculture: towards 2010: an FAO studyFood & Agriculture Org.

Andrade, F.H. and V.O. Sadras. 2000. Bases para el manejo del maíz, el girasol y la sojaINTA, Buenos Aires (Argentina). EEA Balcarce.

AQUASTAT, F. 2002. AQUASTAT database.

Ashcroft, P., J. Catt, P. Curran, J. Munden and R. Webster. 1990. The relation between reflected radiation and yield on the Broadbalk winter wheat experiment†. REMOTE SENSING 11: 1821-1836.

Asrar, G., M. Fuchs, E. Kanemasu and J. Hatfield. 1984. Estimating absorbed photosynthetic radiation and leaf area index from spectral reflectance in wheat. Agronomy journal 76: 300-306.

Ayers, R. and D. Westcot. 1985. Water quality for agriculture. FAO Irrigation and drainage paper 29 Rev. 1. Food and Agricultural Organization. Rome.

Barton, K. 2016. MuMIn: Multi-Model Inference.

Bates, D., M. Maechler, B. Bolker and S. Walker. 2015. Fitting Linear Mixed-Effects Models using "lme4". Journal of Statistical Software 67: 1-48. doi:10.18637/jss.v067.i01.

Bhatti, A., D. Mulla and B. Frazier. 1991. Estimation of soil properties and wheat yields on complex eroded hills using geostatistics and thematic mapper images. Remote Sensing of Environment 37: 181-191.

Biswas, A. and B.C. Si. 2011. Scales and locations of time stability of soil water storage in a hummocky landscape. Journal of Hydrology 408: 100-112.

Brevik, E.C., T.E. Fenton and A. Lazari. 2006. Soil electrical conductivity as a function of soil water content and implications for soil mapping. Precision Agriculture 7: 393-404.

Burnham, K.P. and D.R. Anderson. 2003. Model selection and multimodel inference: a practical information-theoretic approachSpringer Science & Business Media.

Calviño, P.A., F.H. Andrade and V.O. Sadras. 2003. Maize yield as affected by water availability, soil depth, and crop management. Agronomy Journal 95: 275-281.

Chen, F., D.E. Kissel, L.T. West and W. Adkins. 2000. Field-scale mapping of surface soil organic carbon using remotely sensed imagery. Soil Science Society of America Journal 64: 746-753.

Chen, P.-Y., G. Fedosejevs, M. Tiscareno-Lopez and J.G. Arnold. 2006. Assessment of MODIS-EVI, MODIS-NDVI and VEGETATION-NDVI composite data using agricultural measurements: an example at corn fields in western Mexico. Environmental monitoring and assessment 119: 69-82.

Condon, A., R. Richards, G. Rebetzke and G. Farquhar. 2004. Breeding for high water-use efficiency. Journal of Experimental Botany 55: 2447-2460.

Corwin, D. and S. Lesch. 2003. Application of soil electrical conductivity to precision agriculture. Agronomy Journal 95: 455-471.

Corwin, D. and S. Lesch. 2005. Apparent soil electrical conductivity measurements in agriculture. Computers and electronics in agriculture 46: 11-43.

Corwin, D. and S. Lesch. 2005. Characterizing soil spatial variability with apparent soil electrical conductivity: I. Survey protocols. Computers and electronics in agriculture 46: 103-133.

Corwin, D., S. Lesch, P. Shouse, R. Soppe and J. Ayars. 2003. Identifying soil properties that influence cotton yield using soil sampling directed by apparent soil electrical conductivity. Agronomy Journal 95: 352-364.

da Silva, A.P., A. Nadler and B. Kay. 2001. Factors contributing to temporal stability in spatial patterns of water content in the tillage zone. Soil and Tillage Research 58: 207-218.
Delegido, J., J. Verrelst, C. Meza, J. Rivera, L. Alonso and J. Moreno. 2013. A red-edge spectral index for remote sensing estimation of green LAI over agroecosystems. European Journal of Agronomy 46: 42-52.
Djaman, K. and S. Irmak. 2012. Soil water extraction patterns and crop, irrigation, and evapotranspiration water use efficiency of maize under full and limited irrigation and rainfed settings. Transactions of the ASABE 55: 1223-1238.
Dodds, W.K., W.W. Bouska, J.L. Eitzmann, T.J. Pilger, K.L. Pitts, A.J. Riley, et al. 2008. Eutrophication of US freshwaters: analysis of potential economic damages. Environmental Science & Technology 43: 12-19.
Evans, R.G. and E.J. Sadler. 2008. Methods and technologies to improve efficiency of water use. Water resources research 44.
Evett, S.R., R.C. Schwartz, J.A. Tolk and T.A. Howell. 2009. Soil profile water content determination: spatiotemporal variability of electromagnetic and neutron probe sensors in access tubes. Vadose Zone Journal 8: 926-941.
Famiglietti, J., J. Devereaux, C. Laymon, T. Tsegaye, P. Houser, T. Jackson, et al. 1999. Ground-based investigation of soil moisture variability within remote sensing footprints during the Southern Great Plains 1997 (SGP97) Hydrology Experiment. Water Resources Research 35.
FAO. 2002. Crops and drops: Making the best use of water for agriculture. World Food Day Rome.
FAO. 2015. Statistical Pocketbook World food and agriculture. FAO.
Fipps, G. 1995. Soil Moisture ManagementTexas Agricultural Extension Service, Texas A&M University System, College Station.
Fleming, K., D. Westfall, D. Wiens and M. Brodahl. 2000. Evaluating farmer defined management zone maps for variable rate fertilizer application. Precision Agriculture 2: 201-215.
Fleming, K.L., D.G. Westfall, D.W. Wiens, L.E. Rothe, J.E. Cipra and D.F. Heermann. 1999. Evaluating farmer developed management zone maps for precision farming. Precision Agriculture: 335-343.
Fridgen, J.J., N.R. Kitchen, K.A. Sudduth, S.T. Drummond, W.J. Wiebold and C.W. Fraisse. 2004. Management zone analyst (MZA). Agronomy Journal 96: 100-108.
Gao, X., A.R. Huete, W. Ni and T. Miura. 2000. Optical–biophysical relationships of vegetation spectra without background contamination. Remote Sensing of Environment 74: 609-620.
Gao, X., P. Wu, X. Zhao, J. Wang and Y. Shi. 2014. Effects of land use on soil moisture variations in a semi- arid catchment: implications for land and agricultural water management. Land Degradation & Development 25: 163-172.
Gitelson, A. and M.N. Merzlyak. 1994. Quantitative estimation of chlorophyll-a using reflectance spectra: experiments with autumn chestnut and maple leaves. Journal of Photochemistry and Photobiology B: Biology 22: 247-252.
Gitelson, A. and M.N. Merzlyak. 1994. Spectral reflectance changes associated with autumn senescence of Aesculus hippocastanum L. and Acer platanoides L. leaves. Spectral features and relation to chlorophyll estimation. Journal of Plant Physiology 143: 286-292.
Gitelson, A.A., Y.J. Kaufman and M.N. Merzlyak. 1996. Use of a green channel in remote sensing of global vegetation from EOS-MODIS. Remote Sensing of Environment 58: 289-298.
Gitelson, A.A., Y.J. Kaufman, R. Stark and D. Rundquist. 2002. Novel algorithms for remote estimation of vegetation fraction. Remote Sensing of Environment 80: 76-87.

Gitelson, A.A. and M.N. Merzlyak. 1997. Remote estimation of chlorophyll content in higher plant leaves. International Journal of Remote Sensing 18: 2691-2697.
Gitelson, A.A., A. Viña, T.J. Arkebauer, D.C. Rundquist, G. Keydan and B. Leavitt. 2003. Remote estimation of leaf area index and green leaf biomass in maize canopies. Geophysical Research Letters 30.
Groeteke, J., L. Dotterer and J. Shanahan. 2014. Variable Rate Irrigation. Crop Insights 24.
Gupta, S., R. Dowdy and W. Larson. 1977. Hydraulic and thermal properties of a sandy soil as influenced by incorporation of sewage sludge. Soil Science Society of America Journal 41: 601-605.
Hanks, R. 1983. Yield and water-use relationships: An overview. Limitations to efficient water use in crop production: 393-411.
Hanson, B. and K. Kaita. 1997. Response of electromagnetic conductivity meter to soil salinity and soil-water content. Journal of irrigation and Drainage Engineering 123: 141-143.
Hawley, M.E., T.J. Jackson and R.H. McCuen. 1983. Surface soil moisture variation on small agricultural watersheds. Journal of Hydrology 62: 179-200.
2010. Spatial irrigation scheduling for variable rate irrigation. Proceedings of the New Zealand Grassland Association, New Zealand Grassland Association.
Hedley, C., I. Yule, C. Eastwood, T. Shepherd and G. Arnold. 2004. Rapid identification of soil textural and management zones using electromagnetic induction sensing of soils. Soil Research 42: 389-400.
Hedley, C., I. Yule, M. Tuohy and I. Vogeler. 2009. Key performance indicators for simulated variable-rate irrigation of variable soils in humid regions. Transactions of the ASABE 52: 1575-1584.
Hedley, C.B. and I.J. Yule. 2009. Soil water status mapping and two variable-rate irrigation scenarios. Precision Agriculture 10: 342-355.
Henninger, D., G. Petersen and E. Engman. 1976. Surface soil moisture within a watershed—variations, factors influencing, and relationship to surface runoff. Soil Science Society of America Journal 40: 773-776.
Hezarjaribi, A. and H. Sourell. 2007. Feasibility study of monitoring the total available water content using non- invasive electromagnetic induction- based and electrode- based soil electrical conductivity measurements. Irrigation and Drainage 56: 53-65.
Holzman, M., R. Rivas and M. Piccolo. 2014. Estimating soil moisture and the relationship with crop yield using surface temperature and vegetation index. International Journal of Applied Earth Observation and Geoinformation 28: 181-192.
Howell, T., J. Steiner, A. Schneider, S. Evett and J. Tolk. 1997. Seasonal and maximum daily evapotranspiration of irrigated winter wheat, sorghum, and corn—Southern High Plains. Transactions of the ASAE 40: 623-634.
Howell, T.A. 2001. Enhancing water use efficiency in irrigated agriculture. Agronomy journal 93: 281-289.
Huete, A., K. Didan, T. Miura, E.P. Rodriguez, X. Gao and L.G. Ferreira. 2002. Overview of the radiometric and biophysical performance of the MODIS vegetation indices. Remote sensing of environment 83: 195-213.
Huete, A., C. Justice and W. van Leeuwen. 1999. MODIS vegetation index (MOD13) algorithm theoretical basis document. Greenbelt: NASA Goddard Space Flight Centre, http://modarch. gsfc. nasa. gov/MODIS/LAND/# vegetation-indices.

Hupet, F. and M. Vanclooster. 2002. Intraseasonal dynamics of soil moisture variability within a small agricultural maize cropped field. Journal of Hydrology 261: 86-101.
Isla, R., R. Aragüés and A. Royo. 2003. Spatial variability of salt-affected soils in the middle Ebro valley (Spain) and implications in plant breeding for increased productivity. Euphytica 134: 325-334.
Johl, S.S. 2013. Irrigation and Agricultural Development: Based on an International Expert Consultation, Baghdad, Iraq, 24 February-1 March 1979Elsevier.
Kerry, R., M. Oliver and Z. Frogbrook. 2010. Sampling in precision agriculture. Geostatistical applications for precision agriculture. Springer. p. 35-63.
Khosla, R., K. Fleming, J. Delgado, T. Shaver and D. Westfall. 2002. Use of site-specific management zones to improve nitrogen management for precision agriculture. Journal of Soil and Water Conservation 57: 513-518.
Knipling, E.B. 1970. Physical and physiological basis for the reflectance of visible and near-infrared radiation from vegetation. Remote Sensing of Environment 1: 155-159.
Kranz, W.L., S. Irmak, S.J. Van Donk, C.D. Yonts and D.L. Martin. 2008. Irrigation management for corn. Neb Guide, University of Nebraska, Lincoln.
Kumar, R. and L. Silva. 1973. Light ray tracing through a leaf cross section. Applied Optics 12: 2950-2954.
2011. Variable Rate Irrigation 2010 Field Results. 2011 Louisville, Kentucky, August 7-10, 2011, American Society of Agricultural and Biological Engineers.
Lichtenthaler, H.K. 1987. Chlorophyls and carotenoids: Pigments of photosynthetic biomembranes. Methods in enzimology 148 (34): 350-382. Academic Press.
Longchamps, L., R. Khosla, R. Reich and D. Gui. 2015. Spatial and Temporal Variability of Soil Water Content in Leveled Fields. Soil Science Society of America Journal 79: 1446-1454.
Lull, H.W. and K.G. Reinhart. 1955. Soil-moisture measurementSouthern Forest Experiment Station, Forest Service, US Forest Service.
Maas, E.V. and G. Hoffman. 1977. Crop salt tolerance - current assessment. Journal of the irrigation and drainage division 103: 115-134.
Maddonni, G.A., M.a.E. Otegui, B. Andrieu, M. Chelle and J.J. Casal. 2002. Maize leaves turn away from neighbors. Plant Physiology 130: 1181-1189.
Mahey, R., R. Singh, S. Sidhu, R. Narang, V. Dadhwal, J. Parihar, et al. 1993. Pre-harvest state level wheat acreage estimation using IRS-IA LISS-I data in Punjab (India). International Journal of Remote Sensing 14: 1099-1106.
Martin, D., T. Smith, W. Kranz, S. Irmak, S. van Donk and J. Shanahan. 2014. Soil Water Management. Crop Insights 24.
McCulloch, C.E. and J.M. Neuhaus. 2001. Generalized linear mixed modelsWiley Online Library.
McNeill, J. 1980. Electromagnetic terrain conductivity measurement at low induction numbers. Geonics Limited Ontario, Canada.
Mehrjardi, R.T., S. Mahmoodi, M. Taze and E. Sahebjalal. 2008. Accuracy assessment of soil salinity map in Yazd-Ardakan Plain, Central Iran, based on Landsat ETM+ imagery. Am.-Eurasian J. Agric. Environ. Sci 3: 708-712.
Mohanty, B., J. Famiglietti and T. Skaggs. 2000. Evolution of soil moisture spatial structure in a mixed vegetation pixel during the Southern Great Plains 1997 (SGP97) Hydrology Experiment. Water Resources Research 36: 3675-3686.

Moore, I., G. Burch and D. Mackenzie. 1988. Topographic effects on the distribution of surface soil water and the location of ephemeral gullies. Transactions of the ASAE (USA).
Muñoz-Carpena, R., S. Shukla and K. Morgan. 2004. Field devices for monitoring soil water contentUniversity of Florida Cooperative Extension Service, Institute of Food and Agricultural Sciences, EDIS.
Myneni, R.B. and F.G. Hall. 1995. The interpretation of spectral vegetation indexes. Geoscience and Remote Sensing, IEEE Transactions on 33: 481-486.
Myneni, R.B., R. Ramakrishna, R. Nemani and S.W. Running. 1997. Estimation of global leaf area index and absorbed PAR using radiative transfer models. Geoscience and Remote Sensing, IEEE Transactions on 35: 1380-1393.
Nguy-Robertson, A., A. Gitelson, Y. Peng, A. Viña, T. Arkebauer and D. Rundquist. 2012. Green leaf area index estimation in maize and soybean: combining vegetation indices to achieve maximal sensitivity. Agronomy Journal 104: 1336-1347.
Nielsen, D.R., J.W. Biggar and K.T. Erh. 1973. Spatial variability of field-measured soil-water propertiesUniversity of California, Division of Agricultural Sciences.
Omary, M., C. Camp and E. Sadler. 1997. Center pivot irrigation system modification to provide variable water application depths. Applied Engineering in Agriculture 13: 235-239.
Overstreet, L.F. and J. DeJong-Huges. 2009. The importance of soil organic matter in cropping systems of the Northern Great Plains. Section 2d,(University of Minnesota, College of Food, Agricultural and Natural Resource Sciences, 2009) http://www. extension. umn. edu/distribution/cropsystems M 1273.
Pagliai, M., N. Vignozzi and S. Pellegrini. 2004. Soil structure and the effect of management practices. Soil and Tillage Research 79: 131-143.
Paine, J.G., R.S. Goldsmith and B.R. Scanlon. 1998. Electrical conductivity and gamma-ray response to clay, water, and chloride content in fissured sediments, Trans-Pecos Texas. Environmental & Engineering Geoscience 4: 225-239.
Pan, Y.X. and X.P. Wang. 2009. Factors controlling the spatial variability of surface soil moisture within revegetated- stabilized desert ecosystems of the Tengger Desert, Northern China. Hydrological Processes 23: 1591-1601.
Peralta, N.R. and J.L. Costa. 2013. Delineation of management zones with soil apparent electrical conductivity to improve nutrient management. Computers and electronics in agriculture 99: 218-226.
Peralta, N.R., J.L. Costa, M. Balzarini and H. Angelini. 2013. Delineation of management zones with measurements of soil apparent electrical conductivity in the southeastern pampas. Canadian Journal of Soil Science 93: 205-218.
Peters, R.T., K. Desta and L. Nelson. 2013. Practical use of soil moisture sensors and their data for irrigation schedulingWashington State University Extension.
Pinty, B., C. Leprieur and M.M. Verstraete. 1993. Towards a quantitative interpretation of vegetation indices Part 1: Biophysical canopy properties and classical indices. Remote Sensing Reviews 7: 127-150.
Postel, S.L. 2000. Entering an era of water scarcity: the challenges ahead. Ecological applications 10: 941-948.
R Core Team. 2016. R: A language and environment for statistical computing. R Foundation for Statistical Computing, Vienna, Austria. 2016. ISBN 3-900051-07-0.

Rhoades, J. and D. Corwin. 1981. Determining soil electrical conductivity-depth relations using an inductive electromagnetic soil conductivity meter. Soil Science Society of America Journal 45: 255-260.
Rouse, J., R. Haas, J. Schell and D. Deering. 1974. Monitoring vegetation systems in the Great Plains with ERTS. NASA special publication 351: 309.
Russell V, L. 2016. Least-Squares Means: The (R) Package (lsmeans). Journal of Statistical Software 69: 1-33. doi:10.18637/jss.v069.i01.
Sadler, E., R. Evans, K. Stone and C. Camp. 2005. Opportunities for conservation with precision irrigation. Journal of Soil and Water Conservation 60: 371-378.
Sadler, E.J., C.R. Camp, D.E. Evans and J. Millen. 2002. Spatial variation of corn response to irrigation. Transactions of the ASAE 45: 1869-1881.
Schmitz, M. and H. Sourell. 2000. Variability in soil moisture measurements. Irrigation Science 19: 147-151.
Schuster, C., M. Förster and B. Kleinschmit. 2012. Testing the red edge channel for improving land-use classifications based on high-resolution multi-spectral satellite data. International Journal of Remote Sensing 33: 5583-5599.
Sharp, R. and W. Davies. 1985. Root growth and water uptake by maize plants in drying soil. Journal of Experimental Botany 36: 1441-1456.
Sheets, K.R. and J.M. Hendrickx. 1995. Noninvasive soil water content measurement using electromagnetic induction. Water resources research 31: 2401-2409.
Shi, Z., Y. Li, R. Wang and F. Makeschine. 2005. Assessment of temporal and spatial variability of soil salinity in a coastal saline field. Environmental Geology 48: 171-178.
Smith, V.H., G.D. Tilman and J.C. Nekola. 1999. Eutrophication: impacts of excess nutrient inputs on freshwater, marine, and terrestrial ecosystems. Environmental pollution 100: 179-196.
Sosa, D. 2012. Instituto Nacional de Tecnología Agropecuaria (INTA). Manejo de Suelos. Técnicas de toma y remisión de muestras de suelo. Argentina.
Steduto, P. 1996. Water use efficiency. Sustainability of Irrigated Agriculture. Springer. p. 193-209.
Steduto, P., T.C. Hsiao, D. Raes and E. Fereres. 2012. Crop yield response to waterFood and Agriculture Organization of the United Nations Rome.
Stone, J., D. Kirkham and A. Read. 1955. Soil moisture determination by a portable neutron scattering moisture meter. Soil Science Society of America Journal 19: 419-423.
Sudduth, K., N. Kitchen, W. Wiebold, W. Batchelor, G. Bollero, D. Bullock, et al. 2005. Relating apparent electrical conductivity to soil properties across the north-central USA. Computers and Electronics in Agriculture 46: 263-283.
Tanner, C. and T. Sinclair. 1983. Efficient water use in crop production: research or re-search? Limitations to efficient water use in crop production: 1-27.
Teal, R., B. Tubana, K. Girma, K. Freeman, D. Arnall, O. Walsh, et al. 2006. In-season prediction of corn grain yield potential using normalized difference vegetation index. Agronomy Journal 98: 1488-1494.
Teuling, A.J. and P.A. Troch. 2005. Improved understanding of soil moisture variability dynamics. Geophysical Research Letters 32.
Turral, H., J.J. Burke and J.-M. Faurès. 2011. Climate change, water and food security. Food and Agriculture Organization of the United Nations Rome.
Unganai, L.S. and F.N. Kogan. 1998. Drought monitoring and corn yield estimation in Southern Africa from AVHRR data. Remote Sensing of Environment 63: 219-232.

Vachaud, G., A. Passerat de Silans, P. Balabanis and M. Vauclin. 1985. Temporal stability of spatially measured soil water probability density function. Soil Science Society of America Journal 49: 822-828.
Viña, A., A.A. Gitelson, A.L. Nguy-Robertson and Y. Peng. 2011. Comparison of different vegetation indices for the remote assessment of green leaf area index of crops. Remote Sensing of Environment 115: 3468-3478.
Waine, T., B. Blackmore and R. Godwin. 2000. Mapping available water content and estimating soil textural class using electro-magnetic induction. Proceedings of EurAgEng, Paper 00-SW 44.
Walthall, C., W. Dulaney, M. Anderson, J. Norman, H. Fang and S. Liang. 2004. A comparison of empirical and neural network approaches for estimating corn and soybean leaf area index from Landsat ETM+ imagery. Remote Sensing of Environment 92: 465-474.
Wang, L. and J.J. Qu. 2009. Satellite remote sensing applications for surface soil moisture monitoring: A review. Frontiers of Earth Science in China 3: 237-247.
Waskom, R.M., T. Bauder, J. Davis and G. Cardon. 2003. Diagnosing saline and sodic soil problemsColorado State University Cooperative Extension.
Wiegand, C., A. Richardson, D. Escobar and A. Gerbermann. 1991. Vegetation indices in crop assessments. Remote Sensing of Environment 35: 105-119.
Yong-Ling, W., G. Peng and Z. Zhi-Liang. 2010. A spectral index for estimating soil salinity in the Yellow River Delta Region of China using EO-1 Hyperion data. Pedosphere 20: 378-388.

APPENDIX A

Table A1. Pearson's Correlation (r) between neutron probe (NP) and yield for Site I at different depths and different day of the year (DOY). The r was indicated when a significant (p value < 0.05) correlation coefficients was observed, and non-significant relationship were indicated by a hyphen (-).

	Depth							
DOY	30 cm	60 cm	90 cm	120 cm	150 cm	$\bar{x}$ 30 – 60 cm	$\bar{x}$ 30 – 90 cm	$\bar{x}$ 30 – 150 cm
170	-	-	-	-	-	-	-	-
175	-	-	-	-	-	-	-	-
177	-	-	-	-	-	-	-	-
181	-	-	-	-	-	-	-	-
184	-	-	-	-	-	-	-	-
188	-	-	-	-	-	-	-	-
191	0.48	-	-	-	-	-	-	-
195	-	-	-	-	-	-	-	-
198	-	-	-	-	-	-	-	-
202	-	-	-	-	-	-	-	-
205	0.55	-	-	-	-	0.48	-	-
209	0.64	-	-	-	-	0.56	-	-
212	0.72	0.55	-	-	-	0.67	0.57	0.53
216	0.77	0.56	-	-	-	0.70	0.61	0.58
219	0.53	0.57	-	0.58	-	0.60	0.56	0.58
222	0.79	0.58	-	0.54	-	0.72	0.61	0.61
226	0.55	0.64	0.72	0.77	0.53	0.61	0.67	0.69
230	0.75	0.60	-	0.68	0.51	0.71	0.63	0.64
233	0.77	0.70	0.52	0.61	0.59	0.76	0.69	0.67
237	0.81	0.70	0.61	0.62	0.72	0.81	0.74	0.73
240	0.84	0.74	0.68	0.68	0.69	0.84	0.80	0.77

Table A2. Pearson's Correlation (r) between neutron probe (NP) and yield for Site II at different depths and different day of the year (DOY). The r was indicated when a significant (*p* value < 0.05) correlation coefficients was observed, and non-significant relationship were indicated by a hyphen (-).

	Depth							
DOY	30 cm	60 cm	90 cm	120 cm	150 cm	$\bar{x}$ 30 – 60 cm	$\bar{x}$ 30 – 90 cm	$\bar{x}$ 30 – 150 cm
159	-	-	-0.4964	-	-	-	-	-
169	-	-	-	-	-	-	-	-
175	-	-	-	-	-	-	-	-
182	-	-0.5033	-	-	-	-0.4940	-0.5292	-
191	-	-	-	-	-	-	-	-
204	-	-	-	-	-	-	-	-
211	-	-	-	-	-	-	-	-
224	-	-	-	-	-	-	-	-
232	-	-	-	-	-	-	-	-
258	-	-	-	-	-	-	-	-
265	-	-	-	-	-	-	-	-
272	-	-	-	-	-	-	-	-